UNIVERSIDADE DE SÃO PAULO
FACULDADE DE ODONTOLOGIA DE BAURU

PAULA SANCHES DOS SANTOS

Microtomographic and histologic evaluation of craniofacial reconstructions in rabbits using different biomaterials

Avaliação microtomográfica e histológica de reconstruções craniofaciais em coelhos utilizando diferentes biomateriais

BAURU
2020

PAULA SANCHES DOS SANTOS

Microtomographic and histologic evaluation of craniofacial reconstructions in rabbits using different biomaterials

Avaliação microtomográfica e histológica de reconstruções craniofaciais em coelhos utilizando diferentes biomateriais

Tese constituída por artigos apresentada a Faculdade de Odontologia de Bauru da Universidade de São Paulo para obtenção do título de Doutor em Ciências no Programa de Ciências Odontológicas Aplicadas, na área de concentração Biologia Oral.

Orientador: Prof. Dr. Gerson Francisco de Assis

BAURU

2020

Santos, Paula Sanches dos

Avaliação microtomográfica e histológica de reconstruções craniofaciais em coelhos utilizando diferentes biomateriais / Paula Sanches dos Santos – Bauru, 2020.

105p. : il. ; 31cm.

Tese (Doutorado) – Faculdade de Odontologia de Bauru. Universidade de São Paulo

Orientador: Prof. Dr. Gerson Francisco de Assis

FOLHA DE APROVAÇÃO

Dedicatória

Dedico esse trabalho ao meu Deus e aos meus pais Edson e Cidinha.

Agradecimentos

"Àquele que é capaz de fazer infinitamente mais do que tudo o que pedimos ou pensamos, de acordo com o seu poder que atua em nós." Bíblia Sagrada (NVI), Efésios 3:20. A **Deus**, meu Pai Eterno e Soberano, que me deu a vida e o privilégio de ser sua filha, por meio de Jesus Cristo. Sem Ele nada disso seria possível. Antes de estar em meus planos, essa conquista já estava em Seus planos e tudo preparou para que eu chegasse até aqui. Sempre esteve ao meu lado, me amando incondicionalmente, me orientando, me levantando e me sustentando. Obrigada Senhor por cada forma de me mostrar seu carinho, cuidado e amor e também pelas pessoas que colocou em meu caminho. Sou eternamente grata e quero sempre viver para te honrar. "Pois dele, por ele e para ele são todas as coisas. A ele seja a glória para sempre! Amém." Bíblia Sagrada (NVI), Romanos 11:36.

Aos meus pais **Edson M. dos Santos e Maria A. M. S. dos Santos (Cidinha)** por toda a ajuda e retaguarda que sempre me deram. Agradeço pelo amor e paciência, pelos esforços e abdicações, pelos ensinamentos e conselhos, pelas orações e palavras de incentivo. Pela companhia de sempre e por se fazerem tão presente em minha vida, inclusive neste trabalho, vibrando com minhas vitórias e participando das minhas aflições. Vocês são meus exemplos de determinação, sabedoria e temor a Deus e continuam sendo até hoje os meus melhores e principais companheiros de vida. Com certeza, sem vocês essa conquista seria muito mais difícil e penosa. Sou privilegiada e grata por tê-los como pais. Essa vitória é nossa!!! Amo vocês.

Ao meu irmão **Filipe S. R. dos Santos**, meu primeiro amigo e companheiro das brincadeiras e artes de criança, meu exemplo de dedicação e determinação aos estudos. Agradeço a ele e à minha cunhada **Vanessa P. S. Ribas** pelo apoio e orações, pela companhia, paciência e preocupação de sempre. Precocemente, quero agradecer ao meu sobrinho **Davi**, que ainda está no "forninho", mas que já é muito amado e me traz muita alegria**.** Estendo meus agradecimentos também à **Dona Nice** (mãe da Vanessa) pela companhia sempre agradável em nossas reuniões familiares.

Aos meus avós maternos **Sebastião** (*in memoriam*) e **Apparecida** que muito me amaram, me incentivaram, se preocuparam com meus projetos e planos. Agradeço a minha avó Apparecida que participa ativamente da minha vida até hoje, vibrando com cada conquista e deixando minha vida mais alegre. À "**Tia Cida**" que considero como uma avó. Suas preocupações, carinhos e caprichos culinários deixam minha vida mais leve e agradável. Aos meus avós paternos, **Cypriano** (*in memoriam*) e **Maria Thereza** (*in memoriam*), que muito me dedicaram carinho e amor na infância e que certamente estariam muito felizes e orgulhosos por essa conquista. Agradeço também aos meus tios, primos, seus respectivos e demais parentes das famílias **Molina Sanches** e **Martins dos Santos,** pela torcida, amizade, encontros e alegrias.

Aos meus irmãos em Cristo, em especial aos da **Igreja Batista do Jardim Bela Vista de Bauru** e da **Igreja Batista do Estoril de Bauru** e à minha amiga mais chegada que irmã, **Flávia Choi Marchesano**. Agradeço muito a todos pelas orações, acompanhamento nas lutas e vitórias, sempre me dando palavras de ânimo e incentivo.

Ao meu orientador **Prof. Dr. Gerson Francisco de Assis**, pela oportunidade dada e pela confiança depositada para que eu pudesse desenvolver o doutorado. Agradeço pela convivência, atenção, amizade e ensinamentos. Sempre muito acessível, com seu jeito descontraído, sincero e humilde, trazendo alegria aos nossos dias.

À **Dra. Tania Mary Cestari**, minha "co-orientadora", que desde o início da minha jornada no laboratório (há 11 anos), me deu todo o suporte necessário e me ensinou a fazer ciência. Sempre muito prestativa, se desdobrando ao máximo para atender a todos e solucionar nossas dúvidas. Obrigada pelos ensinamentos diários que me permitiram grande crescimento. A sua inteligência e o seu amor pela ciência é admirável! Agradeço pelo carinho, atenção, paciência e pela amizade que se desenvolveu ao longo desses anos.

Ao **Prof. Dr. Rumio Taga**, que foi meu primeiro orientador nessa instituição, pessoa de grande admiração e respeito, com quem tive a honra de conviver e aprender durante todo o período de minha iniciação científica, mestrado e até hoje.

Aos demais professores do Laboratório de Histologia da FOB-USP. Ao **Prof. Dr. Gustavo Pompermaier Garlet** pelos conhecimentos proporcionados e exemplo de grande pesquisador que é. À **Profa. Dra. Camila O. Rodini Pegoraro**, com suas palavras de incentivo e conversas a respeito da vida profissional e pelas aulas ministradas.

Agradeço à minha irmãzinha de pesquisa **Daniela Pereira Catanzaro**, pela amizade sincera, por todas as conversas e também pelo seu apoio, sensibilidade e preocupação em sempre me ajudar. Agradeço aos meus colegas do **Laboratório da Disciplina de Histologia da FOB-USP** pela companhia e amizade, pelos momentos de aprendizados e conselhos, pelo respeito e apoio que sempre recebi e também pelos momentos descontraídos, *coffees*, almoços no bandejão e práticas esportivas. Com certeza a presença de cada um de vocês no meu dia a dia deixou tudo com mais cor, leveza e vida, sendo para mim uma terapia diária estar com vocês: **Suellen Paini, Rodrigo Buzo, Luciana Mieli Saito, Nathália Lopes, Rafael Ortiz, Angélica Fonseca, Jéssica Melchiades, Nádia Amôr, Ana Carolina Bighetti, Michelle Soriani Azevedo, Carolina Francisconi, Priscila Colavite, Vinicius Tagliavini, Luan Damasceno, André P. Tabanêz;** e também àqueles que já ganharam asas e voaram: **Ricardo V. N. Arantes, Caroline A. Rocha, Andréia E. Vieira Ribeiro, Ever E. L. Mena, Cláudia Biguetti, Eliana Lippe e Franco Cavalla.** Estendo esses agradecimentos também às técnicas do Laboratório de Histologia, **Danielle S. Ceolin (Dani)** e **Patrícia S. M. Germino (Paty),** e por todos os auxílios técnicos prestados, pela forma com que me acolheram no laboratório desde o início da minha iniciação científica, pelos ensinamentos, alegrias partilhadas, conversas e pela amizade e carinho que se desenvolveram ao longo desse tempo. À secretária **Maria Teresa A. F. M. Silva (Tê)**, agradeço pelas ajudas prestadas com tanto esmero, por seu carinho e cuidado comigo demonstrado diariamente, pelas conversas, mensagens, risadas e amizade. À Dona **Aldivina Mendes da Silva (D. Divina)** pelos deliciosos cafezinhos, pela atenção e conversas sempre muito agradáveis. Às funcionárias da limpeza que se preocupavam em deixar tudo limpinho para que pudéssemos desenvolver nossas atividades em um ambiente agradável.

Aos **Professores da FOB-USP e HRAC-USP** que ministraram disciplinas a mim durante o curso e contribuíram de alguma forma para o meu crescimento.

Aos demais **Alunos de Pós-Graduação da Biologia Oral** que partilharam comigo de aulas, estudos e trabalhos.

Às Disciplinas da FOB-USP que gentilmente abriram suas portas quando precisei de algum serviço ou equipamento, como a **Anatomia**, a **Microbiologia e Imunologia** e a **Radiologia**, e ao **Centro Integrado de Pesquisas (CIP).**

À Secretária da Biologia Oral, **Dalva Ribeiro de Oliveira,** que sempre me auxiliou nas dúvidas e procedimentos a serem tomados, com muita atenção, dedicação e carinho.

Aos funcionários da **Pós-Graduação e Biblioteca**.

Aos funcionários do **Biotério Central da FOB-USP**.

Aos funcionários do **Restaurante Universitário (Bandejão) da FOB-USP**.

À **Faculdade de Odontologia da UNESP de Araraquara**, pelo uso do microtomógrafo, em especial à funcionária: Luana Elis Sabino.

Aos **Membros da Banca**, pela disponibilidade e pelas sugestões e críticas que certamente contribuirão com esse trabalho.

Por fim, agradeço a todos que, de alguma forma, participaram e me auxiliaram nesta caminhada.

...Muito obrigada!

"É melhor ter companhia do que estar sozinho, porque maior é a recompensa do trabalho de duas pessoas. Se um cair, o amigo pode ajudá-lo a levantar-se. [...] Um cordão de três dobras não se rompe com facilidade." **Bíblia Sagrada (NVI), Eclesiastes 4:9,10a e 12b.**

Agradecimentos Institucionais

À **Universidade de São Paulo (USP)**.

À **Faculdade de Odontologia de Bauru da Universidade de São Paulo (FOB – USP)**.

Ao **Prof. Dr. Vahan Agopyan**, digníssimo Reitor da Universidade de São Paulo.

Ao **Prof. Dr. Pedro Vitoriano Oliveira**, digníssimo secretário Geral da Universidade de São Paulo.

Ao **Prof. Dr. Carlos Ferreira dos Santos**, digníssimo Diretor da Faculdade de Odontologia de Bauru da Universidade de São Paulo.

Ao **Prof. Dr. Guilherme dos Reis Pereira Janson**, digníssimo Vice-Diretor da Faculdade de Odontologia de Bauru da Universidade de São Paulo.

Ao **Prof. Dr. José Henrique Rubo**, digníssimo Prefeito do Campus da Faculdade de Odontologia de Bauru da Universidade de São Paulo.

À **Profa. Dra. Izabel Regina Fischer Rubira Bullen,** digníssima Presidente da Comissão de Pós-Graduação, da Faculdade de Odontologia de Bauru da Universidade de São Paulo.

À **Profa. Dra. Marília Afonso Rabelo Buzalaf**, digníssima Coordenadora do Programa de Pós-Graduação em Ciências Odontológicas Aplicadas na área de Biologia Oral, da Faculdade de Odontologia de Bauru da Universidade de São Paulo.

À **Coordenação de Aperfeiçoamento de Pessoal de Nível Superior – Brasil (CAPES)** pelo apoio – Código de Financiamento 001.

Epígrafe

"Por isso dediquei-me a aprender, a investigar, a buscar a sabedoria e a razão de ser das coisas." **Bíblia Sagrada (NVI), Eclesiastes 7:25a**.

ABSTRACT

The aim was to evaluate the bone formation and bone augmentation in two different models of craniofacial reconstructive surgery using comparatively different calcium phosphate-based ceramics or using deproteinized bovine bone (DBB) in association with angiogenic fraction F1 obtained from latex (*Hevea brasiliensis*) and hyaluronic acid hydrogel (HAH). In the article 1, bilateral maxillary sinus augmentation (MSA) was performed using carbonated deproteinized bovine bone (cDBB), sinterized deproteinized bovine bone (sDBB) or porous biphasic calcium phosphate (pBCP) in rabbits. After 2, 4 and 8 weeks the samples were collected and analyzed under microtomography, histomorphometry and immunohistochemistry for TRAP labeling. All treatments promoted maintenance of the MSA volume over time. The bone formation occurred in close contact with the surface of all materials particles. In cDBB group the number of TRAP+ cells maintaining stable during all experimental periods, while in sDBB and pBCP groups a peak was observed at 2 weeks. In all experimental periods, bone formation in sDBB group was higher compared to cDBB group and similar to pBCP group. In the article 2, bilateral cranial bone defects were performed and filled with F1/HAH/DBB or HAH/DBB and the contralateral side with F1/HAH or HAH in rabbits. After 2, 4 and 8 weeks the samples were collected to microtomography and histomorphometry analyzes. The total volume (TV) in the HAH/DBB and F1/HAH/DBB groups were significantly higher than in the HAH and F1/HAH groups. At 2 weeks, the F1/HAH/DBB group presented a greater volume bone (BV) compared to the other groups. In HAH/DBB and F1/HAH/DBB groups the bone tissue grew on the surface and pores of the DBB increasing progressively the maturity and the volume occupied. The DBB structure not changed. In defects of the HAH and F1/HAH groups occurred the invasion of the adjacent tegument with formation of a thin layer of connective tissue and small new bone formation limited to the edges during all periods. In conclusion, cDBB, sDBB and pBCP maintained the MSA volume, favoring bone formation and maturation being safe alternatives in the MSA technique. And, the F1 fraction associated to DBB provided significant increase in the bone formation of the cranial bone defects especially at the initial healing phase, suggesting a promising strategy for the treatment of craniomaxillofacial defects.

Key-words: Biocompatible Materials. Bone Density. Bone Regeneration. Ceramics. Rabbits. X-Ray Microtomography.

RESUMO

O objetivo foi avaliar a formação e o ganho ósseo em dois diferentes modelos de cirurgia reconstrutiva craniofacial, usando comparativamente diferentes cerâmicas à base de fosfato de cálcio ou usando osso bovino desproteinizado (OBD) em associação à fração angiogênica F1 obtida do látex (*Hevea brasiliensis*) e hidrogel de ácido hialurônico (HAH). No artigo 1, o levantamento do seio maxilar (LSM) bilateral foi realizado utilizando osso bovino desproteinizado carbonatado (OBDc), osso bovino desproteinizado sinterizado (OBDs) ou cerâmica bifásica de fosfato de cálcio porosa (BFCp) em coelhos. Após 2, 4 e 8 semanas, as amostras foram coletadas e analisadas sob microtomografia, histomorfometria e imunohistoquímica para marcação de TRAP. Todos os tratamentos promoveram a manutenção do volume do LSM ao longo do tempo. A formação óssea ocorreu em íntimo contato com a superfície das partículas de todos os materiais. No grupo OBDc, o número de células TRAP + manteve-se estável durante todos os períodos experimentais, enquanto nos grupos OBDs e BFCp foi observado um pico em 2 semanas. Em todos os períodos experimentais, a formação óssea no grupo OBDs foi maior em comparação ao grupo OBDc e similar ao grupo BFCp. No artigo 2, defeitos ósseos cranianos bilaterais foram realizados e preenchidos com F1/HAH/OBD ou HAH/OBD e o lado contralateral com F1/HAH ou HAH em coelhos. Após 2, 4 e 8 semanas, as amostras foram coletadas para análises de microtomografia e histomorfometria. O volume total (VT) nos grupos HAH/OBD e F1/HAH/OBD foi significativamente maior que nos grupos HAH e F1/HAH. Em duas semanas, o grupo F1/HAH/OBD apresentou maior volume ósseo (VO) em comparação aos demais grupos. Nos grupos HAH/OBD e F1/HAH/OBD, o tecido ósseo cresceu na superfície e nos poros do OBD, aumentando progressivamente a maturidade e o volume ocupado. A estrutura OBD não foi alterada. Nos defeitos dos grupos HAH e F1/HAH ocorreu invasão do tegumento adjacente com formação de fina camada de tecido conjuntivo e pequena e nova formação óssea limitada às bordas durante todos os períodos. Concluindo, OBDc, OBDs e BFCp mantiveram o volume LSM, favorecendo a formação e maturação óssea, sendo alternativas seguras na técnica de LSM. E a fração F1 associada ao OBD proporcionou aumento significativo na formação óssea dos defeitos ósseos cranianos, principalmente na fase inicial do reparo, sugerindo ser uma estratégia promissora para o tratamento de defeitos craniomaxilofaciais.

Palavras-chave: Materiais Biocompatíveis. Densidade Óssea. Regeneração Óssea. Cerâmica. Coelhos. Microtomografia por Raio-X.

TABLE OF CONTENTS

1 INTRODUCTION

1 INTRODUCTION

The craniofacial region is a complex array of bone, cartilage, soft tissue, nerves and blood vessels (Ward *et al.*, 2010). The lack of sufficient bone volume in the oral and maxillofacial area, especially resulting from cancer surgeries, trauma, chronic infection, maxillary atrophy, congenital and acquired defects can compromise the normal function and aesthetics (Petrovic *et al.*, 2012; Ezirganli *et al.*, 2015; Pilipchuk *et al.*, 2015). Bone grafts or substitute biomaterials are commonly used therapeutic strategies for craniofacial reconstructions such as bone augmentation and repair of bone defects (Ezirganli *et al.*, 2015; Li *et al.*, 2015). The American Academy of Orthopedic Surgeons estimates that over 500,000 bone grafting procedures are performed in the United States each year (Greenwald *et al.*, 2001). To date, autogenous bone is considered the gold standard for bone substitutes because it presents osteogenic, osteoinductive and osteoconductive properties (Amini *et al.*, 2012; Almubarak *et al.*, 2016; Delgado-Ruiz *et al.*, 2018). However, its use involves some disadvantages, such as tendency of resorption, obtaining limited by the quantity in the intraoral area and by the increase in surgical complexity in the extraoral area, leading to the need for hospitalization, general anesthesia, increased risk of infection and increased morbidity (Ozdemir *et al.*, 2013; Esposito *et al.*, 2014; Nkenke e Neukam, 2014; Stacchi *et al.*, 2017). In the attempt to overcome these limitations, researches have proposed and tested the performance of different bone substitutes biomaterials as an alternative to autogenous bone graft (Lutz *et al.*, 2015; Stacchi *et al.*, 2017; Oh *et al.*, 2019).

Bone substitutes biomaterials are divided into allogens, xenogens and alloplastic according to their origin (Papageorgiou *et al.*, 2016). Allogenic graft is obtained from a genetically different donor, but of the same species (Jensen e Terheyden, 2009; Pilipchuk *et al.*, 2015). The bone harvested often from a cadaveric tissue is submitted to various treatments in order to decrease its antigenicity and, depending on the method of processing, to maintain its osteoinductive property (Pilipchuk *et al.*, 2015). The bone allografts is treated with antibiotics, solvents and cold-freeze-disinfection at -80ºC, and can also be lyophilized, demineralized or irradiated (Salai *et al.*, 2000; Nguyen *et al.*, 2007; Holtzclaw *et al.*, 2008). However, allografts are associated with risks of infections (as hepatitis and HIV) and immunoreactions (Amini *et al.*, 2012; Ezirganli *et al.*, 2015).

Xenogeneic grafts are derived from different species than the recipient as coral, porcine, equine or bovine sources (Jensen e Terheyden, 2009; Esposito *et al.*, 2014; Pilipchuk *et al.*, 2015). Among these, the deproteinized bovine bone (DBB) has been one of the most used, well documented and effective in reconstructive implantology (Lutz *et al.*, 2015; Fienitz *et al.*, 2017). Therefore, it has been used as a control group or substitute bone control material in several studies (Cordaro *et al.*, 2008; Jensen *et al.*, 2009; Jun *et al.*, 2014; Calasans-Maia *et al.*, 2015; Mordenfeld *et al.*, 2015). The DBB is produced with bovine cancellous bone by deproteinization process at high temperatures and chemical cleaning procedures, resulting in a mineral, inorganic bone matrix of natural, porous and non-antigenic hydroxyapatite (Accorsi-Mendonca *et al.*, 2008; Calasans-Maia *et al.*, 2009). This biomaterial presents natural bone architecture, biocompatibility, osteoconduction and slow resorption (Yildirim *et al.*, 2000; Iezzi *et al.*, 2012; Kolerman *et al.*, 2012; Mordenfeld *et al.*, 2015).

Alloplastic graft are materials synthetically produced that can present different forms: polymers, ceramics, metals and composites (Jensen e Terheyden, 2009; Matassi *et al.*, 2011; Esposito *et al.*, 2014). In this sense, calcium phosphate-based ceramics such as hydroxyapatite (HA), beta tricalcium phosphate (β-TCP) and biphasic calcium phosphate (BCP) have been used for teeth or bone replacement, bone augmentation or repair (Legeros, 2008; Pilipchuk *et al.*, 2015). These ceramics are biocompatible, bioactive and osteoconductive (Legeros, 2008; Zimmermann e Moghaddam, 2011; Yip *et al.*, 2015) and have shown osteoinduction property in animal models (Ozdemir *et al.*, 2013; Santos *et al.*, 2018). BCP is composed of a more stable (HA) and a more resorbable phase (β-TCP) and is currently used and studied with different rates of proportion between the phases, however, the optimal ratio between HA and β-TCP is not yet established (Lim, Kim, *et al.*, 2015).

All non-autogenous bone substitute materials can have different shapes and can be mixed with autogenous bone or with growth factors and cells (Klijn *et al.*, 2010). Depending on their chemical characteristics, they can be slowly resorbing or fast-resorbing over time (Esposito *et al.*, 2014). The presence of pores and concavities in the structure of the biomaterial allowing adequate space through increased surface area for diffusion of nutrients and cells, blood vessel formation, as well as for growing tissues such as bone tissue inside material (Legeros, 2008; Zimmermann e Moghaddam, 2011; Pilipchuk *et al.*, 2015; Denry e Kuhn, 2016). Pores also influence the rate of degradation, so materials with high porosity are more quickly degraded than materials with low porosity (Zimmermann e Moghaddam, 2011).

Despite advances in bone biology and bone substitutes materials studies, limitations and challenges still remain (Issa *et al.*, 2016). And, the ideal bone graft substitute for all situations does not exist, being necessary application of different types of bone substitutes or their association, according to the clinical problem (Janicki e Schmidmaier, 2011). In this sense, investigations in tissue engineering area employing scaffolds alone or in combination with growth factors, cells and/or gene delivery have shown great potential to overcome existing challenges and limits in reconstructive craniofacial surgery (Pilipchuk *et al.*, 2015).

Studies of new bone substitute materials, growth factors and stem cells largely involve the choice of rabbits as an in vivo preclinical model (Li *et al.*, 2015; Peric *et al.*, 2015). The rabbit is the most used animal in musculoskeletal research (Neyt *et al.*, 1998) and among larger animals it is the model most commonly used to bone repair evaluation (Peric *et al.*, 2015), researches on dental implants (Coelho *et al.*, 2009) and surgical strategies for craniofacial application such as maxillary sinus augmentation (MSA) due to the similarity of the rabbit's maxillary sinus to the human maxillary sinus (Muschler *et al.*, 2010) (Lim, Zhang, *et al.*, 2015). The advantages of its use include: low cost, size and ease of handling, maturation of bone tissue in a short period of time, bone density similar to that of humans, considerable amount of data previously existing in the literature and the possibility of creating multiple defects, allowing the evaluation of different treatments in the same animal and reducing risk of errors in the analyzes (Wang *et al.*, 1998; Pearce *et al.*, 2007; Coelho *et al.*, 2009; Pripatnanont *et al.*, 2009; Li *et al.*, 2015). Another advantage of this experimental model is to be able to harvest the entire region of interest, which facilitates its evaluation through various techniques and processes.

In this context, microcomputed tomography (micro-CT) has been increasingly used in preclinical studies, because it is a non-destructive technique that allows obtaining high resolution three-dimensional images, and information to assessing the microstructure of the biomaterial and bone tissue, as well as quantifying the relative and total volume of the region of interest (Chappard *et al.*, 2010; Lambert *et al.*, 2013; Peyrin *et al.*, 2014). In addition, Micro-CT correlated to conventional histological technique can bring interesting findings for the evaluation of craniofacial reconstructions such as MSA and treatment of bone defects with the use of biomaterials.

Given the above, the general aim of this study is to evaluate the potential effects of different biomaterials for craniofacial reconstructions such as large bone defects and bone

augmentation in posterior maxilla by MSA technique. Using rabbit experimental model, the microtomographical and histological evaluations were performed for the purpose of to understand the possible contribution of each treatment/material to bone formation and bone augmentation.

Specifically, the article 1 (in submission) presents the results of investigation of three bone substitutes materials of calcium phosphate-based ceramics in rabbit maxillary sinus augmentation (MSA). Thus, microtomographic, histomorphometric and immunohistochemical for TRAP labeling analyzes were performed to evaluate the bone formation and maintenance of gained bone volume throughout the experimental periods.

The article 2 (in preparation) presents findings in rabbit cranial defect repair model using the angiogenic fraction F1 obtained from latex and carried to the hyaluronic acid hydrogel (HAH) and deproteinized bovine bone (DBB) in order to verify the capacity of different treatments to stimulate bone formation and osteoconduction capacity by microtomographic and histomorphometric analyzes.

2 ARTICLES

2 ARTICLES

The articles presented in this thesis were written according to the instructions and guidelines for article submission of the corresponding journals.

- ARTICLE 1 – Maxillary sinus augmentation using different calcium phosphate-based ceramics: a microtomographic, histomorfometric and immunohistochemical study. Materials Science & Engineering C: Materials for Biological Applications. (Submitted).

- ARTICLE 2 – Microtomographic and histomorphometric evaluations of the *in vivo* effect of the F1 fraction of the latex (*Hevea brasiliensis*) carried to hyaluronic acid hydrogel adsorbed to the deproteinized bovine bone in the process of bone repair. Clinical Oral Implants Research. (In preparation).

2.1 ARTICLE 1 – Maxillary sinus augmentation using different calcium phosphate-based ceramics: a microtomographic, histomorfometric and immunohistochemical study[*].

ABSTRACT

In the present work, the effectiveness of both sinterized deproteinized bovine bone **(sDBB)** and porous biphasic calcium phosphate **(pBCP)** compared to carbonated deproteinized bovine bone **(cDBB)** on stimulating bone formation in maxillary sinus augmentation (MSA) and participation of TRAP positive and negative cells were assessed. A bilateral lifting of the maxillary sinuses (MSs) in 24 rabbits was performed using 200 mm^3 of filling material for sinus according to each experimental group. After 2, 4 and 8 weeks the samples were collected to be analyzed under microtomography, histomorphometry and immunohistochemistry for TRAP labeling. The obtained results showed that all three materials had good biocompatibility and promoted maintenance of the MSA volume over time averaging 213.2 mm^3. In all groups, the bone formation occurred in close contact with the surface of materials particles. In cDBB group the number of TRAP+ cells (4 cells/mm^2) maintaining stable during all experimental periods, while in sDBB and pBCP groups a peak was observed at 2 weeks (8 and 11 cells/mm^2, respectively). In all experimental periods, bone formation in sDBB (mean of 53.0 ± 10.10 mm^3) was higher compared to cDBB group (mean of 43.7±11.60 mm^3) and similar to pBCP group (mean of 47.5±10.40 mm^3). Although, sDBB and pBCP stimulate an initial increase of number of TRAP+ cells compared to cDBB, they maintained the MSA volume and showed good osteoconductive capacity, favoring bone formation and maturation over time. Thus, we conclude that these two biomaterials can also be a safe alternative in the MSA technique.

KEY-WORDS: Biocompatible Materials. Bone Density. Calcium Phosphate. Rabbits. Sinus Floor Augmentation. X-Ray Microtomography.

[*] Santos PS, Cestari TM, Rocha CA, Arantes RVN, Assis GF, Taga R. Maxillary sinus augmentation using different calcium phosphate-based ceramics: a microtomographic, histomorfometric and immunohistochemical study. Materials Science & Engineering C: Materials for Biological Applications. (Submitted).

1 INTRODUCTION

Currently, the placement of titanium dental implants is a common practice in the esthetic and functional rehabilitation of edentulous patients [1]. Therefore, a challenge faced in this rehabilitation is when the patient has alveolar atrophy and pneumatization of the maxillary sinus in the posterior region of maxilla, with insufficient bone volume to implant placement [2]. In this case, an effective and widely used surgical procedure before implant placement is the maxillary sinus floor augmentation (MSA) [3]. In this surgical technique, the maxillary sinus membrane is elevated, creating a space for filling with a graft material [4], promoting an increase of bone height by the deposition of new bone on the sinus bone surface, thus allowing the placement of implants in the region [5, 6].

For MSA procedure, autogenous bone is considered the "gold standard" graft among the materials used [7-9], due to its osteogenic, osteoinductive and osteoconductive properties [10]. However, its use involves several problems, such as: insufficient quantity of bone, need for hospitalization, risk of infection and morbidity in donor area, and the possibility of accelerated graft resorption at the recipient site [11, 12]. Therefore, in the last years, various new bone substitute materials are being proposed as an alternative to autogenous graft in MSA procedures.

Among non-autogenous bone graft materials, the most studied and well documented in the literature is the commercially known Bio-Oss®, a carbonated deproteinized bovine bone, which can be considered a reference between non-autogenous bone substitute materials due to its so successful use [13, 14]. This material undergoes a low heat treatment with temperatures around 300 °C [15], resulting in a carbonated apatite compound (so-called cDBB), non-antigenic and considered protein free [8, 16]. Another deproteinized bovine bone material with similarities of production to Bio-Oss® is Gen-Ox®inorg, however, it is heat-treated sintered at 1000°C and shows greater crystallinity and absence of organic waste, (so-called sDBB) [17, 18]. Both materials have excellent osteoconductive properties allowing bone deposition directly on their

surface [19-22]. Another material to be highlighted is the calcium phosphate biphasic ceramic (BCP), an alloplastic biomaterial composed of two phases: HA (hydroxyapatite) and β-TCP (beta-tricalcium phosphate) [23-25] which presents excellent bioactivity and osteoconductivity. In this latter material, the β-TCP phase is more soluble, promoting osteogenic activity and new bone deposition on its surface, while the HA phase is more stable, maintaining the repair space and the total bone volume gained on the long term [26]. BCP performance is therefore influenced by differences in the HA and β-TCP proportions, but an optimal relationship between them is not yet known in the literature [27]. The previous study of Santos *et al*. (2018) [25] showed that a new HA/β-TCP 70%:30% porous BCP (pBCP) when implanted in a heterotopic region of mice, led to punctual bone formation on its surface, indicating having osteoinductive capacity. In the same work, when implanted in rabbit mandibular critical-size defect, this pBCP exhibited high osteoconductive capacity, promoting bone formation similarly to autogenous bone graft and maintaining repaired tissue volume. These bone formations occurred initially within the pores and concavities of the pBCP particles, highlighting the importance of their presence. According to Hannink and Arts (2011); Zhang et al. (2015) and Perez and Mestres (2016) [28-30] , the concavities and pores in the material particles increase their surface area, facilitating vascularization, protein adsorption and adhesion of osteogenic progenitor cells and, consequently, ceramic dissolution and bone formation.

It is known that differences in origin, shape, size, porosity and rate of degradation of the various available bone substitute materials indicated for the MSA procedures can influence their biological behavior, tissue reactions and act directly on the rate and time of bone formation [31] and can induce cell types such as macrophages and multinucleated giant cells (MNGCs) to influence or support bone repair [15]. Thus, it is evident that the choice of bone graft material is an important step for the MSA procedure to be successful. The present study sought to evaluate the efficiency of sDBB and pBCP in the technique of MSA in rabbits compared to cDBB, using

as comparison parameter the bone formation capacity, quality of newly formed bone and maintenance of gained bone volume.

2 MATERIALS AND METHODS

2.1 Biomaterials evaluated

i. Particles (size ranging from 0.5-0.75 mm) of porous biphasic calcium phosphate **(pBCP)** GenPhos XP®, Baumer S.A., Brazil), a composite of 70% hydroxyapatite and 30% tricalcium phosphate;

ii. Particles (size ranging from 0.5-1.0 mm) of sintered and deproteinized bovine bone **(sDBB)** (Gen-Ox®inorg, Baumer S.A., Brazil);

iii. Particles (size ranging from 0.25-1.0 mm) of carbonated and deproteinized bovine bone **(cDBB)** (Bio-Oss®, Geistlich, Switzerland).

2.2 Animals

Twenty four male white New Zealand rabbits (*Oryctolagus cuniculus*) with 20 weeks of age and weighed an average of 3.7 ± 0.21kg (mean ± SDM) were used. The animals were kept in the institutional animal care facilities and were fed *ad libitum*. The experimental procedures and protocols used in this work were approved by the Animal Committee of University of São Paulo, Bauru, SP, Brazil (CEEPA Process n. 028/2013). Bilateral lifting of the maxillary sinuses (total=48 sinuses) were performed in accordance with the experimental groups: I. cDBB (6MSs/period), II. sDBB (5MSs/period) and III. pBCP (5MSs/period) (see Fig. 1A).

2.3 Surgical procedures

Preoperatively the rabbits were sedated and anesthetized by intramuscular injection of 10 mg/kg xylazine and 50 mg/kg ketamine (Ceva Saúde Animal Ltda, Brazil) based on the

specifications of "The Institutional Animal Care and Use Committee" (University of California, San Francisco). All MSA surgeries were performed by an experienced surgeon following previously described procedures [32]. After trichotomy and asepsis with iodine alcohol of the surgical area, a U-shaped incision was made in the tegument of nasal region and the soft tissues with the periosteum were reflected to expose the upper nasal bone of wall of the sinus and the nasoincisal suture line. With the use of a round bur (diameter of 4mm), two contralateral nasal bone windows were outlined and fenestrae were made by osteotomy under continuous sterile saline irrigation. Posteriorly the antral mucosa was gently pushed inside using a curette dentin and both created spaces that were filled with biomaterials according to each treatment group. The volume of filling material was standardized in 200 mm^3 per sinus. The bone windows created were covered with a resorbable membrane (GenDerm®, Baumer S.A., Brazil) to prevent fibrous connective tissue ingrowth into augmented space of the sinuses and the suture was performed with silk thread. After suturing, topical antibacterial rifamycin was applied on the surgical wound (Rifocina® Spray, Sanofi-Aventis, Brazil). The postoperative care consisted of subcutaneous injection of 0.1 mL/kg body weight of anti-inflammatory ketoprofen (Ketofen 1%®, Merial, Brazil) during 3 days and of 10mg/kg body weight of antibiotic enrofloxacin 2.5% (Flotril® 2.5%; Intervet-Schering-Plough, Brazil) during 7 days.

2.4 Sample collection and microtomography

At experimental periods of 2, 4 and 8 weeks (8 animals/period), the rabbits were killed and the samples of the maxillary sinuses were dissected and fixed in 10% phosphate-buffered formalin pH 7.2 for 7 days. Subsequently, the specimens were submitted to analysis in a microcomputed tomography (micro-CT, SkyScan 1176, Belgium). The X-ray beam source was operated at 80 kV and 300 μA. A Cu + Al filter was used and the sample was rotated 180 °

with a rotation step of 0.5°. 3D-images of each MSA were reconstructed, aligned and evaluated using the NRecon, DataViewer and CTAn softwares (package 64 bits, SkyScan, Bruker), respectively. In each MS was determined the width, height and length using the as a showed in the Figure 1B1. The total volume (TV) of MSA was obtained through of images in the coronal plane selecting manually the region of interest (Figure 1B2).

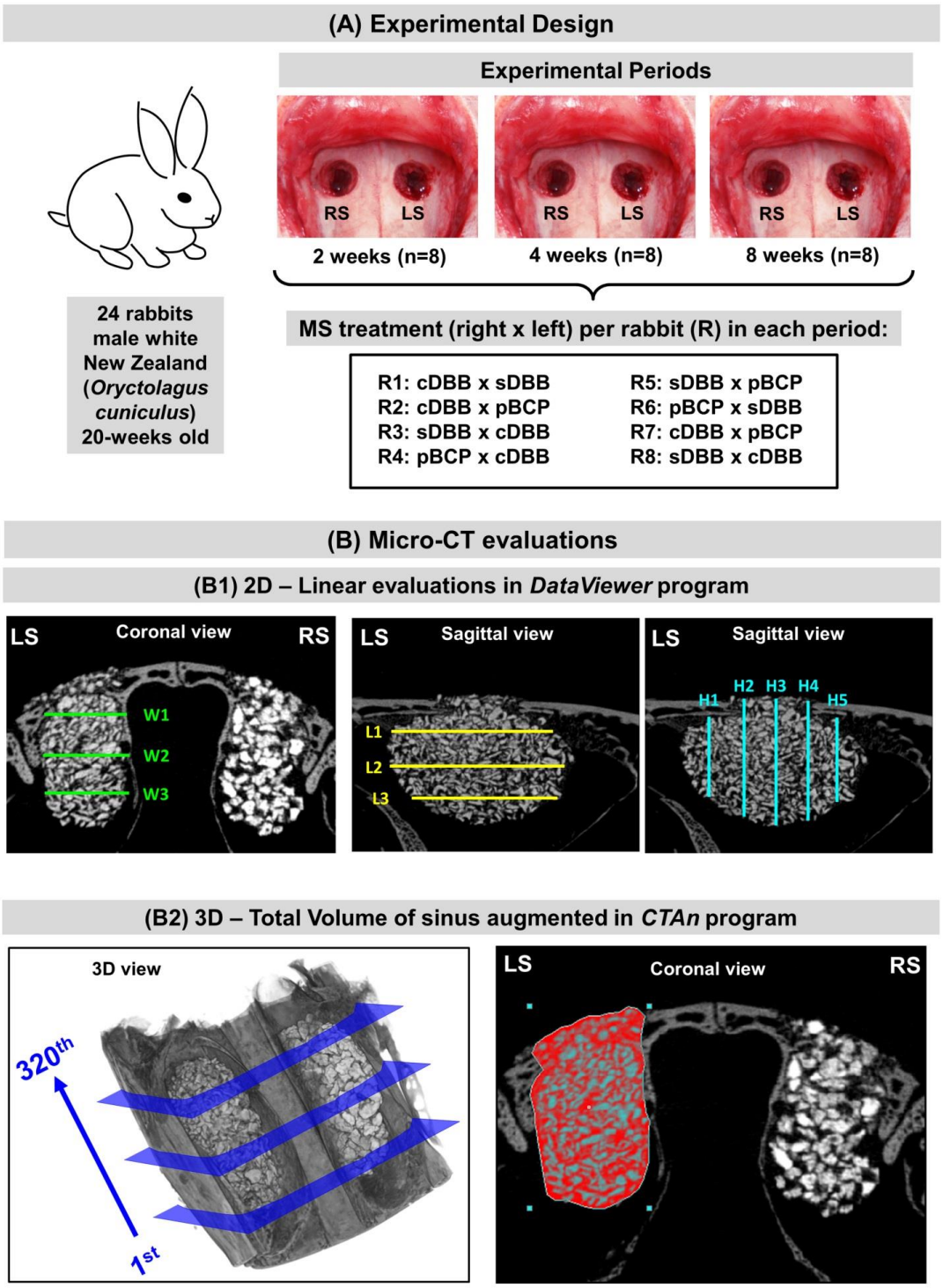

Figure 1. Material and Methods: (A) Experimental Design: 24 rabbits divided in the experimental periods of 2, 4 and 8 weeks (8 animals/period), and the treatment used in the right (RS) and left sinus (LS) per rabbit (R) in each period. **(B) Micro-CT evaluations: (B1) 2D - Linear evaluations of sinus augmented in *DataViewer* program:** *Coronal view plane* with determination of width (average of tree measurements - green line) of each maxillary sinus augmentation (MSA) individually analyzed (RS and LS) and *Sagittal views* with determination of height (average of five measurements – blue lines) and length (average of tree measurements – yellow lines) of each MSA individually analyzed (RS and LS). **(B2) 3D - Total Volume of sinus augmented in *CTAn* program:** *3D view* of bilateral sinuses augmented and adjacent native bone showing a total of 320 slices/images obtained (representative coronal slices in blue) and one 2D-*Coronal view* showing MSA area (LS) manually selected in red and individually analyzed.

2.5 Histological procedures

After microtomographic analysis, the samples were decalcified in 4.13% ethylenediaminetetraacetic acid (Titriplex III - Merck KGaA, Damstadt, Germany) plus 0.44% sodium hydroxide for approximately 11 weeks and histologically processed for embedding in polymer-enriched paraffin Histosec (Merck KGaA, Damstadt, Germany). The coronal semi-serial 5-µm thick sections were obtained and stained with Hematoxylin-Eosin (HE) [33] or submitted to immunohistochemistry technique. Histological sections were scanned into high-resolution images at 20x magnification using the Aperio ScanScope CS Slide Scanner (Aperio Technologies, Leica Biosystems Imaging, Inc., Vista, CA, USA). The digital images generated in .svs format were viewed and pictures obtained using the ImageScope software (Version 12.4, Aperio Technologies, Leica Biosystems Imaging, Inc., Vista, CA, USA).

2.6 Evaluation of the volume density and total volume of structures present in the MSA

The volume density (%) of newly formed bone, biomaterial, inflammatory infiltrate, connective tissue and bone marrow was determined in two histological sections from each sample using a Zeiss Axioskop light microscope equipped with a 20x objective lens and a Kpl 8x eyepiece containing a Zeiss II Integrating graticule of 100 points. The volume density (Vvi) or volume fraction occupied by each component in the examined specimen was determined by a standard stereological point-counting volumetry method [34]. Each elevated maxillary sinus was analysed by superimposing the graticule over 80 histological fields (40 fields/section) selected by systematic sampling [34] and noting the points pi over a determined component (i) and the total of points P over the entire examined area. The volume density (Vvi) of each component was calculated by the ratio Vvi = pi/P. The total volume or absolute volume of each component (i) present in the MSA was obtained indirectly, using the equation TVi = (TV-MSA x Vvi)/100, where TV-MSA was determined by micro-CT analysis and Vvi by histomorphometry.

2.7 Immunohistochemical procedures

For identification and quantification of multinucleated giant cell (MNGC)/osteoclast activities in MSA, the mouse monoclonal antibody against tartrate-resistant acid phosphatase (TRAP) of human origin (Santa Cruz biotechnology sc-376875) was used in the immunoperoxidase technique. The tissue paraffin-embedded sections obtained in silanized histological glass slides have undergone deparaffinization in xylene and rehydration in graded ethanol. Thereafter, the sections were pretreated with sodium citrate buffer (10mM Sodium Citrate, 0.05% Tween 20, pH 6.0) in a pressure cooker at 15 psi/121 degrees C for 5 min for antigen retrieval. During 10 min the endogenous peroxidase activity was blocked with hydrogen peroxide block (DHP-125, Spring Bioscience Corp) and serum proteins with a 7% milk solution (Molico®) under 15 min. The tissue cuts were incubated with primary antibody against TRAP diluted 1:250 in antibody diluent (ADS-125, Spring Bioscience Corporation) for 60 min in wet chamber at room temperature. The primary antibody was omitted for negative control and the bone tissue adjacent to MSA containing osteoclast was used for positive control. After washing three times in PBS for 10 min, the sections were then incubated with biotin-conjugated secondary antibody goat anti-mouse IgG (ab6788) at a concentration of 1:400 in PBS during 1 h. With application of 3-3'-diaminobenzidine solution for 5 min, the bound complexes were visualized. Finally, the sections were counterstained with Harris hematoxylin.

2.8 Determination of the numbers of TRAP-positive and TRAP-negative cells

The numbers of TRAP-positive and TRAP-negative cells were determined in 40 histological fields/section using a Zeiss Axioskop light microscope equipped with a 20x objective and a Kpl 8x eyepiece containing a Zeiss II Integrating graticule of 100 points. The number of TRAP-immunolabeled (TRAP+) and TRAP-negative (TRAP-) cells, both containing two or more

nuclei, were counted in the all MSA region. The total number of TRAP+ cells and TRAP- cells was expressed in mm^2 of tissue.

2.9 Statistical analysis

The quantitative data obtained were first submitted to the variance homogeneity test for each variable of Hartley, Cochran and Bartlett. Subsequently, the data were compared between groups and experimental periods by two-way analysis of variance (ANOVA). For the variables that showed statistical differences, the means were contrasted with each other by the Tukey test. All tests were performed using the Statistica software (Version 10.0; StatSoft Inc., Tulsa, OK, USA) and the significance level was set at 5%.

3 RESULTS

3.1 Microtomographic analysis

Microtomographic images (Figure 2A-B) and morphometric results (Table of Figure 2C) showed that width, height, length and TV of MSA were similar in all groups (p=0.784, p=0.808, p=0.279 and p=0.054, respectively), remaining stable over the evaluation period (p=0.146, p=0.761, p= 0.094 and p= 0.106, respectively), and being in mean 4.1 ± 0.40 mm, 6.4 ± 0.60 mm, 9.8 ± 1.20 mm and 213.2 ± 36.20 mm^3, respectively. The radiodensity of all materials did not change over the periods. However, sDBB and pBCP particles showed higher radiodensity than the cDBB particles and neighbouring bone tissue. The radiodensity of cDBB and of the animal's bone tissue presented really close, making impossible the differentiation and volumetric quantification of neoformed bone tissue and biomaterial. At 2 weeks, the spaces between the particles were radiolucent indicating to be filled with soft tissue. Over time the radiodensity of these areas increased due to their occupation by mineralized tissue/bone.

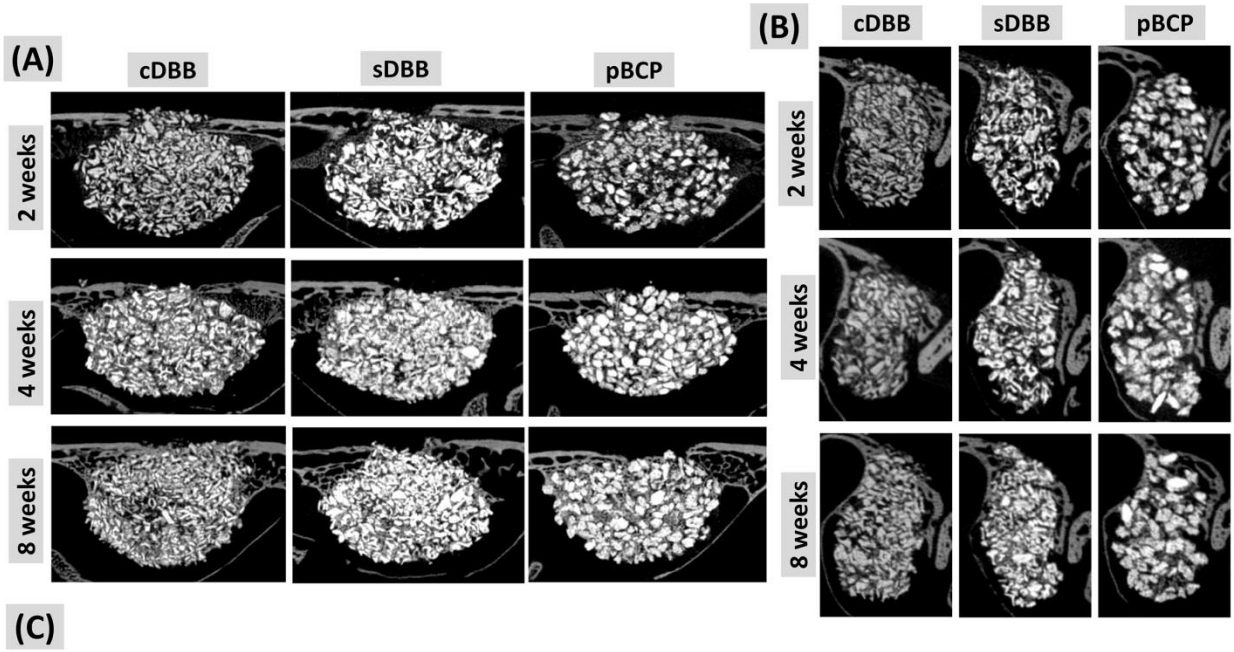

(C)

Micro-CT – Linear and volumetric measures of MSA

Measure	2 weeks			4 weeks			8 weeks		
	cDBB	sDBB	pBCP	cDBB	sDBB	pBCP	cDBB	sDBB	pBCP
Width (mm)	4.08 ± 0.45	4.17 ± 0.39	4.17 ± 0.20	3.92 ± 0.37	3.83 ± 0.44	4.06 ± 0.21	4.31 ± 0.12	4.10 ± 0.55	4.10 ± 0.25
Height (mm)	6.65 ± 0.20	6.29 ± 0.42	6.62 ± 0.22	6.21 ± 0.63	6.79 ± 0.58	6.34 ± 1.00	6.19 ± 0.90	6.33 ± 0.47	6.51 ± 1.04
Length (mm)	10.21 ± 0.28	9.90 ± 0.97	10.83 ± 0.88	9.61 ± 1.64	9.93 ± 0.64	9.01 ± 0.64	8.59 ± 1.48	10.37 ± 0.88	9.87 ± 1.49
Total Volume (mm^3)	220.05 ± 29.30	224.42 ± 23.83	242.80 ± 21.31	193.71 ± 32.27	226.10 ± 31.76	195.74 ± 37.65	181.61 ± 43.35	231.49 ± 26.33	211.69 ± 46.06

Figure 2. Micro-CT results: (A-B) Sagittal (A) and coronal (B) slices of MSA filled with cDBB, sDBB and pBCP in the each experimental period. Note that, the amount of material particles and total area of MSA were similar in all groups and periods evaluated. In the sDBB group, the particles presented radiodensity higher than in the group cDBB, whereas the size and irregular shape of the particles were similar between these groups. The particles of pBCP exhibited radiodensity similar to sDBB, however larger size and more uniform shape. At 2 weeks, note that the spaces between the particles are radiolucent, indicating absence of mineralized bone tissue. At 8 weeks, areas with radiodensity similar to the adjacent bone tissue are present in the interparticle spaces, pointing to new bone formation. **(C)** Table containing mean ± SDM (standard deviation of the mean) of linear and volumetric measures of MSA obtained for each group in each experimental period.

3.2 Histomorphometric and immunohistochemistry analysis

The photomicrographs of the histological sections of MSA stained with HE and immunolabeled for TRAP cells of each group and experimental period are showed in the Figures 3, 4 and 5. The bar graphs for total volume of structures in the MSA and number of TRAP+ and TRAP- cells are showed in the Figure 6.

In all groups, the sinusal membrane showed uniform contour with integrity during 2 (Figs. 3A1, B1 and C1), 4 (Figs. 4A1, B1 and C1) and 8 weeks (Figs. 5A1, 5B1 and 5C1) and presence of small foci of inflammation represented less than 1% or was absent. At 2 weeks the MSA was filled with large amount of biomaterial particles (mean of 95.9mm³) (Figs. 3A2-3, 3B2-3 and 3C2-3, 4A2-3, 4B2-3 and 4C2-3, 5A2-3, 5B2-3 and 5C2-3). It was verified by the statistical analysis an interaction on biomaterial TV when compared periods and materials (p=0,022). Between 2 and 8 weeks (Graph A of Fig. 6), the sinus filled with sDBB maintained the volume stable, while those filled with cDBB and pBCP decreased 34.3% and 22.4%, respectively. At 2 weeks, the immature neoformed bone tissue was present on the surface of the biomaterial particles in all groups and within pBCP concavities (Figs. 3A2-3, B2-3 and C2-3). Over time, bone growth, remodeling and maturation occurred in all treatment groups recovering more than 70% of theirs surfaces (Figs. 5A1, 5B1 and 5C1). The bone TV showed statistical differences regarding the experimental period and material; however, there was no interaction between both (Graph B of Fig. 6). Between 2 and 8 weeks, bone TV increased on average 22.9% in all groups occupying gradually the spaces between particles replacing the connective tissue. However, the bone TV increased by bone tissue accumulation over time was higher in the sDBB group (mean of 53.0 ± 10.10mm³) compared to cDBB group (mean of 43.7±11.60mm³) and similar to pBCP (mean of 47.5±10.40mm³). Between 2 and 8 weeks, the amount of marrow bone increased in all groups, so in the sDBB group it went from 2.56±3.20mm³ to 35.40±13.20mm³, in cDBB from 0.63±0.70mm³ to 28.18±9.20mm³ and in pBCP from 0.44 ± 0.50 mm³ to 39.34 ± 11.90 mm³) (see Figs. 5A2, 5B2, 5C2 and Graph C of Fig. 6).

Regarding to immunolabeling for TRAP, the positive cells were present on the surface of materials near to areas of new bone formation and also bone resorption at 2 (Figure 3A4-5, B4-5 and C4-5), 4 (Figure 4A4-5, B4-5 and C4-5) and 8 weeks (Figure 5A4-5, B4-5 and C4-

5). Two-way ANOVA showed interaction between materials and periods (p=0.000749) for number of TRAP+ cells in the surface of biomaterial. In the cDBB, the number of TRAP+ cells maintained stable until 8 weeks. At 2 weeks, a greater amount of TRAP+ cells was present in sDBB (8 cells/mm^2) and pBCP (11 cells/mm^2) surfaces compared to cDBB (4 cells/mm^2). At 4 weeks, the number of TRAP+ cells in the sDBB (4 cells/mm^2) and pBCP (5 cells/mm^2) surfaces reduced to similar level of cDBB (2 cells/mm^2) and maintaining similar at 8 weeks (Graph D of Fig. 6). In the surface of biomaterials some multinucleated giant cells were negative for TRAP and two-way ANOVA showed interaction between periods and materials (p=0.003). In cDBB, sDBB and pBCP groups, the number of TRAP- cells did not showed differences between them, being in mean 4 cells/mm^2 at 2 and 4 weeks. At 8 weeks, the number of TRAP- cells reduced 75% in cDBB and sDBB, while in pBCP it was similar to observed in 4-weeks period (Graph E of Fig. 6). On the order hand, the number of bone TRAP+ cells i.e. osteoclasts were present on bone surfaces in area of bone resorption. Two-way ANOVA showed only statistical differences regarding the experimental periods (p=0.000051). At 2 weeks, these cells were few frequent in all groups (mean of 2 cells/mm^2), decreasing at 4 weeks (mean of 1 cell/mm^2) and staying like that until 8 weeks (Graph F of Fig. 6).

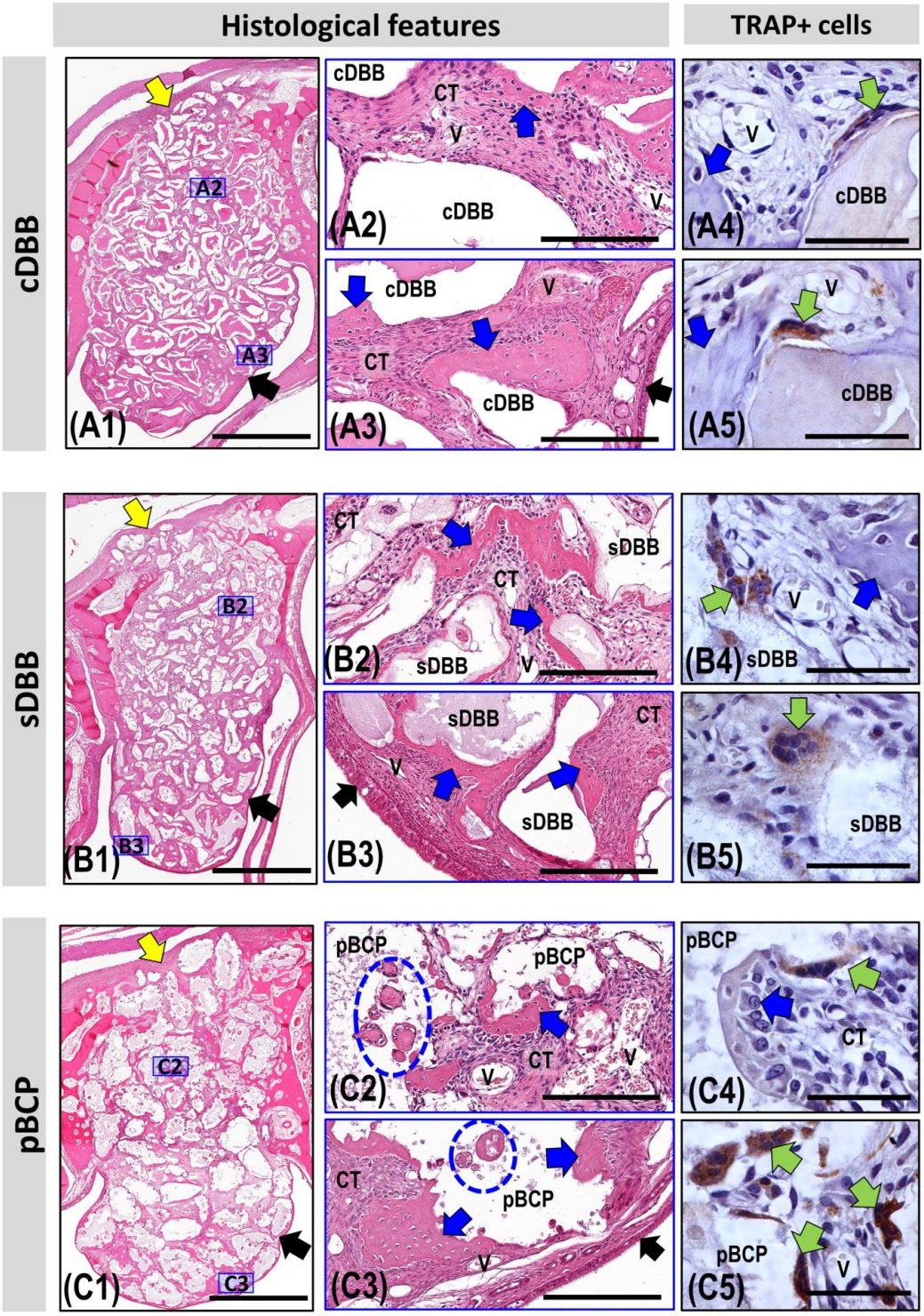

Figure 3: Histological and immunolabeling for TRAP cells images of MSA filled with cDBB (A), sDBB (B) and pBCP (C) at 2 weeks. Histological features: the panoramic views (A1, B1 and C1) show the bone window access (yellow arrows), sinusal membrane integrity (black arrows) and biomaterial particles filling the maxillary sinus cavity. HE, Bar=2mm. Details of osteotomy (A2, B2 and C2) and submucosa (A3, B3 and C3) regions show areas of immature bone formation (blue arrows) on the surface of biomaterial particles (cDBB, sDBB or pBCP), and the space of particles filled by connective tissue (CT) with many cells and blood vessels (V). Note the sinusal membrane integrity (black arrows). Observe in pBCP group (C2-3) that the bone formation occurs within the pores and concavities (area surrounded in dashed blue line). HE, Bar=200µm**. TRAP+ cells :** Higher magnification of cDBB (A4-5), sDBB (B4-5) and pBCP (C4-5) groups exhibit multinucleated cells immunolabeled for TRAP (green arrows) on the particles surface and adjacent to small vessel (V) and new bone (blue arrow). Immunoperoxidase/DAB, Bar= 40 µm.

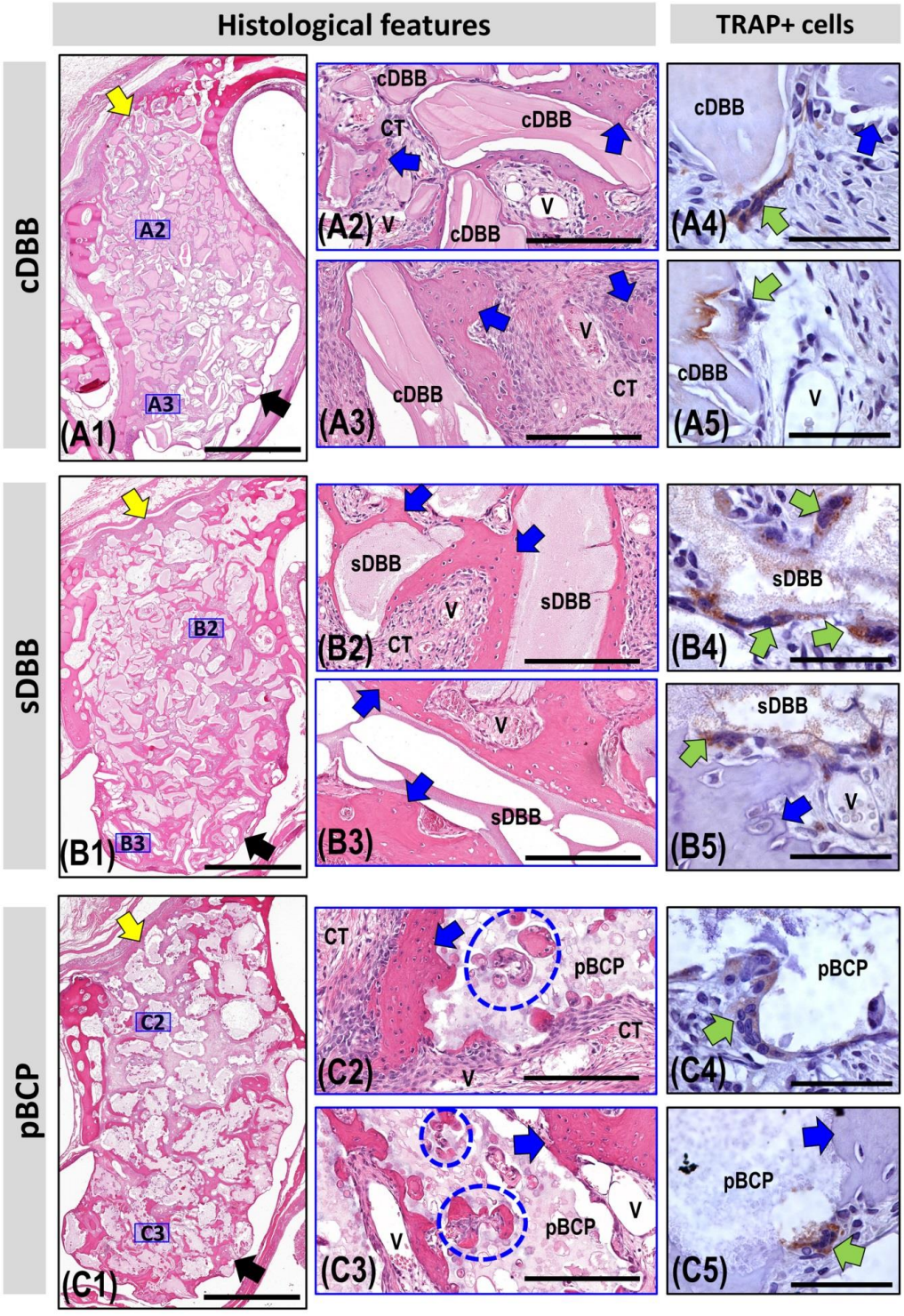

Figure 4: Histological and immunolabeling for TRAP cells images of MSA filled with cDBB (A), sDBB (B) and pBCP (C) at 4 weeks. Histological features: the panoramic views (A1, B1 and C1) show no closure of the bone window access (yellow arrows), sinusal membrane integrity (black arrows) and biomaterial particles filling large part of the maxillary sinus cavity. HE, Bar=2mm. Details of osteotomy (A2, B2 and C2) and submucosa (A3, B3 and C3) regions show a higher and more mature bone formation (blue arrows), recovering the biomaterial particles (cDBB, sDBB or pBCP), than 2 weeks period. However, the space between particles still are filled by richly cellularized and vascularized (V) connective tissue (CT). Observe in pBCP group (C2-3) the bone formation within the pores and concavities (area surrounded in dashed blue line). HE, Bar=200µm**. TRAP+ cells:** Higher magnification of cDBB (A4-5), sDBB (B4-5) and pBCP (C4-5) groups exhibit multinucleated cells immunolabeled for TRAP (green arrows) on the particles surface with variable size and format. Immunoperoxidase/DAB, Bar= 40 µm.

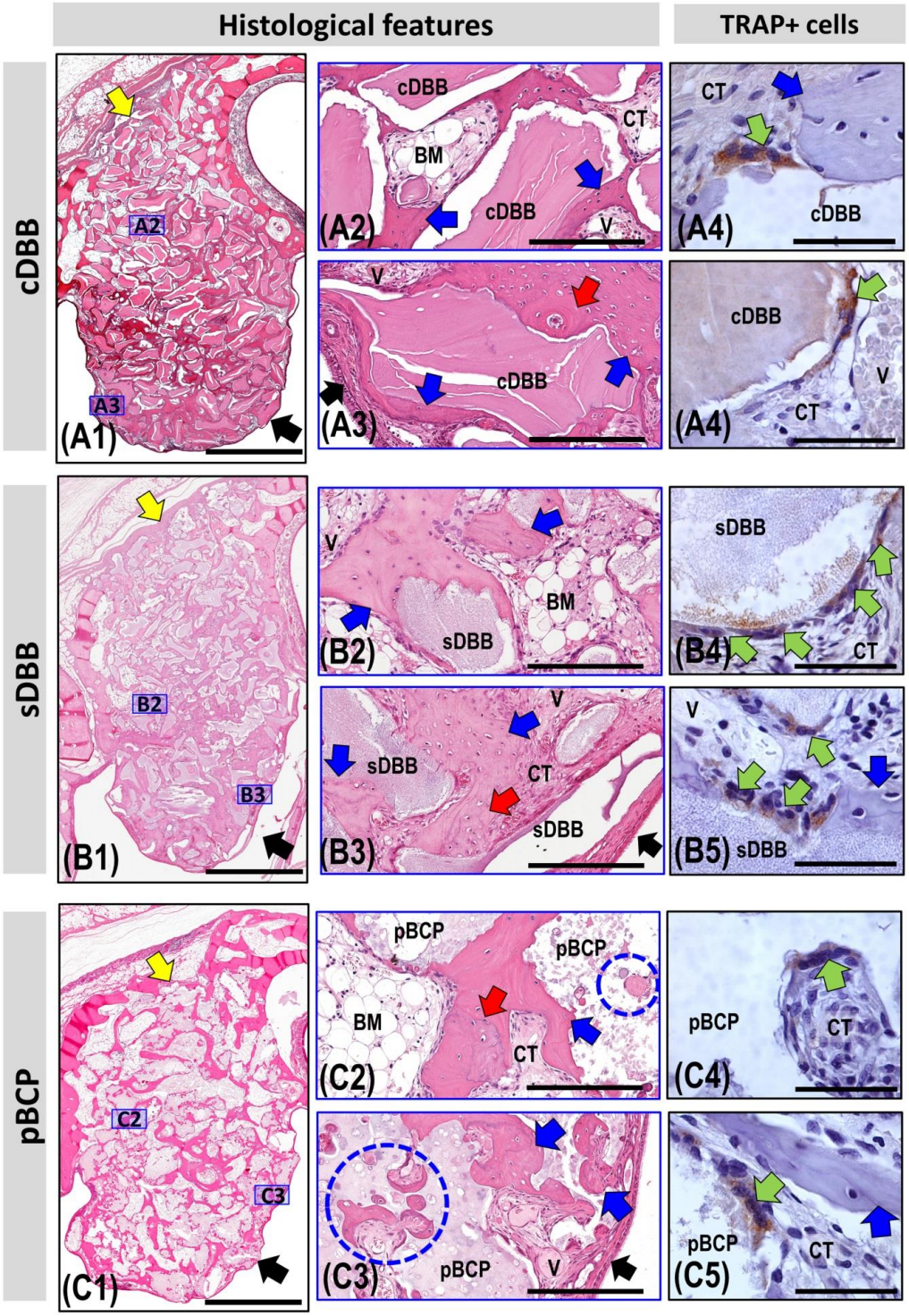

Figure 5: Histological and immunolabeling for TRAP cells images of MSA filled with cDBB (A), sDBB (B) and pBCP (C) at 8 weeks. Histological features: the panoramic views (A1, B1 and C1) show partial closing of bone window (yellow arrows), integral aspect of sinusal membrane (black arrows) and similar quantity of material particles observed in previous periods. HE, Bar=2mm. Details of osteotomy (A2, B2 and C2) and submucosa (A3, B3 and C3) regions show a large part of space between biomaterial particles (cDBB, sDBB or pBCP) occupied by mature bone (blue arrows) with lamellar structure (red arrows) and bone marrow (BM) formations. A small part of spaces between particles are filled by connective tissue (CT). Observe in pBCP group (C2-3) the bone formation within the pores and concavities (area surrounded in dashed blue line). HE, Bar=200µm**. TRAP+ cells:** Higher magnification of cDBB (A4-5), sDBB (B4-5) and pBCP (C4-5) groups exhibit multinucleated cells immunolabeled for TRAP (green arrows) on the particles surface near the bone formation (blue arrows). Immunoperoxidase/DAB, Bar= 40 µm.

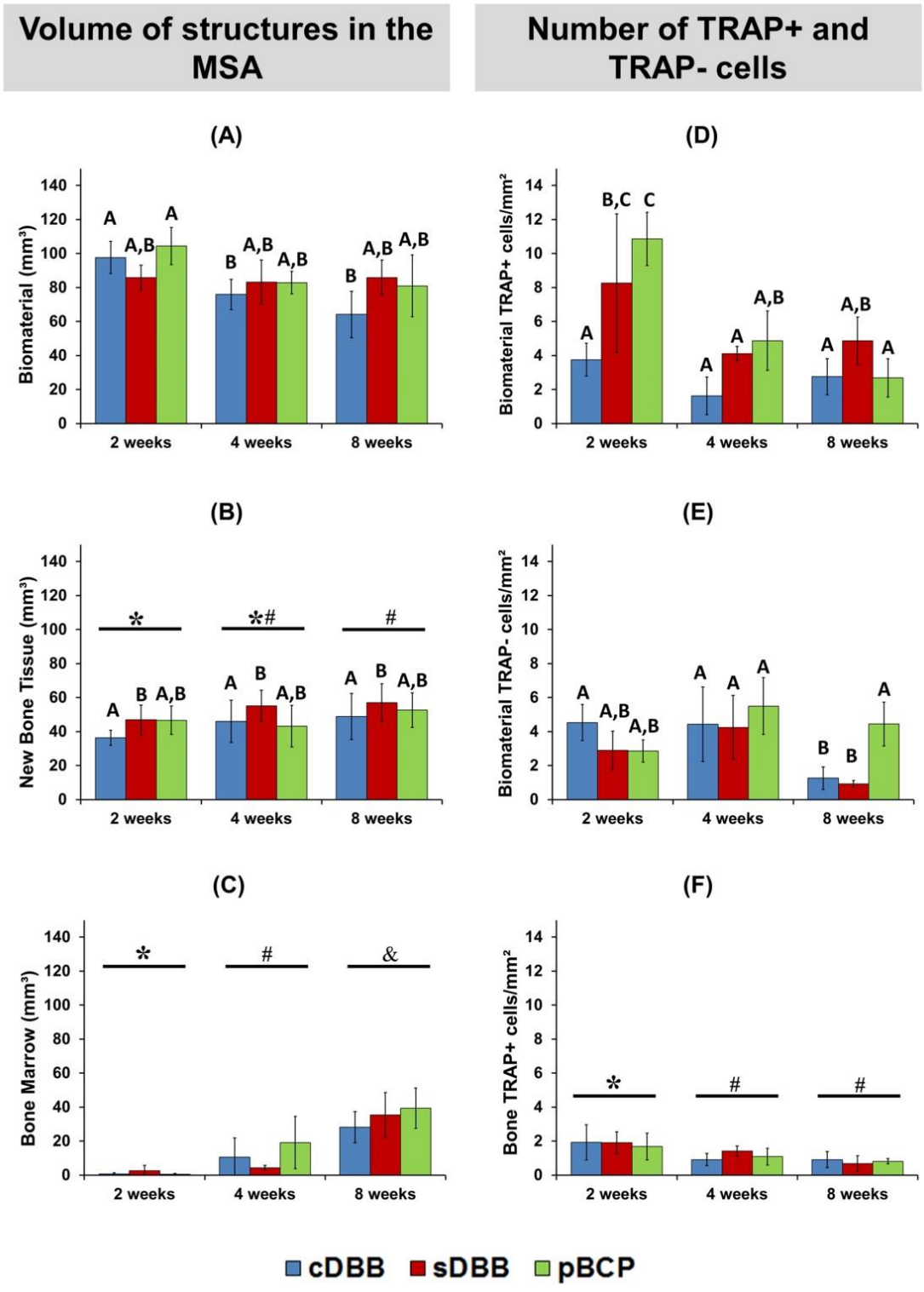

Figure 6: Histomorphometric results. Bar graphs of mean ± SDM for total volume of biomaterial (A), new bone tissue (B) and bone marrow (C) present in the MSA in each group and experimental period, as well as, number of TRAP+ cells (D) and TRAP- cells (E) in the biomaterials surface and, number of TRAP+ cells in the bone surface (F). Different letters represent differences among groups within the period, and different symbols represent differences among periods; $p < 0.05$.

4 DISCUSSION

Bone substitutes have wide applicability in the field of oral surgery and implantology, playing a key role for treating bone and peri-implant defects and maxillary sinus floor augmentation [35]. The biological performance of each bone substitutes varies during treatment period according to origin and physico-chemical properties. In the present study, different calcium phosphate-based ceramics used as bone substitutes were evaluated in rabbit's MSA experimental model by micro-CT, histomorphometric and immunohistochemistry analyzes.

The micro-CT is a non-invasive technique used for obtaining high resolution three-dimensional images [36]. This method was used to obtain the height, width, length and TV of MSAs. No statistical differences were observed among groups and experimental periods indicating first a similar MS anatomy between rabbits and second a maintenance of TV of MSAs. Other studies using the same rabbit's model also showed that the TV of MSAs after treatment with cDBB, sDBB (sintering at 700°C) and BCPs (30:70, 60:40 and 70:30 ratios) were preserved until 8 weeks [32, 37] and 24 weeks [38], while with β-TCP [32] occurred a marked decrease in the volume initially filled. In the latter case, this reduction occurred due to quick reabsorption of β-TCP and to the action of air forces in the sinuses that promoted its expansion. The data reported above indicate that the use of slow resorptive ceramics favors the maintenance of augmented sinus volume resisting sinus cavity re-expansion and providing long-term three-dimensional bone stability [39]. As noted in other studies [40, 41], we also had difficulties in quantifying new formed bone and cDBB particles using micro-CT. Both have similar radiodensities and it is difficult to distinguish between them.

As for the total volume (TV) of each component of the MSA, at 2 weeks no statistical differences were observed in TV of MSA (mean of 229 mm^3, $p>0.97$) and TV of biomaterials (mean 96.05 mm^3, $p>0.23$), between groups. Although, TV of MSA and of sDBB and pBCP

maintained stable during all experimental periods, the TV of cDBB particles reduced 34.3% at 8 weeks indicating that this materials was slowly degraded over time by via passive dissolution and cellular processes [42, 43]. In the cDBB, no sintering HA particles maintained the crystallite size of the small sized hydroxyapatite (15nm) and with carbonate in its structures, similarly to occurring in the natural mineral bone structure [44]. On the other hand, in the sDBB processed at 1000^{o}C, the HA crystallite size increase for 39nm and carbonate content is deleted [17, 44], decreasing its degradability compared to cDBB as observed here. Similarly, Riachi et al. (2012) [45] showed that DBB sintered at 1200ºC (2.7 mm particle size) had a higher crystallinity and smaller solubility in water compared to cDBB (1 mm particle size) and it was associated to small volume loss in MSA filled with sDBB (23.4 ± 3.6%) than cDBB (33.4 ± 3.1%) four years radiographic follow-up.

It is known that multinucleated giant cells (MNGCs) observed in the materials surface are formed by fusion of monocytes and macrophages and have been observed in the degradation process via phagocytosis [15, 46].The MNGCs should be considered as a "functional syncytium" of macrophages, which react similarly to their mononuclear precursors in response to material [47]. Therefore, in current work, these cells were TRAP+ and TRAP- immunolabeled, and they were not associated with inflammatory processes. At 2 weeks, the numbers of TRAP+ cells in pBCP and sDBB surfaces were similar and 220% higher than number of TRAP- cells. The number of TRAP+ cells in cDBB surface was in mean 60% smaller than observed in the other materials and similar to number of TRAP- cells. According to previous study [32], the presence of TRAP+ cells at initial period of MSA regeneration were associated with calcium phosphate ceramic (CPC) surface preparation for bone tissue deposition by osteoblasts. In our study at 2 weeks, the new bone volume (BV) in the MSA filled with sDBB was similar to pBCP (mean of 46.8mm^3) and 29% higher than cDBB (36.3mm^3). It should be noted that other studies revealed that MNGCs present on the surface of

CPC represent a source of growth factors for tissue repair, such as vascular endothelial growth factor (VEGF), an essential factor involved in the process of vascularization and bone formation at the repair site [48, 49]. In this way, MNGCs can be considered currently as a tissue repair phenotype, with release of M2 macrophage-related cytokines and growth factors [50].

In the following period, the number of TRAP+ cells in pBCP and sDBB groups decreased to equivalent values of the cDBB. Between 2 and 8 weeks, a higher increase of BV was observed in cDBB (34.5%) than in the sDBB (21.7%) and pBCP (12.9%) groups. Recent study of Hung et al. (2019) [51] in mini-pigs showed after 12 weeks similar new bone formation for both treatments, cDBB (25.6 ± 2.5%) and BCP 60:40 (24.6 ± 1.5%). However, Lambert et al. (2013) [38] had observed that the bone formation after 6 months of MSA surgeries in rabbits filled with cDBB was smaller than with BCP 60:40 and pure β-TCP. Comparatively, the rabbit bone metabolism is 3 times faster than in humans [52]. Therefore, the period between 6 and 8 weeks of rabbit bone repair when occurs the peak of bone formation and substitution of immature primary bone tissue for mature lamellar bone tissue, correspond to the period of 18 and 24 weeks in the human. Regarding clinical studies MSA biopsy after 24 weeks of treatment with DBB (sintered or carbonated) and pBCP 60:40 also showed no statistically significant differences to new formed bone [53-55].

The bone remodeling dynamic process verified by local bone tissue maturity and quantity of osteoclasts on the surface of the new bone was similar in the three treatment groups over the periods. Thus, temporally, the number of bone TRAP+ cells / osteoclasts was significantly higher at 2 weeks, reducing 0.55 times at 4 weeks and remaining stable for up to 8 weeks. These results indicated that the major bone remodeling occurred in the early periods after surgeries, coinciding with the period of greater bone formation. From 4 weeks onwards, when the most of the spaces between particles was filled with a mixture of immature and mature bone tissue plus bone marrow, there was a gradual reduction in bone formation and

resorption rate accompanied by greater bone tissue maturity and bone marrow formation until 8 weeks.

5 CONCLUSIONS

Within the limits of this study, using the MSA technique in rabbits to check the efficiency of sDBB and pBCP in comparison with cDBB in stimulating bone formation showed that all bone substitutes evaluated allowed new bone formation on its surface, indicating they have excellent osteoconductive properties, reaching at the end of 8 weeks to an adequate bone maturity. However, these materials presented different bone growth rate, due to its differences in physicochemical properties. The maxillary sinus augmented volume was kept in all experimental periods by the three evaluated materials. Based in the results, it was concluded that both sDBB and pBCP can be used clinically as alternatives to cDBB and autogenous graft in the MSA procedures.

6 DECLARATION OF INTERESTS

The authors declare that they have no known competing financial interests or personal relationships that could have appeared to influence the work reported in this paper.

7 FUNDING SOURCES

“This study was financed in part by the Coordenação de Aperfeiçoamento de Pessoal de Nível Superior – Brasil (CAPES) – Finance Code 001”

8 ACKNOWLEDGMENTS

This study was financed in part by the Coordenação de Aperfeiçoamento de Pessoal de Nível Superior – Brasil (CAPES) – Finance Code 001. We thank Danielle Santi Ceolin and Patricia de Sá Mortágua Germino for their assistance with the histotechnical processing.

9 REFERENCES

[1] S.S. Wallace, S.J. Froum, Annals of periodontology / the American Academy of Periodontology, 8 (2003) 328-343.
[2] M. Pettinicchio, T. Traini, G. Murmura, S. Caputi, M. Degidi, C. Mangano, A. Piattelli, Clinical oral investigations, 16 (2012) 45-53.
[3] M. Del Fabbro, G. Rosano, S. Taschieri, European journal of oral sciences, 116 (2008) 497-506.
[4] E. Nkenke, F. Stelzle, Clinical oral implants research, 20 Suppl 4 (2009) 124-133.
[5] M. Esposito, M.G. Grusovin, J. Rees, D. Karasoulos, P. Felice, R. Alissa, H. Worthington, P. Coulthard, European journal of oral implantology, 3 (2010) 7-26.
[6] D.Z. Lee, S.T. Chen, I.B. Darby, Clinical oral implants research, 23 (2012) 918-924.
[7] R.J. Klijn, G.J. Meijer, E.M. Bronkhorst, J.A. Jansen, Tissue engineering. Part B, Reviews, 16 (2010) 493-507.
[8] C.M. Schmitt, H. Doering, T. Schmidt, R. Lutz, F.W. Neukam, K.A. Schlegel, Clinical oral implants research, 24 (2013) 576-585.
[9] R. Lutz, S. Berger-Fink, P. Stockmann, F.W. Neukam, K.A. Schlegel, Clinical oral implants research, 26 (2015) 644-648.
[10] P. Galindo-Moreno, G. Avila, J.E. Fernandez-Barbero, F. Mesa, F. O'Valle-Ravassa, H.L. Wang, Clinical oral implants research, 19 (2008) 755-759.
[11] T. Jensen, S. Schou, P.A. Svendsen, J.L. Forman, H.J. Gundersen, H. Terheyden, P. Holmstrup, Clinical oral implants research, 23 (2012) 902-910.
[12] M. Esposito, P. Felice, H.V. Worthington, The Cochrane database of systematic reviews, 5 (2014) CD008397.
[13] S. Vandeweghe, C. Leconte, D. Ono, P.G. Coelho, R. Jimbo, Implant dentistry, 22 (2013) 339-343.
[14] M.D. Calasans-Maia, C.F. Mourao, A.T. Alves, S.C. Sartoretto, M.J. de Uzeda, J.M. Granjeiro, Clinical implant dentistry and related research, 17 Suppl 2 (2015) e586-593.
[15] Z. Peric Kacarevic, F. Kavehei, A. Houshmand, J. Franke, R. Smeets, D. Rimashevskiy, S. Wenisch, R. Schnettler, O. Jung, M. Barbeck, The International journal of artificial organs, 41 (2018) 789-800.
[16] A. Berberi, A. Samarani, N. Nader, Z. Noujeim, M. Dagher, W. Kanj, R. Mearawi, Z. Salemeh, B. Badran, BioMed research international, 2014 (2014) 320790.
[17] T. Accorsi-Mendonca, M.B. Conz, T.C. Barros, L.A. de Sena, A. Soares Gde, J.M. Granjeiro, Brazilian oral research, 22 (2008) 5-10.
[18] R. Manfro, F.S. Fonseca, M.C. Bortoluzzi, W.R. Sendyk, Journal of maxillofacial and oral surgery, 13 (2014) 464-470.
[19] M. Yildirim, H. Spiekermann, S. Biesterfeld, D. Edelhoff, Clinical oral implants research, 11 (2000) 217-229.
[20] T.M. Cestari, J.M. Granjeiro, G.F. de Assis, G.P. Garlet, R. Taga, Clinical oral implants

research, 20 (2009) 340-350.
[21] F.S. Rocha, L.M. Ramos, J.D. Batista, D. Zanetta-Barbosa, E.A. Ferro, P. Dechichi, The Journal of oral implantology, 37 (2011) 511-518.
[22] M. Ayna, Y. Acil, A. Gulses, The International journal of periodontics & restorative dentistry, 35 (2015) 541-547.
[23] G. Daculsi, O. Laboux, O. Malard, P. Weiss, Journal of materials science. Materials in medicine, 14 (2003) 195-200.
[24] R.Z. LeGeros, Chemical reviews, 108 (2008) 4742-4753.
[25] P.S. Santos, T.M. Cestari, J.B. Paulin, R. Martins, C.A. Rocha, R.V.N. Arantes, B.C. Costa, C.M. Dos Santos, G.F. Assis, R. Taga, Journal of biomedical materials research. Part B, Applied biomaterials, 106 (2018) 1546-1557.
[26] S.V. Dorozhkin, Journal of materials science. Materials in medicine, 24 (2013) 1335-1363.
[27] H.C. Lim, K.T. Kim, J.S. Lee, U.W. Jung, S.H. Choi, The International journal of oral & maxillofacial implants, 30 (2015) 1280-1286.
[28] G. Hannink, J.J. Arts, Injury, 42 Suppl 2 (2011) S22-25.
[29] J. Zhang, D. Barbieri, H. ten Hoopen, J.D. de Bruijn, C.A. van Blitterswijk, H. Yuan, Journal of biomedical materials research. Part A, 103 (2015) 1188-1199.
[30] R.A. Perez, G. Mestres, Materials science & engineering. C, Materials for biological applications, 61 (2016) 922-939.
[31] L.S. De Souza Nunes, R.V. De Oliveira, L.A. Holgado, H. Nary Filho, D.A. Ribeiro, M.A. Matsumoto, Clinical oral implants research, 21 (2010) 584-590.
[32] A.C.C. Bighetti, T.M. Cestari, P.S. Santos, R.V.N. Arantes, S. Paini, G.F. Assis, B.C. Costa, F.A. de Oliveira, C.K. Tokuhara, R.C. de Oliveira, R. Taga, Journal of biomedical materials research. Part B, Applied biomaterials, 108 (2020) 282-297.
[33] L.G. Luna, Manual of histologic staining methods of the Armed Forces Institute of Pathology, McGraw-Hill Book Company, New York, 1968, pp. 36-38.
[34] E.R. Weibel, Int Rev Cytol, 26 (1969) 235-302.
[35] G. Iezzi, A. Piattelli, A. Giuliani, C. Mangano, L. Manzon, M. Degidi, F. Iaculli, A. Scarano, A. Filippone, V. Perrotti, Current pharmaceutical biotechnology, 18 (2017) 19-32.
[36] M.S. Irie, G.D. Rabelo, R. Spin-Neto, P. Dechichi, J.S. Borges, P.B.F. Soares, Braz Dent J, 29 (2018) 227-238.
[37] H.C. Lim, M.L. Zhang, J.S. Lee, U.W. Jung, S.H. Choi, The International journal of oral & maxillofacial implants, 30 (2015) 65-72.
[38] F. Lambert, A. Leonard, G. Lecloux, S. Sourice, P. Pilet, E. Rompen, The International journal of oral & maxillofacial implants, 28 (2013) 393-402.
[39] H. Xu, Y. Shimizu, S. Asai, K. Ooya, Clinical oral implants research, 15 (2004) 126-133.
[40] R.J. Miron, L. Wei, D.D. Bosshardt, D. Buser, A. Sculean, Y. Zhang, Clinical oral investigations, 18 (2014) 471-478.
[41] Y. Zhang, D. Jing, D. Buser, A. Sculean, F. Chandad, R.J. Miron, Clinical oral investigations, 20 (2016) 589-595.
[42] J. Lu, M. Descamps, J. Dejou, G. Koubi, P. Hardouin, J. Lemaitre, J.P. Proust, Journal of biomedical materials research, 63 (2002) 408-412.
[43] Z. Sheikh, M.N. Abdallah, A.A. Hanafi, S. Misbahuddin, H. Rashid, M. Glogauer, Materials, 8 (2015) 7913-7925.
[44] F.d.P.d. Desterro, M.S. Sader, G.D.d.A. Soares, G.M. Vidigal Jr, Brazilian dental journal, 25 (2014) 282-288.
[45] F. Riachi, N. Naaman, C. Tabarani, N. Aboelsaad, M.N. Aboushelib, A. Berberi, Z. Salameh, International journal of dentistry, 2012 (2012) 737262.
[46] A.K. McNally, J.M. Anderson, Experimental and molecular pathology, 79 (2005) 126-

135.
[47] M. Barbeck, A. Motta, C. Migliaresi, R. Sader, C.J. Kirkpatrick, S. Ghanaati, Journal of biomedical materials research. Part A, 104 (2016) 413-418.
[48] S. Ghanaati, M. Barbeck, C. Orth, I. Willershausen, B.W. Thimm, C. Hoffmann, A. Rasic, R.A. Sader, R.E. Unger, F. Peters, C.J. Kirkpatrick, Acta biomaterialia, 6 (2010) 4476-4487.
[49] Y.Q. Yang, Y.Y. Tan, R. Wong, A. Wenden, L.K. Zhang, A.B. Rabie, International journal of oral science, 4 (2012) 64-68.
[50] D.P. Vasconcelos, M. Costa, I.F. Amaral, M.A. Barbosa, A.P. Aguas, J.N. Barbosa, Biomaterials, 37 (2015) 116-123.
[51] C.C. Hung, E. Fu, H.C. Chiu, H.C. Liang, Journal of periodontology, (2019).
[52] W.E. Roberts, R.K. Smith, Y. Zilberman, P.G. Mozsary, R.S. Smith, American journal of orthodontics, 86 (1984) 95-111.
[53] L. Cordaro, D.D. Bosshardt, P. Palattella, W. Rao, G. Serino, M. Chiapasco, Clinical oral implants research, 19 (2008) 796-803.
[54] T. Fienitz, O. Moses, C. Klemm, A. Happe, D. Ferrari, M. Kreppel, Z. Ormianer, M. Gal, D. Rothamel, Clinical oral investigations, 21 (2017) 787-794.
[55] J.S. Oh, Y.S. Seo, G.J. Lee, J.S. You, S.G. Kim, The International journal of oral & maxillofacial implants, 34 (2019) 233-242.

2.2 ARTICLE 2 - Microtomographic and histomorphometric evaluations of the *in vivo* effect of the F1 fraction of the latex (*Hevea brasiliensis*) carried to hyaluronic acid hydrogel adsorbed to the deproteinized bovine bone in the process of bone repair[*].

ABSTRACT

The aim of this study was to evaluate the bone formation using the angiogenic fraction F1 obtained from latex (*Hevea brasiliensis*) and hyaluronic acid hydrogel (HAH) associated with deproteinized bovine bone (DBB) during the process of rabbit cranial repair. 8-mm bilateral bone defects were performed in 30 rabbits. In F1 groups, one of the defects was filled with F1/HAH plus DBB (F1/HAH/DBB subgroup) and the other with F1/HAH (F1/HAH subgroup). In control groups, one defect was filled with HAH plus DBB (HAH/DBB subgroup) and the contralateral with HAH (HAH subgroup). After 2, 4 and 8 weeks the samples were collected to 3D and 2D analyzes (micro-CT and histomorphometry, respectively). 3D-analyzes showed that total volume (TV) in the HAH/DBB and F1/HAH/DBB groups (251.52±29.77 mm^3) were significantly higher than in the HAH and F1/HAH groups (98.13±8.37 mm^3). The DBB structure not changed, presenting 68.69±9.74% of pores and 1064.00±128.68 mm^2 of total surface area. 2D-analyzes showed that, at 2 weeks, the F1/HAH/DBB group presented a greater volume bone (BV) (41.36 ± 3.13 mm^3) with a statistically significant difference compared to HAH/DBB group (33.65 ± 5.54 mm^3) and to HAH and F1/HAH groups (8.59 ± 2.32 mm^3 and 7.36 ± 2.03 mm^3, respectively). Between 2 and 8 weeks, in HAH/DBB and F1/HAH/DBB groups the bone tissue grew on the surface and pores of biomaterial trabeculae and gradually gained maturity, occupying 21.78% of defect and DBB 31.25%. In the HAH or F1/HAH groups was observed the invasion of the adjacent tegument (occupying 73.87% of defect region), formation of a thin layer of connective tissue (12.76%) and small new bone formation limited to the defect edges (11.01%) during all periods. The present results showed that DBB block-shaped provided the vertical bone gain and the F1 associated with DBB increased significantly the bone formation in rabbit cranial defects especially at the early healing phase, suggesting it be a promising strategy for the treatment of craniomaxillofacial defects.

Keywords: Angiogenesis Inducing Agents. Biocompatible Materials. Bone Regeneration. Rabbits. X-Ray Microtomography.

[*] Santos PS, Paini S, Bighetti ACC, Cestari TM, Arantes RVN, Garlet GP, Taga R, Assis GF. Microtomographic and histomorphometric evaluations of the *in vivo* effect of the F1 fraction of the latex (*Hevea brasiliensis*) carried to hyaluronic acid hydrogel adsorbed to the deproteinized bovine bone in the process of bone repair. Clinical Oral Implants Research. (In preparation).

1 INTRODUCTION

Extensive bone defects in the cranio-maxillofacial region still represent a major clinical challenge currently, which may be due to trauma, infections, tumors or genetic disorders (Dos Santos Kotake et al., 2017; Garcia-Gareta, Coathup, & Blunn, 2015) and exceed the patient's physiological regenerative capacity (Li et al., 2015). For the treatment of these defects, several bone graft materials have been used in order to an aesthetic and functional restoration of this area, which requires rapid and predictable angiogenesis and bone neoformation (J. W. Park, Kang, & Hanawa, 2016). Among bone substitute materials, deproteinized bovine bone (DBB) has been extensively investigated, because its physical-chemical structure is comparable to that of human spongy bone and its porous nature considerably increases its surface area (Iezzi et al., 2012). The DBB is originated of bovine cancellous bone that by process of deproteinization at high temperatures and chemical cleaning procedures, results in a mineral or inorganic bone matrix of natural, porous and non-antigenic hydroxyapatite (Accorsi-Mendonca et al., 2008; Calasans-Maia, Ascoli, Novellino, Rossi, & Granjeiro, 2009), biocompatible, osteoconductive (Iezzi et al., 2012; Kolerman, Samorodnitzky-Naveh, Barnea, & Tal, 2012) and slow resorption (Mordenfeld, Lindgren, & Hallman, 2015; Yildirim, Spiekermann, Biesterfeld, & Edelhoff, 2000). Its osteoconductive property allows the newly formed bone tissue to be deposited directly on the surface of its particles or trabeculae (Ayna, Acil, & Gulses, 2015; Cestari, Granjeiro, de Assis, Garlet, & Taga, 2009; Rocha et al., 2011; Traini, Valentini, Iezzi, & Piattelli, 2007).

Another critical and highly relevant phenomenon in bone repair is angiogenesis (Hu & Olsen, 2017; L. H. Nguyen et al., 2012). The invasion of blood vessels in this region will provide oxygen, nutrients and minerals, as well as factors and cells that will participate in the repair process (Cui, Dighe, & Irvine, 2013; Kusumbe, Ramasamy, & Adams, 2014). Spontaneous vascular growth occurs in a few micrometers per day, which limits large tissue

constructions (Rouwkema, Rivron, & van Blitterswijk, 2008). Therefore, failures in revascularization can lead to loss of mechanical resistance over time, poor osseointegration and graft osteonecrosis (Almubarak et al., 2016; L. H. Nguyen et al., 2012). Hence, recent advances in the area of bone tissue engineering point to the importance of including angiogenic factors in therapy, aiming at an effective bone repair (Aravamudhan et al., 2013; L. H. Nguyen et al., 2012; Zimmermann et al., 2015). Thus, therapeutic angiogenesis has been suggested as a treatment for the repair of fractures in acute injuries, non-union defects and osteogenic distraction (Almubarak et al., 2016; Hankenson, Dishowitz, Gray, & Schenker, 2011). It is known that angiogenesis is mainly modulated by the vascular endothelial growth factor (VEGF) and osteogenesis induced mainly by bone morphogenetic proteins (BMPs) however, these two processes are also influenced by other growth factors during the repair phase, such as: fibroblast growth factor (FGF), platelet-derived growth factor (PDGF), angiopoetin (Ang), insulin growth factor (IGF) and transforming growth factor beta (TGF-β) (Almubarak et al., 2016; Cui et al., 2013). Therefore, currently preclinical research has investigated the possibility of the association of osteogenic and angiogenic factors to enhance and guide bone neoformation (Cui et al., 2013; Kempen et al., 2009; Shi & Wang, 2010; Xiao et al., 2011). In this sense, other substances of natural origin have been investigated to promote tissue regeneration. Among them is the latex of the rubber tree (*Hevea brasiliensis*) which presents high biocompatibility and stimulates neovascularization, cell adhesion and formation of the extracellular matrix (Mrue et al., 2004), important properties also in the bone repair process. It has been suggested that such latex properties are due to growth factors present in it capable of acting in human tissue, however its mechanisms are not yet fully understood (Issa et al., 2012; Penhavel, Tavares, Carneiro, & Sousa, 2016). In this context, the FrHb1 (F1) fraction extracted from the latex of the rubber tree (*Hevea brasiliensis*) has shown promising results regarding its response in tissue regeneration (Dos Santos Kotake et

al., 2017) and has important biological properties, such as increase angiogenic activity (Mendonca, Mauricio, Teixeira Lde, Lachat, & Coutinho-Netto, 2010), cell adhesion and extracellular matrix formation (Mrue et al., 2004), besides presenting potential to stimulate bone formation (Balabanian, Coutinho-Netto, Lamano-Carvalho, Lacerda, & Brentegani, 2006; Machado et al., 2015). Therefore, its use has been proposed in several clinical situations in medicine and dentistry (Arnez 2008; Mendonça, 2008).

For the therapeutic application of the F1 fraction, it is necessary to associate it with an appropriate carrier substance that has an effect on the action of this fraction of the látex. Therefore, hyaluronic acid (HAc) has been noted as an important component in the construction of new biomaterials for tissue engineering and regenerative medicine (Khan & Ahmad, 2013). It is a biodegradable and hydrophilic polymer found naturally in the extracellular matrix (Garg, Singh, Arora, & Murthy, 2012; Kogan, Soltes, Stern, & Gemeiner, 2007) and has been used in the manufacture of hydrogels to promote the release of proteins/growth factors or drugs into the target tissue (Hilborn, 2011; Hulsart-Billstrom et al., 2013; Khan & Ahmad, 2013; Son et al., 2015).

Therefore, the aim of this study was to verify if the F1 fraction obtained from the latex of *Hevea brasilienses* carried to the hyaluronic acid hydrogel (HAH) adsorbed on the surface of deproteinized bovine bone (DBB) favors angiogenesis and osteogenesis in cranial defects created experimentally in rabbits.

2 MATERIALS AND METHODS

2.1 Biomaterials evaluated:

- Hyaluronic acid hydrogel (HAH) – Polireumin® sodium hyaluronate (FIDIA Farmaceutici SpA, Abano Terme, Italy).

- F1 fraction (peak 1) of natural latex derived from *Hevea brasiliensis* – kindly provided by Department of Biochemistry and Immunology of Medicine School of Ribeirão Preto - University of São Paulo.
- Sintered and deproteinized bovine bone (DBB) block (Gen-Ox®inorg, Baumer S.A., Brazil).

2.2 Animals

Thirty male white New Zealand rabbits (*Oryctolagus cuniculus)* were used with 20 weeks of age with an average body mass of 3.9 ± 0.07kg (mean ± SDM). The animals were maintained in the institutional animal care facilities throughout the experimental period with fed *ad libitum*. All experimental procedures and protocols used in this investigation were approved by the Animal Committee of University of São Paulo, Bauru, SP, Brazil (CEEPA Process n. 027/2013 and 003/2017). Bilateral defects were performed in the region of the parietal bones. In F1 groups (n = 15), the effect of the angiogenic fraction F1 on the bone repair process carried to hyaluronic acid hydrogel (HAH) and associated or not to DBB was evaluated (F1/HAH/DBB and F1/HAH subgroups, respectively). In control groups (n = 15) bone repair was assessed using HAH associated or not to DBB (HAH/DBB and HAH subgroups, respectively). The experimental periods of each group were 2, 4 and 8 weeks (5 animals/period/subgroup).

2.3 Vehicle preparation and association with F1

The 1% HAc solution used in the control group was prepared from 7.5 mL of sterile 2% HAc in 7.5 mL of serum physiological to obtain a 15 mL solution of 1% HAc. The fraction derived from the natural latex of *Hevea brasilienses* is obtained through a chromatographic processing of the serum of the natural latex associated with liquid ammonia.

Through chromatographic processing, several bands (peaks) are observed, the first fraction being called F1. The separation of the F1 fraction is performed biochemically using chromatographic columns and the resulting solution is lyophilized and stored in a solid state (Ferreira, Mendonça, Coutinho-Netto, & Mulato, 2009). In the F1 group, a mixture of F1 and HAc was used; therefore, 15mg of F1 was dissolved in 7.5 mL of saline, obtaining 7.5 mL of 2% F1. Then, 7.5 mL of 2% HAc was mixed with 7.5 mL of 2% F1 to obtain 15 mL of 1% F1 in 1% HAc. In order to eliminate the bacterial presence of the fraction obtained, micro filtration was performed and the substances were stored in a 2 mL aliquot in sterile flasks at a temperature of 4º C until the experiment. For the F1/HAH/DBB subgroup, the flasks were opened in laminar flow and DBB block with 8 mm in diameter and 4 mm in height was deposited. Then they were transferred to a kitassato flask and vacuumed for 60 seconds in a laminar flow hood and stored again at 4ºC until their use in the surgical procedure.

2.4 Surgical procedures

The surgeries were performed with the rabbits under sedation and anesthesia obtained by intramuscular injection of 10 mg/kg xylazine and 50 mg/kg ketamine (Ceva Saúde Animal Ltda, Brazil) based on the specifications of "The Institutional Animal Care and Use Committee" (University of California, San Francisco). After trichotomy and disinfection with 1% polyvinylpyrrolidone aqueous solution in the parietal bone region, a 4 cm semilunar incision was performed, partially exposing the parietal bones. The periosteum was detached and, under constant irrigation with sterile physiological saline solution, bilateral bone defects were performed with a trephine drill (of 8 mm internal diameter) located laterally to the animal's midline and filled according to the treatment group. Posteriorly, the flaps were repositioned and sutured with silk thread. The postoperative care consisted of subcutaneous injection of 0.1 mL/kg body weight of anti-inflammatory ketoprofen (Ketofen 1%®, Merial,

Brazil) during 3 days and of 10mg/kg body weight of antibiotic enrofloxacin 2.5% (Flotril® 2.5%; Intervet-Schering-Plough, Brazil) during 7 days.

2.5 Sample collection and microtomography analysis

The skull regions were collected at 2, 4 and 8 weeks post-surgery and the samples was fixed in 10% phosphate-buffered formalin pH 7.2 for 7 days. Subsequently, the specimens were submitted to analysis in a microcomputed tomography (micro-CT, SkyScan 1176, Belgium). The X-ray beam source was operated at 80 kV and 300 µA. A Cu + Al filter was used and the sample was rotated 180 ° with a 0.5° rotation step, generating an acquisition time of 15 minutes per sample. 3D-images were reconstructed using the NRecon software, 2D-images were aligned in the coronal, transaxial, and sagittal planes using the DataViewer software. 3D-analyzes were performed using CTAn software, therefore, total volume of defect region (TV) was determined through of images in the coronal plane selecting manually the region of interest (ROI) and then, the images were binarized and the optimum threshold values (grey values) were calculated in order to quantify bone volume (BV, optimum interval of 46-121) or DBB volume (DBBV, optimum interval of 121-255). In addition, for HAH/DBB and F1/HAH/DBB groups, the following parameters were also evaluated regarding DBB block: percentage of biomaterial (DBBV/TV), percentage of pores, trabecular thickness (DBB Tb.Th), trabecular separation (DBB Tb.Sp) and DBB surface. All softwares used are of package 64 bits, SkyScan, Bruker.

2.6 Histological procedures and histomorphometric analysis

The samples were decalcified in 4.13% ethylenediaminetetraacetic acid (Titriplex III; Merck KGaA, Darmstadt, Germany) plus 0.44% sodium hydroxide. After, the specimens were embedded in polymer-enriched paraffin Histosec (Merck KGaA, Damstadt, Germany),

and latero-lateral semiserial 5-μm-thick sections were obtained and stained with hematoxylin and eosin (HE). Histological sections were scanned into high-resolution images at 40x magnification using the Aperio ScanScope CS Slide Scanner (Aperio Technologies, Leica Biosystems Imaging, Inc., Vista, CA, USA). The digital images generated in .svs format were viewed and pictures obtained using the ImageScope software (Version 12.4, Aperio Technologies, Leica Biosystems Imaging, Inc., Vista, CA, USA). The vertical thickness (T) of defect region was determined by ImageScope software in all treatment groups, at 1x magnification. The average vertical thickness of each defect region was obtained by seven measures to HAH/DBB and F1/HAH/DBB groups and two measures to HAH and F1/HAH groups. The diameter (d) was obtained by a central measure in each the defect. Therefore, the total volume (TV) for histological sections stained with HE was calculated using the following formula for the cylinder volume: $TV=A\times T$; where $A=\pi(d/2)^2$ (according to Cestari et al., 2009).

The volume density (% or Vvi) of each structure present in defect region (biomaterial, newly formed bone, connective tissue, bone marrow, inflammatory infiltrate) was determined in five coronal cross-sections of each sample applying a standard stereological point-counting volumetry method (Weibel, 1969). Using light microscope at 20x magnification and by superimposing the graticule over 250 histological fields (50 fields/section) was determined the points (pi) over a specific component (i) and the total of points (P) over the entire examined area. Therefore, the Vvi was calculated by the ratio Vvi = pi/P. Posteriorly total volume or absolute volume of each component (TVi) was calculated by formula $TVi=Vvi\times TV$ (using the TV previously obtained by ImageScope system) (Cestari et al., 2009).

2.7 Statistical analysis

First, all quantitative data were submitted to normality test (Kolmogorov-Smirnov). When this parameter was satisfied, the data were compared between groups per periods by one-way analysis of variance (ANOVA) and Bartlett's test, followed by Tukey's Multiple Comparison Test in order to compared influence of each treatment and time in the bone gain and regeneration. The data obtained regarding DBB block were also compared between two groups (HAH/DBB and F1/HAH/DBB) by Student's T-Test. When normality test was not satisfied, the non-parametric Kruskal–Wallis and the Dunn's Multiple Comparison post-hoc tests were applied. Finally, to evaluate the strength of the linear relationship between micro-CT and histomorphometric data for TV, BV and DBBV in defect region, Pearson's correlation coefficient was used. All tests were performed using the GraphPad Prism 5 software for windows (GraphPad Software Inc., San Diego, CA, USA) and the significance level was set at $p<0.05$, i.e. value taken to reject the null hypothesis.

3 RESULTS

3.1 Microtomographic analysis

Microtomographic images (Figure 1A-D) showed that in all evaluated defects, bone formation occurred in a centripetal way, i.e., from the edges towards the center of the defect. In the HAH/DBB and F1/HAH/DBB groups (Fig. 1A-B), the DBB block presented more hyperdense in relation to the parietal bone throughout the study period being easily distinguishable from the newly formed bone inside the defect facilitating binarization during 3D-analyzes. The trabecular structure of the DBB relative to its origin was maintained in all experimental periods and the new bone (isodense areas) that was formed at the edge of the defect invaded the trabecular spaces of the DBB forming a bone bridge between the original bone and the implanted material, and reaching the center of the defect until 8 weeks. In HAH

and F1/HAH groups the interior of the defects remained strongly hypodense throughout the evaluation period, indicating the absence of mineralized material in this region, and a slight formation of bone tissue at the edge of the defect, demonstrating bone non-union and non-closure of the defect in these groups. By morphometric analysis in the micro-CT (Figure 1E-F), the total volume (TV) of the graft region was of 251.52 ± 29.77 mm^3, with 51.62 ± 5.61 mm^3 of bone tissue that was easily observed on the surface of the trabeculae of the DBB block in HAH/DBB and F1/HAH/DBB groups. In contrast, in HAH and F1/HAH groups the TV and BV were from 98.13 ± 8.37 mm^3 and 15.15 ± 3.33 mm^3, respectively. By 3D-analyzes it was possible to obtain the data from the implanted DBB. The DBBV volume (DBBV) was similar and remained constant throughout the experimental period in HAH/DBB and F1/HAH/DBB groups, averaging 64.86 ± 17.15 mm^3 (ranging from 57.03 ± 13.32 mm^3 to 81.00 ± 19.02 mm^3, $p > 0.10$). The DBB structure remained intact during the eight weeks of implantation, containing 30.91 ± 9.34% of DBB block (ranging from 40.16 ± 13.63% to 25.51 ± 3.62%) and 68.69 ± 9.74% of pores (ranging from 57.44 ± 16.02% to 74.49 ± 3.62%). Characteristically, each DBB block was formed by trabeculae with a thickness (DBB Tb.Th) of 0.19 ± 0.04 mm (ranging from 0.16 ± 0.04 mm to 0.22 ± 0.06 mm), separated (DBB Tb.Sp) by 0.42 ± 0.05 mm and with an average total surface area (DBB surface) of 1064.00 ± 128.68 mm^2 (ranging from 1000.00 ± 120.80 mm^2 to 1117 ± 59.99 mm^2).

3.2 Histomorphometric analysis

The photomicrographs of the histological sections of defect region of each group and experimental period are showed in the Figures 2 and 3. The bar graphs of total volume and of each structures volume are showed in the Figure 4A. The volume of the grafted area was greater in HAH/DBB and F1/HAH/DBB groups (average of 206.08 ± 13.88 mm^3) than HAH and F1/HAH groups (average of 94.07 ± 11.88 mm^3), distancing the tegument from the defect

area in the first two groups, and with the tegument occupying a large part of the defect in groups without DBB (compare Fig 2A and 2C with Fig 2B and 2D). In defects of HAH/DBB and F1/HAH/DBB groups, 30.66% (64.11 ± 14.79 mm^3) and 31.86% (64.68 ± 5.72 mm^3) was filled by DBB block in the evaluation period, respectively (see graph A2 of Fig 4). At 2 weeks, the spaces intertrabeculae of the material was filled on average 18.15% (37.51 ± 4.33 mm^3) by new bone formation present on the surface of the DBB near the defect border, 46.34% (95.77 ± 9.36 mm^3) by connective tissue and only 1.75% filled by bone marrow (3.62 ± 1.62 mm^3) (see Fig 3A-B and graphs A3-5 of Fig 4). In that same period, the bone volume was 22.91% higher in F1/HAH/DBB (41.36 ± 3.13 mm^3) compared to HAH/DBB (33.65 ± 5.54 mm^3), and $p<0.05$. Between 2 and 8 weeks occurred an extension and progressive maturation of bone formation occupying a large part of DBB surface and growing towards the center of the defect, however presenting less thickness (compare Fig 3A with Fig 3B) and maintaining the volume of newly formed bone tissue (see graph A3 of Fig 4). Over the periods, the connective tissue volume decreased while the bone marrow volume increased, fact noticed mainly in HAH/DBB group. In the HAH and F1/HAH groups, the absence of the DBB block led to the collapse of the tegument which was occupying 73.87% (69.49 ± 7.82 mm^3) of defect region and the new bone formation was restricted to small area near the defect border (see Fig 2B and 2D and Fig 3C-D). In these defects, only 11.01% (10.36 ± 2.82 mm^3) was occupied by new bone tissue and 12.76% (12.01 ± 4.68 mm^3) by connective tissue.

3.3 Correlation between data obtained by microtomographic and histomorphometric analyzes (PEARSON correlation)

The scatter plots with trendline in Figure 4B show the results obtained in Pearson's correlation regarding the data obtained for TV, DBBV and BV in the two methods of evaluation: mCT-morphometry (3D) and histomorphometry (2D). Correlation, or correlation

coefficient, statistically represents the strength and direction of the linear relationship between two random variables (Lee Rodgers & Nicewander, 1988). For the analyzed data, it was possible to observe that Pearson correlation coefficient was strong or very strong. Thus, for TV the R^2 was 0.9594 (Graph B1 of Fig 4) and for BV it was 0.9453 (Graph B2 of Fig 4), indicating a very strong relationship between the mCT-morphometry and histomorphometry. DBBV presented R^2 equal to 0.6015 (Graph B3 of Fig 4), characterizing a strong correlation. Such results were possible due to the high density of the material evaluated (DBB block), which can be easily deferred from bone tissue by the micro-CT binarization technique and that, despite being submitted to demineralization in histotechnical processing, the histological structure is preserved and the area occupied by the material is also clearly different of the other constituents in the histological section stained by HE as can be verified in the histological photomicrographs presented in this work.

4 DISCUSSION

The capacity of bioactive molecules, growth factors and/or cells with a carrier in combination, or not, with bone substitute materials to increase bone healing and to improve vascularization has been an intensive research topic. This strategy of the tissue engineering has been contributed to solve difficult problems related to the reconstruction of large bone defects in the cranio-maxillofacial. Therefore, in this study were evaluated the effects of the angiogenic F1 fraction of the latex carried to the HAH in combination or not with DBB block in bone repair. For this purpose, the model of rabbits cranial bone defects was used in this investigation, which is well established in the literature and is commonly used to mimic orthopedic situations and to test biomaterials (Delgado-Ruiz, Calvo-Guirado, & Romanos, 2015; Li et al., 2015). In this context, 8-mm bilateral cranial bone defects are considered critical size for up to 24 weeks, according to a study conducted in our laboratory (Arantes,

2016). Based on this knowledge, and to exclude treatment bias, we chose to insert HAH in all treatment groups. Regarding the final evaluation period of this present study (8 weeks) is sufficient period to certify the capability of bone formation in the experimental groups in the rabbit, because is the time that denotes the remodeling phase of bone healing (Pripatnanont, Nuntanaranont, & Vongvatcharanon, 2009).

An important point in this study was the possibility to differentiate and quantify biomaterial and new bone formation in the three-dimensional analysis of the micro-CT, also expanding the parameters and characteristics related to the DBB (percentage of biomaterial, percentage of pores, trabecular thickness, trabecular separation and DBB surface). These evaluations occurred due to DBB used presenting high crystallinity, which is obtained in its deproteinization process at a temperature of 950 to 1000ºC (Accorsi-Mendonca *et al.*, 2008). It was also possible to observe great variability in the radiodensity and thickness of the trabeculae of the implanted DBB blocks, even if within groups. These differences probably occurred due to the location or region of the medullary bone from which the block was extracted (the closer to the cortical, the denser it will be the trabeculae; and the closer to the center of the medullary canal, the less dense it will be) (Endo et al., 2016). It is known that a 3D interconnected porous structure is a fundamental feature in a substitute bone material in order to allow cell penetration and access to metabolic requirements (Son et al., 2015). In this context, porosity and surface area of the biomaterial influence in providing of an adequate framework for bone ingrowth into biomaterial pores (T. B. Nguyen & Lee, 2014). In this study, it was possible to verify that the structure of the DBB remained constant regarding its evaluated parameters and characteristics throughout the evaluation period, without statistically significant differences, and provided mechanical support for cells and tissues to infiltrate and grow within and in close contact with its highly porous macrostructure (68.69 ± 9.74% of pores).

Histologic analysis is considered the gold standard for the evaluation bone repair and provides important data regarding cellularity as well as the morphology and dynamics of bone remodeling (Yeom, Blanchard, Kim, Zunt, & Chu, 2008); however this 2D-analysis may be insufficient for the complete assessment of bone microstructure and biomaterial. Therefore, micro-CT is a 3D-analysis and can be used to solve some limitations of the conventional technique, mapping the mineral elements of the region of interest and revealing significant changes in the evaluated mineral structure. In this context, several studies have shown a reasonable correlation between histomorphometric and micro-CT analysis (S. Y. Park et al., 2011; Romao et al., 2015; Yeom et al., 2008). Thus, the 3D-microtomographic and 2D-histomorphometric values of TV, BV and DBBV in this investigation were noted and compared in order to verify the correlation between them. Pearson's correlation analysis showed strong or very strong correlation between the values of micro-CT and histomorphometric in all parameters analyzed.

As seen in the results presented here, the defects evaluated microtomographically and histomorphometrically presented, in general, two distinct patterns of repair mainly linked to the presence or absence of the DBB block. In the defects that contained the DBB (HAH/DBB and F1/HAH/DBB groups), the bone substitute material remained stable, with constant volume, working like a scaffold and an artificial bridge between the bony edges during evaluation time, maintaining the area for the bone growth. In addition, the implantation of DBB block promoted a gain in height and the maintenance of conformation, avoiding the invasion of adjacent soft tissues until the last study period. On the other hand, defects without DBB (HAH and F1/HAH groups) did not show repair ability until the last evaluated period and were filled by a thin layer of connective tissue, small bone formations restricted to the edges and mostly by invasion of the adjacent tegument (that occupied 73.87% of the defect volume during the 8 weeks of evaluation). Other authors have already reported the importance

of implanting filling materials such as calcium phosphate ceramics in defects in the craniofacial region, because they favor bone formation and growth, as well as vertical bone gain (Cestari et al., 2009; Pripatnanont et al., 2009; Rocha et al., 2011).

The repair process does not only involve the formation of new bone tissue; however it also depends directly on neovascularization for the supply of nutrients, excretion of metabolites and transport of cells and oxygen (Diomede et al., 2020; Wernike et al., 2010). Therefore, during repair occurs a coordinated process of bone synthesis by osteoblasts and blood vessel formation by endothelial cells, so-named osteogenic-angiogenic coupling (Harris, Rutledge, Cheng, Blanchette, & Jabbarzadeh, 2013; Kanczler & Oreffo, 2008; Son et al., 2015). In this way, the osteoblasts secrete angiogenic growth factors, such as VEGF (vascular endothelial growth factor) that trigger signaling responses in the endothelial cells. In turn, osteogenic growth factors, such as BMP (bone morphogenetic protein) are released from endothelial cells and promote osteoblast differentiation and mineralization (Hu & Olsen, 2017; Sivaraj & Adams, 2016). Growth factors are bioactive molecules responsible locally by modulation of cellular activities (Devescovi, Leonardi, Ciapetti, & Cenni, 2008), among which BMP and VEGF play keys role in osteogenesis and angiogenesis processes, respectively (Hankenson, Gagne, & Shaughnessy, 2015; Kempen et al., 2009; Zeng et al., 2019). In large bone defects, especially, inadequate vascularization may jeopardize the successful repair since diffusion of oxygen and nutrients is only limited to a distance of 150–200 μm (L. H. Nguyen et al., 2012). Therefore, the development of approaches to accelerate and increase vascular growth in association with bone substitute materials is essential for effective repair (Harris et al., 2013). In this current study, the association of the angiogenic F1 fraction with HAH plus filling material DBB for bone defects treatment showed to favor greater bone volume at 2 weeks probably due to F1's capacity of neoformation of blood vessels previously described in other works with tissue repair (Andrade et al., 2011;

Balabanian et al., 2006; Dias et al., 2019; Mendonca et al., 2010; Sampaio et al., 2010) and to F1 possibly to be associated with the regulation of growth factors (Dias et al., 2019). Accordingly, (Balabanian et al., 2006) verified that the use of granules of natural latex extracted from *Hevea brasiliensis* rubber tree implanted inside of rat alveolar sockets after tooth extraction also accelerated process of bone formation during the initial period of repair. As previously mentioned a filling material such as DBB is required in the treatment of large bone defects for forming a 3D structure and maintain the mechanical stability of the region. In addition, the association of this material with angiogenic or osteogenic factors for example impedes rapid tissue diffusion and can to exert a synergistic effect on the bone formation (Gonzaga et al., 2019; Issa et al., 2016). In this way, a recent study performed by our research group showed that the use of F1 incorporated to DBB granule-shaped is favorable for bone formation in rat cranial critical size bone defects and that the concentration of the F1 protein as well as the filler material used in the combination can influence the repair process. In addition, the authors conclude that F1 can be a promising bioactive material for using in bone tissue engineering (Paini et al., 2020).

Regarding the hyaluronic acid, this biomaterial and its derivatives have been commonly used as scaffolds (Patterson et al., 2010) or as cells/growth factors carriers (Bae et al., 2014; de Santana & de Santana, 2015; J. Kim et al., 2007; S. K. Kim et al., 2016; Son et al., 2015) or, as in the case of this study under discussion, in combination with additional scaffold materials for bone tissue engineering (Hulsart-Billstrom et al., 2015; Son et al., 2015). The study of (Barreiros et al., (2014) evaluated the effects of F1 protein carried in the HAH in the treatment of crushed sciatic nerves of rats and observed that this combined use showed best results compared to HAH alone. In the present study, the use of HAH plus F1 in the treatment of cranial bone defects model showed no statistical difference in bone formation

compared to defects treated with HAH alone (occupying 10.93% and 11.10% of TV, respectively) and between 2, 4 and 8 weeks.

The molecular mechanisms associated to F1 fraction still remain poorly understood (Dias et al., 2019). Therefore, further studies employing molecular and immunoassay method may contribute to a better understanding of the targets and the pathways of action of the F1 in the bone biology field, allowing an adequate correlation and corroboration of morphological findings presented in this study.

5 CONCLUSIONS

Within the limits of this study, in the rabbit cranial bone defects, the osteoconductive material DBB block-shaped showed stable, providing the vertical bone gain and maintaining the area for the bone growth. The defects treated with HAH or HAH plus F1 results in fibrous connective tissue formation and surrounding soft tissues collapse into the defect. The F1 fraction with HAH plus DBB showed to favor significantly greater new bone formation in the early repair period. Based in this results, it we concluded that this therapy can be a suitable alternative in the treatment of bone defects in the cranio-maxillofacial region, however, further studies are needed to confirm these results.

6 DECLARATION OF INTERESTS

The authors declare that they have no known competing financial interests or personal relationships that could have appeared to influence the work reported in this paper.

7 FUNDING SOURCES

“This study was financed in part by the Coordenação de Aperfeiçoamento de Pessoal de Nível Superior – Brasil (CAPES) – Finance Code 001”

8 ACKNOWLEDGMENTS

This study was financed in part by the Coordenação de Aperfeiçoamento de Pessoal de Nível Superior – Brasil (CAPES) – Finance Code 001. We thank Danielle Santi Ceolin and Patricia de Sá Mortágua Germino for their assistance with the histotechnical processing.

9 REFERENCES

Accorsi-Mendonca, T., Conz, M. B., Barros, T. C., de Sena, L. A., Soares Gde, A., & Granjeiro, J. M. (2008). Physicochemical characterization of two deproteinized bovine xenografts. *Braz Oral Res, 22*(1), 5-10.

Almubarak, S., Nethercott, H., Freeberg, M., Beaudon, C., Jha, A., Jackson, W., . . . Bahney, C. (2016). Tissue engineering strategies for promoting vascularized bone regeneration. *Bone, 83*, 197-209. doi: 10.1016/j.bone.2015.11.011

Andrade, T. A., Iyer, A., Das, P. K., Foss, N. T., Garcia, S. B., Coutinho-Netto, J., . . . Frade, M. A. (2011). The inflammatory stimulus of a natural latex biomembrane improves healing in mice. *Braz J Med Biol Res, 44*(10), 1036-1047. doi: 10.1590/s0100-879x2011007500116

Arantes, R. V. N. (2016). *Avaliação microtomográfica e histomorfométrica do processo de reparo de defeitos ósseos em calvária de coelhos tratados com diferentes materiais de enxerto.* (Doutorado Tese), Faculdade de Odontologia de Bauru, Universidade de São Paulo.

Aravamudhan, A., Ramos, D. M., Nip, J., Subramanian, A., James, R., Harmon, M. D., . . . Kumbar, S. G. (2013). Osteoinductive small molecules: growth factor alternatives for bone tissue engineering. *Curr Pharm Des, 19*(19), 3420-3428.

Arnez, M. F. M. (2008). *Osseointegração de implantes em defeitos circunferenciais utilizando proteínas angiogênicas purificadas do látex, osso autógeno e regeneração óssea guiada. Estudo comparativo em mandíbulas de cães.* (Dissertação Mestrado), Faculdade de Odontologia de Ribeirão Preto, Universidade de São Paulo.

Ayna, M., Acil, Y., & Gulses, A. (2015). Fate of a Bovine-Derived Xenograft in Maxillary Sinus Floor Elevation After 14 Years: Histologic and Radiologic Analysis. *Int J Periodontics Restorative Dent, 35*(4), 541-547. doi: 10.11607/prd.2135

Bae, M. S., Ohe, J. Y., Lee, J. B., Heo, D. N., Byun, W., Bae, H., . . . Kwon, I. K. (2014). Photo-cured hyaluronic acid-based hydrogels containing growth and differentiation factor 5 (GDF-5) for bone tissue regeneration. *Bone, 59*, 189-198. doi: 10.1016/j.bone.2013.11.019

Balabanian, C. A., Coutinho-Netto, J., Lamano-Carvalho, T. L., Lacerda, S. A., & Brentegani, L. G. (2006). Biocompatibility of natural latex implanted into dental alveolus of rats. *J Oral Sci, 48*(4), 201-205.

Barreiros, V. C., Dias, F. J., Iyomasa, M. M., Coutinho-Netto, J., de Sousa, L. G., Fazan, V. P., . . . Issa, J. P. (2014). Morphological and morphometric analyses of crushed sciatic nerves after application of a purified protein from natural latex and hyaluronic acid hydrogel. *Growth Factors, 32*(5), 164-170. doi: 10.3109/08977194.2014.952727

Calasans-Maia, M. D., Ascoli, F. O., Novellino, A. T. A. N., Rossi, A. M., & Granjeiro, J. M. (2009). Comparative histological evaluation of tibial bone repair in rabbits treated with xenografts. *Acta Ortopédica Brasileira, 17*(6), 340-343.

Cestari, T. M., Granjeiro, J. M., de Assis, G. F., Garlet, G. P., & Taga, R. (2009). Bone repair and augmentation using block of sintered bovine-derived anorganic bone graft in cranial bone defect model. *Clin Oral Implants Res, 20*(4), 340-350. doi: 10.1111/j.1600-0501.2008.01659.x

Cui, Q., Dighe, A. S., & Irvine, J. N., Jr. (2013). Combined angiogenic and osteogenic factor delivery for bone regenerative engineering. *Curr Pharm Des, 19*(19), 3374-3383.

de Santana, R. B., & de Santana, C. M. (2015). Human intrabony defect regeneration with rhFGF-2 and hyaluronic acid - a randomized controlled clinical trial. *J Clin Periodontol, 42*(7), 658-665. doi: 10.1111/jcpe.12406

Delgado-Ruiz, R. A., Calvo-Guirado, J. L., & Romanos, G. E. (2015). Critical size defects for bone regeneration experiments in rabbit calvariae: systematic review and quality evaluation using ARRIVE guidelines. *Clin Oral Implants Res, 26*(8), 915-930. doi: 10.1111/clr.12406

Devescovi, V., Leonardi, E., Ciapetti, G., & Cenni, E. (2008). Growth factors in bone repair. *Chir Organi Mov, 92*(3), 161-168. doi: 10.1007/s12306-008-0064-1

Dias, F. J., Fazan, V. P. S., Cury, D. P., de Almeida, S. R. Y., Borie, E., Fuentes, R., . . . Watanabe, I. S. (2019). Growth factors expression and ultrastructural morphology after application of low-level laser and natural latex protein on a sciatic nerve crush-type injury. *Plos One, 14*(1), e0210211. doi: 10.1371/journal.pone.0210211

Diomede, F., Marconi, G. D., Fonticoli, L., Pizzicanella, J., Merciaro, I., Bramanti, P., . . . Trubiani, O. (2020). Functional Relationship between Osteogenesis and Angiogenesis in Tissue Regeneration. *Int J Mol Sci, 21*(9). doi: 10.3390/ijms21093242

Dos Santos Kotake, B. G., Goncalves Gonzaga, M., Coutinho-Netto, J., Ervolino, E., Tocchini de Figueiredo, F. A., & Mardegan Issa, J. P. (2017). Bone repair of critical sized defects in Wistar rats treated with autogenic, allogenic or xenogenic bone grafts alone or in combination with natural latex fraction F1. *Biomed Mater*. doi: 10.1088/1748-605X/aa9504

Endo, K., Yamada, S., Todoh, M., Takahata, M., Iwasaki, N., & Tadano, S. (2016). Structural strength of cancellous specimens from bovine femur under cyclic compression. *PeerJ, 4*, e1562. doi: 10.7717/peerj.1562

Ferreira, M., Mendonça, R. J., Coutinho-Netto, J., & Mulato, M. (2009). Angiogenic properties of natural rubber latex biomembranes and the serum fraction of Hevea brasiliensis. *Brazilian Journal of Physics, 39*(3), 564-569.

Garcia-Gareta, E., Coathup, M. J., & Blunn, G. W. (2015). Osteoinduction of bone grafting materials for bone repair and regeneration. *Bone, 81*, 112-121. doi: 10.1016/j.bone.2015.07.007

Garg, T., Singh, O., Arora, S., & Murthy, R. (2012). Scaffold: a novel carrier for cell and drug delivery. *Crit Rev Ther Drug Carrier Syst, 29*(1), 1-63.

Gonzaga, M. G., Dos Santos Kotake, B. G., de Figueiredo, F. A. T., Feldman, S., Ervolino, E., Dos Santos, M. C. G., & Issa, J. P. M. (2019). Effectiveness of rhBMP-2 association to autogenous, allogeneic, and heterologous bone grafts. *Microsc Res Tech, 82*(6), 689-695. doi: 10.1002/jemt.23215

Hankenson, K. D., Dishowitz, M., Gray, C., & Schenker, M. (2011). Angiogenesis in bone regeneration. *Injury, 42*(6), 556-561. doi: 10.1016/j.injury.2011.03.035

Hankenson, K. D., Gagne, K., & Shaughnessy, M. (2015). Extracellular signaling molecules to promote fracture healing and bone regeneration. *Adv Drug Deliv Rev, 94*, 3-12. doi: 10.1016/j.addr.2015.09.008

Harris, G. M., Rutledge, K., Cheng, Q., Blanchette, J., & Jabbarzadeh, E. (2013). Strategies to direct angiogenesis within scaffolds for bone tissue engineering. *Curr Pharm Des, 19*(19), 3456-3465.

Hilborn, J. (2011). In vivo injectable gels for tissue repair. *Wiley Interdiscip Rev Nanomed Nanobiotechnol, 3*(6), 589-606. doi: 10.1002/wnan.91

Hu, K., & Olsen, B. R. (2017). Vascular endothelial growth factor control mechanisms in skeletal growth and repair. *Dev Dyn, 246*(4), 227-234. doi: 10.1002/dvdy.24463

Hulsart-Billstrom, G., Bergman, K., Andersson, B., Hilborn, J., Larsson, S., & Jonsson, K. B. (2015). A uni-cortical femoral defect model in the rat: evaluation using injectable hyaluronan hydrogel as a carrier for bone morphogenetic protein-2. *J Tissue Eng Regen Med, 9*(7), 799-807. doi: 10.1002/term.1655

Hulsart-Billstrom, G., Piskounova, S., Gedda, L., Andersson, B. M., Bergman, K., Hilborn, J., . . . Bowden, T. (2013). Morphological differences in BMP-2-induced ectopic bone between solid and crushed hyaluronan hydrogel templates. *J Mater Sci Mater Med, 24*(5), 1201-1209. doi: 10.1007/s10856-013-4877-6

Iezzi, G., Degidi, M., Piattelli, A., Mangano, C., Scarano, A., Shibli, J. A., & Perrotti, V. (2012). Comparative histological results of different biomaterials used in sinus augmentation procedures: a human study at 6 months. *Clin Oral Implants Res, 23*(12), 1369-1376. doi: 10.1111/j.1600-0501.2011.02308.x

Issa, J. P., Defino, H. L., Sebald, W., Coutinho-Netto, J., Iyomasa, M. M., Shimano, A. C., . . . Pitol, D. L. (2012). Biological evaluation of the bone healing process after application of two potentially osteogenic proteins: an animal experimental model. *Gerodontology, 29*(4), 258-264. doi: 10.1111/j.1741-2358.2011.00526.x

Issa, J. P., Gonzaga, M., Kotake, B. G., de Lucia, C., Ervolino, E., & Iyomasa, M. (2016). Bone repair of critical size defects treated with autogenic, allogenic, or xenogenic bone grafts alone or in combination with rhBMP-2. *Clin Oral Implants Res, 27*(5), 558-566. doi: 10.1111/clr.12622

Kanczler, J. M., & Oreffo, R. O. (2008). Osteogenesis and angiogenesis: the potential for engineering bone. *Eur Cell Mater, 15*, 100-114. doi: 10.22203/ecm.v015a08

Kempen, D. H., Lu, L., Heijink, A., Hefferan, T. E., Creemers, L. B., Maran, A., . . . Dhert, W. J. (2009). Effect of local sequential VEGF and BMP-2 delivery on ectopic and orthotopic bone regeneration. *Biomaterials, 30*(14), 2816-2825. doi: 10.1016/j.biomaterials.2009.01.031

Khan, F., & Ahmad, S. R. (2013). Polysaccharides and their derivatives for versatile tissue engineering application. *Macromol Biosci, 13*(4), 395-421. doi: 10.1002/mabi.201200409

Kim, J., Kim, I. S., Cho, T. H., Lee, K. B., Hwang, S. J., Tae, G., . . . Sun, K. (2007). Bone regeneration using hyaluronic acid-based hydrogel with bone morphogenic protein-2 and human mesenchymal stem cells. *Biomaterials, 28*(10), 1830-1837. doi: 10.1016/j.biomaterials.2006.11.050

Kim, S. K., Cho, T. H., Han, J. J., Kim, I. S., Park, Y., & Hwang, S. J. (2016). Comparative study of BMP-2 alone and combined with VEGF carried by hydrogel for maxillary alveolar bone regeneration. *Tissue Eng Regen Med, 13*(2), 171-181. doi: 10.1007/s13770-015-0046-y

Kogan, G., Soltes, L., Stern, R., & Gemeiner, P. (2007). Hyaluronic acid: a natural biopolymer with a broad range of biomedical and industrial applications. *Biotechnol Lett, 29*(1), 17-25. doi: 10.1007/s10529-006-9219-z

Kolerman, R., Samorodnitzky-Naveh, G. R., Barnea, E., & Tal, H. (2012). Histomorphometric analysis of newly formed bone after bilateral maxillary sinus augmentation using two different osteoconductive materials and internal collagen membrane. *Int J Periodontics Restorative Dent, 32*(1), e21-28.

Kusumbe, A. P., Ramasamy, S. K., & Adams, R. H. (2014). Coupling of angiogenesis and osteogenesis by a specific vessel subtype in bone. *Nature, 507*(7492), 323-328. doi: 10.1038/nature13145

Lee Rodgers, J., & Nicewander, W. A. (1988). Thirteen Ways to Look at the Correlation Coefficient. *The American Statistician, 42*(1), 59-66. doi: 10.1080/00031305.1988.10475524

Li, Y., Chen, S.-K., Li, L., Qin, L., Wang, X.-L., & Lai, Y.-X. (2015). Bone defect animal models for testing efficacy of bone substitute biomaterials. *Journal of Orthopaedic Translation, 3*(3), 95-104. doi: http://dx.doi.org/10.1016/j.jot.2015.05.002

Machado, E. G., Issa, J. P., Figueiredo, F. A., Santos, G. R., Galdeano, E. A., Alves, M. C., . . . Cunha, M. R. (2015). A new heterologous fibrin sealant as scaffold to recombinant human bone morphogenetic protein-2 (rhBMP-2) and natural latex proteins for the repair of tibial bone defects. *Acta Histochem, 117*(3), 288-296. doi: 10.1016/j.acthis.2015.03.006

Mendonça, R. (2008). *Purificação e caracterização de uma proteína angiogênica, indutora de fibroplasia e cicatrizante presente no látex natural da seringueira Hevea brasiliensis.* (Doutorado Tese), Faculdade de Medicina de Ribeirão Preto, Universidade de São Paulo.

Mendonca, R. J., Mauricio, V. B., Teixeira Lde, B., Lachat, J. J., & Coutinho-Netto, J. (2010). Increased vascular permeability, angiogenesis and wound healing induced by the serum of natural latex of the rubber tree Hevea brasiliensis. *Phytother Res, 24*(5), 764-768. doi: 10.1002/ptr.3043

Mordenfeld, A., Lindgren, C., & Hallman, M. (2015). Sinus Floor Augmentation Using Straumann(R) BoneCeramic and Bio-Oss(R) in a Split Mouth Design and Later Placement of Implants: A 5-Year Report from a Longitudinal Study. *Clin Implant Dent Relat Res*. doi: 10.1111/cid.12374

Mrue, F., Netto, J. C., Ceneviva, R., Lachat, J. J., Thomazini, J. A., & Tambelini, H. (2004). Evaluation of the biocompatibility of a new biomembrane. *Materials research, 7*(2), 277-283.

Nguyen, L. H., Annabi, N., Nikkhah, M., Bae, H., Binan, L., Park, S., . . . Khademhosseini, A. (2012). Vascularized bone tissue engineering: approaches for potential improvement. *Tissue Eng Part B Rev, 18*(5), 363-382. doi: 10.1089/ten.TEB.2012.0012

Nguyen, T. B., & Lee, B. T. (2014). A combination of biphasic calcium phosphate scaffold with hyaluronic acid-gelatin hydrogel as a new tool for bone regeneration. *Tissue Eng Part A, 20*(13-14), 1993-2004. doi: 10.1089/ten.TEA.2013.0352

Paini, S., Bighetti, A. C. C., Cestari, T. M., Arantes, R. V. N., Santos, P. S., Mena-Laura, E. E., ... Assis, G. F. (2020). Concentration-dependent effects of latex F1-protein fraction incorporated into deproteinized bovine bone and biphasic calcium phosphate on the repair of critical-size bone defects. *J Biomed Mater Res B Appl Biomater*. doi: 10.1002/jbm.b.34664. (In press)

Park, J. W., Kang, D. G., & Hanawa, T. (2016). New bone formation induced by surface strontium-modified ceramic bone graft substitute. *Oral Dis, 22*(1), 53-61. doi: 10.1111/odi.12381

Park, S. Y., Kim, K. H., Koo, K. T., Lee, K. W., Lee, Y. M., Chung, C. P., & Seol, Y. J. (2011). The evaluation of the correlation between histomorphometric analysis and micro-computed tomography analysis in AdBMP-2 induced bone regeneration in rat calvarial defects. *J Periodontal Implant Sci, 41*(5), 218-226. doi: 10.5051/jpis.2011.41.5.218

Patterson, J., Siew, R., Herring, S. W., Lin, A. S., Guldberg, R., & Stayton, P. S. (2010). Hyaluronic acid hydrogels with controlled degradation properties for oriented bone regeneration. *Biomaterials, 31*(26), 6772-6781. doi: 10.1016/j.biomaterials.2010.05.047

Penhavel, M. V., Tavares, V. H., Carneiro, F. P., & Sousa, J. B. (2016). Effect of Hevea brasiliensis latex sap gel on healing of acute skin wounds induced on the back of rats. *Rev Col Bras Cir, 43*(1), 48-53. doi: 10.1590/0100-69912016001010

Pripatnanont, P., Nuntanaranont, T., & Vongvatcharanon, S. (2009). Proportion of deproteinized bovine bone and autogenous bone affects bone formation in the treatment of calvarial defects in rabbits. *Int J Oral Maxillofac Surg, 38*(4), 356-362. doi: 10.1016/j.ijom.2009.02.015

Rocha, F. S., Ramos, L. M., Batista, J. D., Zanetta-Barbosa, D., Ferro, E. A., & Dechichi, P. (2011). Bovine anorganic bone graft associated with platelet-rich plasma: histologic analysis in rabbit calvaria. *J Oral Implantol, 37*(5), 511-518. doi: 10.1563/AAID-JOI-D-09-00091.1

Romao, M. M., Marques, M. M., Cortes, A. R., Horliana, A. C., Moreira, M. S., & Lascala, C. A. (2015). Micro-computed tomography and histomorphometric analysis of human alveolar bone repair induced by laser phototherapy: a pilot study. *Int J Oral Maxillofac Surg, 44*(12), 1521-1528. doi: 10.1016/j.ijom.2015.08.989

Rouwkema, J., Rivron, N. C., & van Blitterswijk, C. A. (2008). Vascularization in tissue engineering. *Trends Biotechnol, 26*(8), 434-441. doi: 10.1016/j.tibtech.2008.04.009

Sampaio, R. B., Mendonca, R. J., Simioni, A. R., Costa, R. A., Siqueira, R. C., Correa, V. M., . . . Jorge, R. (2010). Rabbit retinal neovascularization induced by latex angiogenic-derived fraction: an experimental model. *Curr Eye Res, 35*(1), 56-62. doi: 10.3109/02713680903374216

Shi, Z. B., & Wang, K. Z. (2010). Effects of recombinant adeno-associated viral vectors on angiopoiesis and osteogenesis in cultured rabbit bone marrow stem cells via co-expressing hVEGF and hBMP genes: a preliminary study in vitro. *Tissue Cell, 42*(5), 314-321. doi: 10.1016/j.tice.2010.07.007

Sivaraj, K. K., & Adams, R. H. (2016). Blood vessel formation and function in bone. *Development, 143*(15), 2706-2715. doi: 10.1242/dev.136861

Son, S. R., Sarkar, S. K., Nguyen-Thuy, B. L., Padalhin, A. R., Kim, B. R., Jung, H. I., & Lee, B. T. (2015). Platelet-rich plasma encapsulation in hyaluronic acid/gelatin-BCP hydrogel for growth factor delivery in BCP sponge scaffold for bone regeneration. *J Biomater Appl, 29*(7), 988-1002. doi: 10.1177/0885328214551373

Traini, T., Valentini, P., Iezzi, G., & Piattelli, A. (2007). A histologic and histomorphometric evaluation of anorganic bovine bone retrieved 9 years after a sinus augmentation procedure. *J Periodontol, 78*(5), 955-961. doi: 10.1902/jop.2007.060308

Weibel, E. R. (1969). Stereological principles for morphometry in electron microscopy cytology. *Int Rev Cytol, 26*, 235-302.

Wernike, E., Montjovent, M. O., Liu, Y., Wismeijer, D., Hunziker, E. B., Siebenrock, K. A., . . . Klenke, F. M. (2010). Vegf Incorporated into Calcium Phosphate Ceramics Promotes Vascularisation and Bone Formation in Vivo. *Eur Cell Mater, 19*, 30-40.

Xiao, C., Zhou, H., Liu, G., Zhang, P., Fu, Y., Gu, P., . . . Fan, X. (2011). Bone marrow stromal cells with a combined expression of BMP-2 and VEGF-165 enhanced bone regeneration. *Biomed Mater, 6*(1), 015013. doi: 10.1088/1748-6041/6/1/015013

Yeom, H., Blanchard, S., Kim, S., Zunt, S., & Chu, T. M. (2008). Correlation between micro-computed tomography and histomorphometry for assessment of new bone formation in a calvarial experimental model. *J Craniofac Surg, 19*(2), 446-452. doi: 10.1097/SCS.0b013e318052fe05

Yildirim, M., Spiekermann, H., Biesterfeld, S., & Edelhoff, D. (2000). Maxillary sinus augmentation using xenogenic bone substitute material Bio-Oss in combination with venous blood. A histologic and histomorphometric study in humans. *Clin Oral Implants Res, 11*(3), 217-229.

Zeng, J. H., Qiu, P., Xiong, L., Liu, S. W., Ding, L. H., Xiong, S. L., . . . Zhang, T. (2019). Bone repair scaffold coated with bone morphogenetic protein-2 for bone regeneration in murine calvarial defect model: Systematic review and quality evaluation. *Int J Artif Organs, 42*(7), 325-337. doi: 10.1177/0391398819834944

Zimmermann, A., Pelegrine, A. A., Peruzzo, D., Martinez, E. F., de Mello e Oliveira, R., Aloise, A. C., & Ferreira, L. M. (2015). Adipose mesenchymal stem cells associated with xenograft in a guided bone regeneration model: a histomorphometric study in rabbit calvaria. *Int J Oral Maxillofac Implants, 30*(6), 1415-1422. doi: 10.11607/jomi.4164

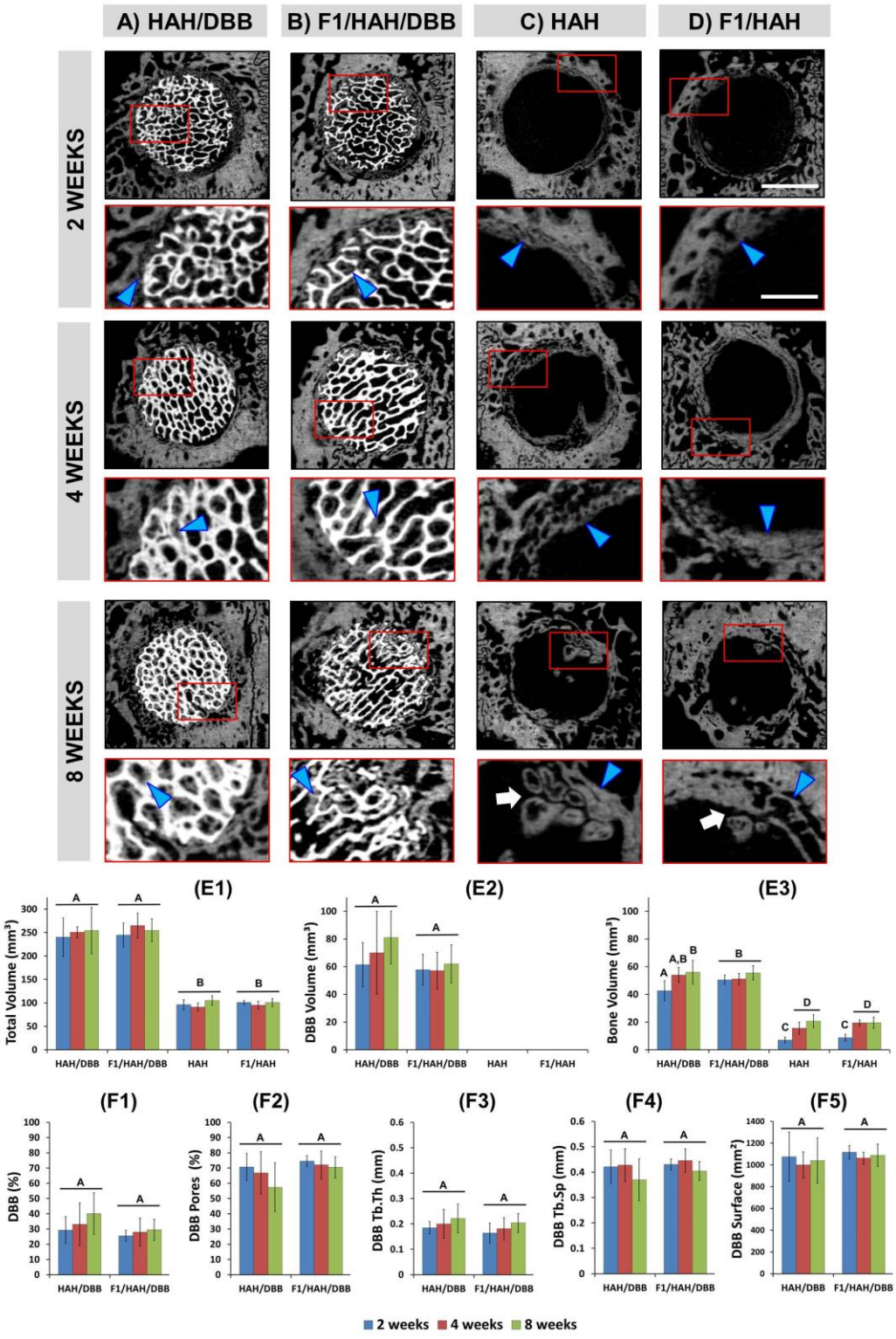

Figure 1: Micro-CT transaxial slice of calvaria defects in different experimental groups and periods and micro-CT 3D-analyzes. A and B) Defects show hyperdense DBB porous block and isodense areas of the newly formed bone (blue arrowheads) into the DBB pores near to defect edge with progressive increase in its density over time. **C and D)** Defect shows large hypodense area referring to the soft tissue and small formation of new bone (blue arrowheads) at the defect edge of the defect without bone union (white arrows). Bars=4mm and 1.5 mm. **E1-3)** Bar graphs of mean ± SDM for Total Volume of Defect Region (TV), DBB Volume (DBBV) and Bone Volume (BV) analyzed on the micro-CT and **F1-5)** Bar graphs of mean ± SDM for DBB percentage, DBB pores percentage, DBB trabecular thickness (DBB Tb.Th), DBB trabecular separation (DBB Tb.Sp) and DBB surface. Different letters represent differences among groups and periods ($p < 0.05$).

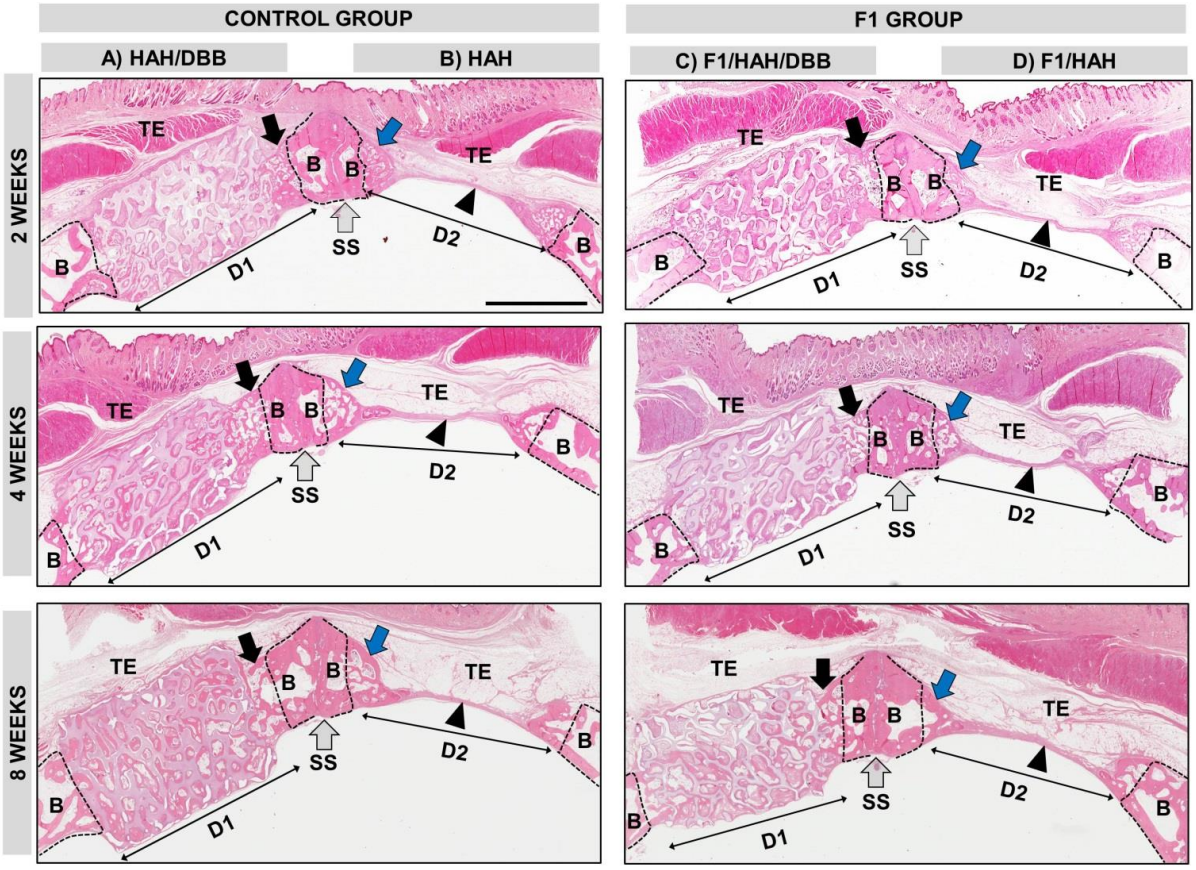

Figure 2 – Panoramic histological view of bilateral defects Control Groups and F1 Groups at 2, 4 and 8 weeks. **A and C)** Defects filled with HAH/DBB (D1 in A) and F1/HAH/DBB (D1 in C) shows the material block occupying all defect space and maintaining the tegument in the original position. Note the bone formation (black arrows) at defect border (B), invading the pores of the biomaterial arranged in different directions. **B and D)** In the contralateral side defect filled with HAH (D2 in B) and F1/HAH (D2 in D) shows small bone formation (blue arrows) in the border (B), fibrous connective tissue (black arrowheads) and invagination of the tegument (TE). SS= Sagital suture. HE, bar = 4mm.

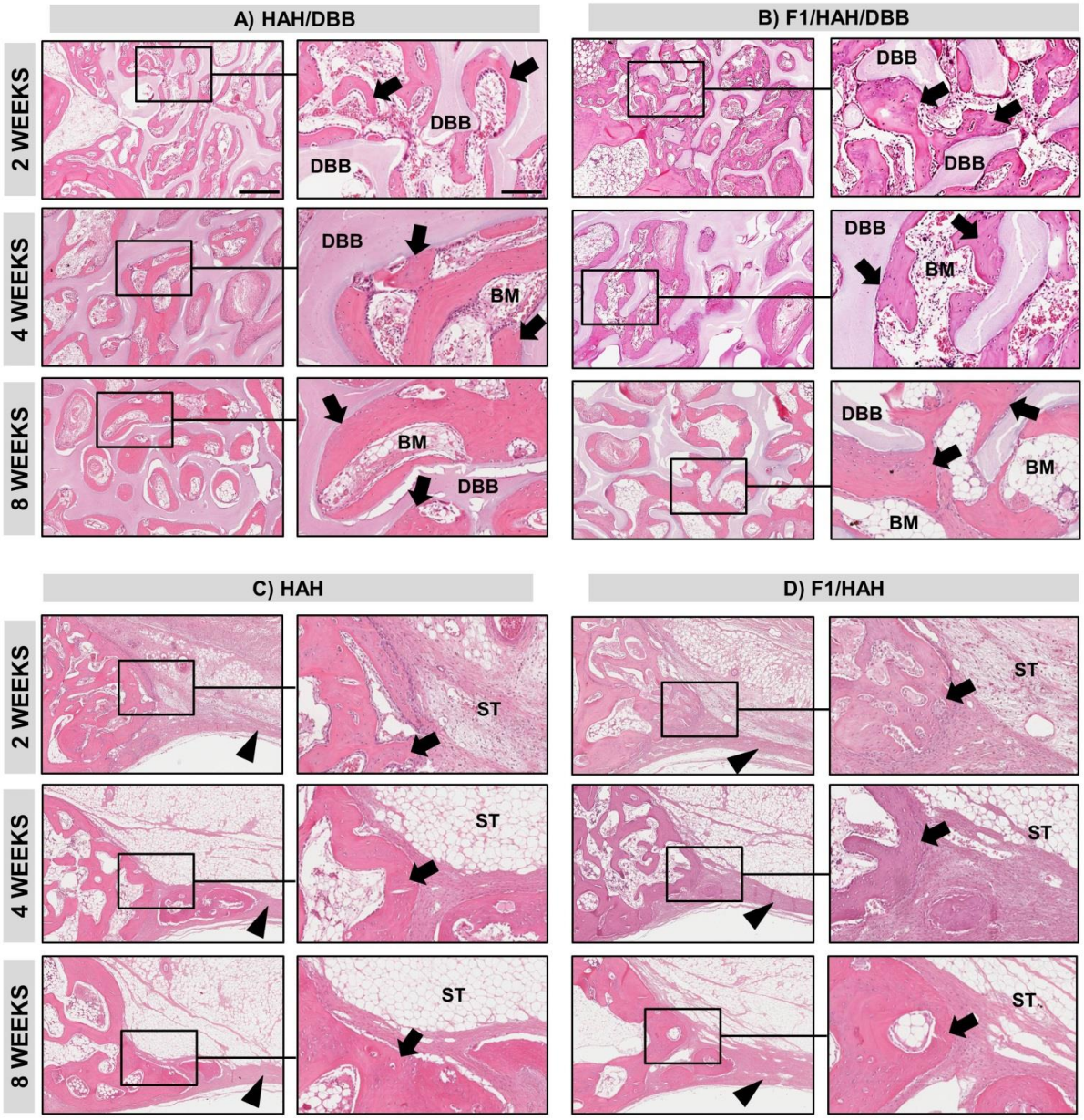

Figure 3 –Histological view of defects region of different experimental groups at 2, 4 and 8 weeks. A and B) Details show bone formation (black arrows) deposited directly to the surface of the DBB and surrounding the immature bone marrow at 2 and 4 weeks. At 8 weeks, the most of DBB pores show filled by lamellar bone tissue (black arrows) and mature bone marrow (BM); **C and D)** In all periods, the defects show the surrounding soft tissues (ST) collapsed into the defect, formation of a thin layer of fibrous connective tissue (black arrowheads) above to dura-mater surface and small bone formation (black arrows) limited to the defect border. HE, Bars=500µm and 150µm.

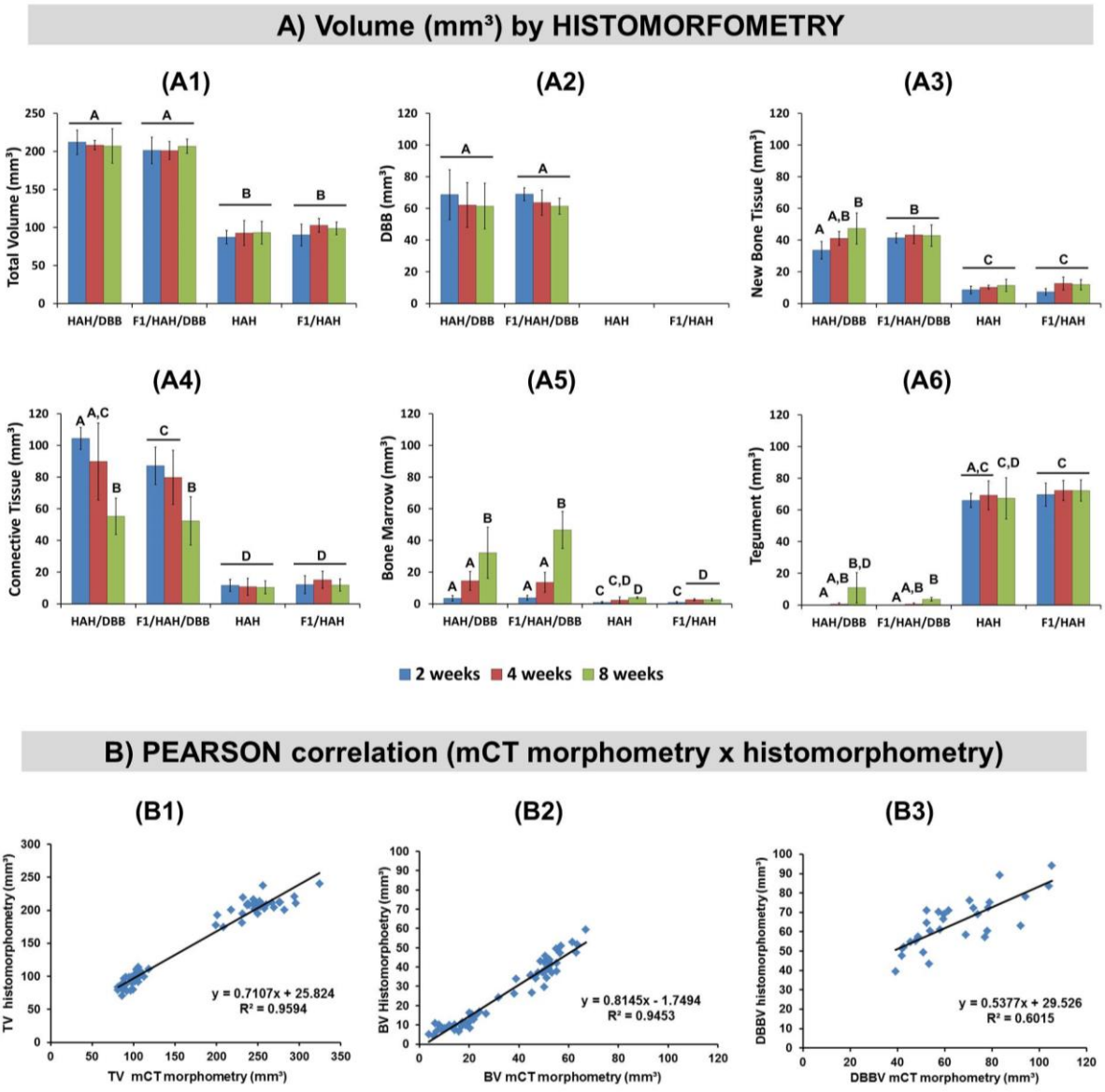

Figure 4: Volume of each structure in the defect by histomorphometric analysis (A) and Pearson Correlation between mCT morphometry and histomorphometry analysis (B). A) Bar graphs of mean ± SDM for Total Volume of Defect Region (A1), DBB Volume (A2), Bone Volume (A3), Connective Tissue Volume (A4), Bone Marrow Volume (A5) and Tegument Volume (A6). Different letters represent differences among groups and periods ($p < 0.05$). **B)** Correlation graphs for Total Volume (B1), DBB Volume (B2) and Bone Volume (B3) between mCT and histomorphometric analysis.

3 DISCUSSION

3 DISCUSSION

In this present thesis, the process of bone repair and bone augmentation was investigated in two different models of craniofacial reconstructive surgery, maxillary sinus augmentation (article 1) or critical size bone defect (article 2), and using different therapeutic approaches, such as calcium phosphate-based bone substitute materials used alone (article 1) or in combination with F1 protein fraction obtained from latex of *Hevea brasiliensis* (article 2).

Maxillary sinus augmentation (MSA) is a surgical technique widely applied in order to promote a significant vertical bone increase of the atrophic maxilla and allowing the placement of implants (Nkenke e Stelzle, 2009; Lee *et al.*, 2012). This technique is considered an adequate model for testing the behavior of substitute bone materials, because it is a closed and protected place and has a high local bone regeneration potential which can be maximized with filling biomaterials (Sauerbier *et al.*, 2011; Lim, Zhang, *et al.*, 2015). In this way, the bone regeneration in MSA can be obtained applying different options. The blood clot can be used as a filling material; however, the regenerated bone is progressively reabsorbed while the sinus re-expands due to positive intra-sinus air pressure (Lambert *et al.*, 2011). A similar phenomenon occurs with the use of autogenous bone, in which constant bone remodeling generated in the face of sinus forces leads to a significant and rapid decrease in the bone volume previously gained by the remodeling of autogenous bone particles and their replacement by fine bone trabeculae (Lambert *et al.*, 2011; Rocha, 2015). Other option to bone gain in MSA are substitute bone materials that are not resorbable or have slow resorption which seem to resist re-expansion of the sinus cavity, providing long-term three-dimensional bone stability (Xu *et al.*, 2004).

In this way, in the first article was verified that the three slow reabsorption calcium phosphate-based ceramics used contributed to maintaining the elevated maxillary sinus (MS) volume. The non-autogenous bone substitute material most successfully used, most studied clinically and histologically and established in the literature for MSA is the calcium phosphate-based ceramic carbonated deproteinized bovine bone so-called Bio-Oss® (cDBB). This material is considered reference among non-autogenous bone-substitute materials and gold standard as deproteinized bovine bone, therefore being used as group control in the study of article 1 (Jensen *et al.*, 2009; Sbordone *et al.*, 2011; Jensen *et al.*, 2012b; a; Manfro *et al.*,

2014; Moon *et al.*, 2015; Mordenfeld *et al.*, 2015). The other bone substitute materials used in this research, sintered deproteinized bovine bone (sDBB) and porous biphasic calcium phosphate (pBCP) are products of national manufacture and lower cost. Recent animal studies reveal that both sDBB and pBCP present excellent osteoconductive capacity, good bioactivity and slow resorption (Cestari *et al.*, 2009; Rocha *et al.*, 2011; Santos *et al.*, 2018; Paini *et al.*, 2020). The comparative microtomographic, histomorphometric and immunohistochemical study, in article 1, of sDBB and pBCP compared to cDBB using the MSA model in rabbits showed that the maintenance of elevated MS volume was statistically similar between the materials and periods evaluated, however the volume of bone tissue newly formed was favorable in the MSs filled with sDBB compared to the cDBB and similar to pBCP group.

Bone has a natural ability to regenerate, however, when the defect size is very extensive, its auto regeneration may be impaired. To solve this problem, the critical size bone defects are often treated with calcium phosphate-based ceramic, because it work as bridging structure to provide a pathway of connection to both the ends of the defects, occupy the anatomy of the defect site, avoiding soft tissue prolapse and while contribute to process of bone repair (Rh Owen *et al.*, 2018). Experimentally, Cestari *et al.* (2009) evaluated DBB block-shaped (substitute bone material used in article 2) in cranial critical size defects of *Cavia porcellus* during 12 weeks and observed that the defects without filling (control group) did not repaired and presented limited bone formation only their edges with central fibrous repair and collapsed tegument. On the other hand, the authors report that defects filled with DBB maintained the initial 3D-structure and the material filling contributed to promote the bone formation and stable bone thickness augmentation. In this sense, a systematic review of preclinical studies of bone regeneration concluded that the defects filled with bioceramic scaffolds better permitted the bone formation in contrast unfilled defects, which showed a small spontaneous bone formation (Brunello *et al.*, 2020).

In the critical size bone defects, the revascularization may be impaired, leading to fibrous healing. Therefore, the formation of efficient vascular networks is another crucial factor in the repair process for transport of nutrient, cells, waste and oxygen (Naderi *et al.*, 2011). As stated, the angiogenesis and osteogenesis are process influenced by growth factors during the repair phase (Cui *et al.*, 2013; Almubarak *et al.*, 2016). These growth factors are important polypeptides that work by binding to specific surface receptors of the cell membrane to initiate signaling pathways that regulate proliferation, survival, migration and differentiation cellular (Dias *et al.*, 2019). In this context, has been investigated that the

proper use of angiogenic factors in scaffold biomaterials through the engineered tissues can provide an enough neovascularization and to enhance and guide bone neoformation (Wernike *et al.*, 2010; Naderi *et al.*, 2011; Harris *et al.*, 2013). In this way, angiogenic fraction F1 obtained from the latex of the rubber tree (*Hevea brasiliensis*) has been investigated due to its ability to stimulate angiogenic activity and possibly contribute with bone formation. A recent study performed in our laboratory with rat cranial critical size bone defects showed that the F1 incorporated to DBB promoted a higher bone formation that when incorporated to pBCP and that F1 revealed to be a promising bioactive material for using in bone tissue engineering (Paini *et al.*, 2020). In the article 2, the use of F1 with HAH and associated to porous DBB block-shaped promoted a greater bone formation at 2 weeks compared to others groups, this result may have been influenced by the action of F1, improving vascularization and accelerating repair in the early stages of the process. The hydrogel is a safety biomaterial degraded *in vivo* and is used for delivery of growth factors to the defect site (Kim *et al.*, 2016). The HAH is degraded by hyaluronidase enzyme to nontoxic products that are easily processed by the body, however, presents poor mechanical strength (Sharma *et al.*, 2014). Its use in study of article 2 showed favorable when applied in combination to DBB and able to carrier the angiogenic factor F1.

Architecture of the calcium phosphate-based ceramics is considered a fundamental aspect in tissue bone engineering that influence its biological properties (Brunello *et al.*, 2020). An appropriate architecture should facilitate the flow of nutrients and elimination of waste products, as well as favor angiogenesis and cell ingrowth, proliferation and differentiation in the defect site (Abdulghani e Mitchell, 2019; Jeong *et al.*, 2019). In this context, the porosity (micro and macroporosity) is considered key factor for bone regeneration; increasing the specific surface area available for bioactive molecules adsorption, supporting cell migration into the defect site and, improving the available surface area for cell–scaffold binding and interaction with the surrounding tissues (Samavedi *et al.*, 2013; Zhang *et al.*, 2019). Thus, a porous structure provides an ideal environment for bone tissue ingrowth and repair (Naderi *et al.*, 2011; Ginebra *et al.*, 2018; Brunello *et al.*, 2020). Ginebra *et al.* (2018) points out that when filling is performed with particles-shaped material, the spaces in between granules outline a macroporous network. Regarding the format of the material, it is necessary to evaluate the most appropriate for each type of surgery. In the article 1, for maxillary sinus augmentation were used the particles-shaped ceramics, because, due to its greater mobility, the particles adapt and mold to the shape and volume of each

maxillary sinus, with well-delimited area. However, particulate grafts implantation requires the use of a barrier membrane in order to cover the osteotomy area and to prevent particulate leakage (Cestari *et al.*, 2009). On the other hand, in the article 2, for cranial critical size bone defects, the ceramic block-shaped was applied, no risk of material leaking and providing the necessary mechanical stability for this type of defect.

In both studies, in groups treated with bone substitutes materials it was possible to observe a similar bone repair process. Firstly, the blood was replaced by connective tissue richly cellularized and vascularized with gradual deposition of bone tissue by active osteoblasts on the surface of the biomaterials. At 2 weeks, the MSs augmented with cDBB, sDBB and pBCP granule-shaped showed on average, 37.9% of connective tissue, 18.7% of bone tissue and 0.5% of bone marrow, while , in the calvaria defect treated with HAH/DBB and F1/HAH/DBB exhibited, on average, 46.3%, 18.1% and 1.7% of connective tissue, bone tissue and bone marrow, respectively. The bone formation occurred of the remaining edges/walls towards the central region, growing on the surface of the biomaterial. Until 8 weeks, the bone tissue and bone marrow showed gradual growth and maturation to replace connective tissue previously and widely present. Therefore, in the last evaluated period, the volume density of connective tissue, bone tissue and bone marrow in the MSs were 20.3%, 25.5% and 16.6%, respectively and in the calvaria defect were 26.0%, 21.8% and 19.0% by, respectively. Due to the slow reabsorption and the osteoconductive characteristics of these substitute bone materials applied here, bone formation occurred in the spaces between its particles and its trabeculae until 8 weeks.

According to Pripatnanont *et al.* (2009), the rate of bone healing in rabbits is 3 times faster than in humans. In this way, in the period between 6 and 8 weeks of repair in the rabbit occurs the peak bone remodeling with the presence of mature or secondary bone tissue replacing immature or primary bone tissue, which would be equivalent in the period between 18 and 24 weeks in humans, period adequate for the placement of dental implants (Roberts *et al.*, 1984; Pripatnanont *et al.*, 2009). In addition, Sohn *et al.* (2010) using different sizes of bone defects in rabbit cranial evaluated the repair process and observed that the major remodeling bone occurred at the beginning of the 8-week period. The authors pointed out that the period of 2-4 weeks refers to the initial phase of repair, being able to assess the stability of the material and tissue reactions, whereas period from 8 weeks onwards indicate the late repair phase and can be evaluated bone incorporation, resorption of materials, bone remodeling and the amount of bone regeneration. Therefore, the final 8-week evaluation

period is of great importance in studies involving rabbits in order to evaluate bone tissue and perform the necessary approaches. As seen, animal models play a key role in many studies (Muschler *et al.*, 2010; Brunello *et al.*, 2020), this is because they allow a greater possibility of comparison with studies in humans due to the ability to mimic complex human physiological processes and bone mechanics that cannot be simulated and replaced by most advanced technologies without using animals (Peric *et al.*, 2015). Another advantage is that the use of animals compared to clinical research, often has a lower cost, greater possibility of standardization and reproducibility (Bigham-Sadegh, 2015).

4 CONCLUSIONS

4 CONCLUSIONS

In conclusion, this study originally demonstrated that:

- cDBB, sDBB and pBCP granules are good osteoconductive materials favoring the bone growth in theirs surface. The slow resorption of these materials could be an advantage in that it helps in keeping the dimensions of the MSA (article 1).
- Although no reduction of sDBB and pBCP was observed along of 8 weeks of MSA, both materials stimulate an initial increase of number of TRAP+ cells compared to cDBB in MSA technique (article 1).
- Porous DBB block-shaped plus HAH is biocompatible and good osteoconductive material for treatment of bone large defects in cranial region and its association with F1 is able to improve the bone formation in the early repair phase (article 2).
- The treatment of bone large defects in cranial region only with HAH or HAH plus F1 results in fibrous connective tissue formation and surrounding soft tissues collapse into the defect (article 2).

REFERENCES

REFERENCES[‡]

ABDULGHANI, S.; MITCHELL, G. R. Biomaterials for In Situ Tissue Regeneration: A Review. **Biomolecules,** v. 9, n. 11, Nov 19 2019. ISSN 2218-273X (Electronic) 2218-273X (Linking). Disponível em: < http://www.ncbi.nlm.nih.gov/pubmed/31752393 >.

ACCORSI-MENDONCA, T. et al. Physicochemical characterization of two deproteinized bovine xenografts. **Braz Oral Res,** v. 22, n. 1, p. 5-10, Jan-Mar 2008. ISSN 1807-3107 (Electronic) 1806-8324 (Linking). Disponível em: < http://www.ncbi.nlm.nih.gov/pubmed/18425238 >.

ALMUBARAK, S. et al. Tissue engineering strategies for promoting vascularized bone regeneration. **Bone,** v. 83, p. 197-209, Feb 2016. ISSN 1873-2763 (Electronic) 1873-2763 (Linking). Disponível em: < http://www.ncbi.nlm.nih.gov/pubmed/26608518 >.

AMINI, A. R.; LAURENCIN, C. T.; NUKAVARAPU, S. P. Bone tissue engineering: recent advances and challenges. **Crit Rev Biomed Eng,** v. 40, n. 5, p. 363-408, 2012. ISSN 0278-940X (Print) 0278-940X (Linking). Disponível em: < http://www.ncbi.nlm.nih.gov/pubmed/23339648 >.

BIGHAM-SADEGH, A. Selection of animal models for pre-clinical strategies in evaluating the fracture healing, bone graft substitutes and bone tissue regeneration and engineering. **Connective Tissue Research,** v. 56, n. 3, p. 175-195, 2015. ISSN 03008207.

BRUNELLO, G. et al. The Impact of Bioceramic Scaffolds on Bone Regeneration in Preclinical In Vivo Studies: A Systematic Review. **Materials (Basel),** v. 13, n. 7, Mar 25 2020. ISSN 1996-1944 (Print) 1996-1944 (Linking). Disponível em: < http://www.ncbi.nlm.nih.gov/pubmed/32218290 >.

CALASANS-MAIA, M. D. et al. Comparative histological evaluation of tibial bone repair in rabbits treated with xenografts. **Acta Ortopédica Brasileira,** v. 17, n. 6, p. 340-343, 2009. ISSN 1413-7852. Disponível em: < http://www.scielo.br/aob >.

CALASANS-MAIA, M. D. et al. Maxillary Sinus Augmentation with a New Xenograft: A Randomized Controlled Clinical Trial. **Clin Implant Dent Relat Res,** v. 17 Suppl 2, p. e586-

[‡] References in accordance with the standard: NBR 6023 - Information and Documentation - References - ABNT.

93, Oct 2015. ISSN 1708-8208 (Electronic) 1523-0899 (Linking). Disponível em: < http://www.ncbi.nlm.nih.gov/pubmed/25535980 >.

CESTARI, T. M. et al. Bone repair and augmentation using block of sintered bovine-derived anorganic bone graft in cranial bone defect model. **Clin Oral Implants Res,** v. 20, n. 4, p. 340-50, Apr 2009. ISSN 1600-0501 (Electronic) 0905-7161 (Linking). Disponível em: < http://www.ncbi.nlm.nih.gov/pubmed/19298288 >.

CHAPPARD, D. et al. Sinus lift augmentation and beta-TCP: a microCT and histologic analysis on human bone biopsies. **Micron,** v. 41, n. 4, p. 321-6, Jun 2010. ISSN 1878-4291 (Electronic) 0968-4328 (Linking). Disponível em: < http://www.ncbi.nlm.nih.gov/pubmed/20060730 >.

COELHO, P. G. et al. Basic research methods and current trends of dental implant surfaces. **J Biomed Mater Res B Appl Biomater,** v. 88, n. 2, p. 579-96, Feb 2009. ISSN 1552-4981 (Electronic) 1552-4973 (Linking). Disponível em: < http://www.ncbi.nlm.nih.gov/pubmed/18973274 >.

CORDARO, L. et al. Maxillary sinus grafting with Bio-Oss or Straumann Bone Ceramic: histomorphometric results from a randomized controlled multicenter clinical trial. **Clin Oral Implants Res,** v. 19, n. 8, p. 796-803, Aug 2008. ISSN 1600-0501 (Electronic) 0905-7161 (Linking). Disponível em: < http://www.ncbi.nlm.nih.gov/pubmed/18705811 >.

CUI, Q.; DIGHE, A. S.; IRVINE, J. N., JR. Combined angiogenic and osteogenic factor delivery for bone regenerative engineering. **Curr Pharm Des,** v. 19, n. 19, p. 3374-83, 2013. ISSN 1873-4286 (Electronic) 1381-6128 (Linking). Disponível em: < http://www.ncbi.nlm.nih.gov/pubmed/23432677 >.

DELGADO-RUIZ, R. A.; CALVO GUIRADO, J. L.; ROMANOS, G. E. Bone grafting materials in critical defects in rabbit calvariae. A systematic review and quality evaluation using ARRIVE guidelines. **Clin Oral Implants Res,** v. 29, n. 6, p. 620-634, Jun 2018. ISSN 1600-0501 (Electronic) 0905-7161 (Linking). Disponível em: < http://www.ncbi.nlm.nih.gov/pubmed/25996344 >.

DENRY, I.; KUHN, L. T. Design and characterization of calcium phosphate ceramic scaffolds for bone tissue engineering. **Dent Mater,** v. 32, n. 1, p. 43-53, Jan 2016. ISSN 1879-0097 (Electronic) 0109-5641 (Linking). Disponível em: < http://www.ncbi.nlm.nih.gov/pubmed/26423007 >.

DIAS, F. J. et al. Growth factors expression and ultrastructural morphology after application of low-level laser and natural latex protein on a sciatic nerve crush-type injury. **PLoS One,** v. 14, n. 1, p. e0210211, 2019. ISSN 1932-6203 (Electronic) 1932-6203 (Linking). Disponível em: < http://www.ncbi.nlm.nih.gov/pubmed/30625210 >.

ESPOSITO, M.; FELICE, P.; WORTHINGTON, H. V. Interventions for replacing missing teeth: augmentation procedures of the maxillary sinus. **Cochrane Database Syst Rev,** v. 5, p. CD008397, 2014. ISSN 1469-493X (Electronic) 1361-6137 (Linking). Disponível em: < http://www.ncbi.nlm.nih.gov/pubmed/24825543 >.

EZIRGANLI, S. et al. Effects of different biomaterials on augmented bone volume resorptions. **Clin Oral Implants Res,** v. 26, n. 12, p. 1482-8, Dec 2015. ISSN 1600-0501 (Electronic) 0905-7161 (Linking). Disponível em: < http://www.ncbi.nlm.nih.gov/pubmed/25264123 >.

FIENITZ, T. et al. Histological and radiological evaluation of sintered and non-sintered deproteinized bovine bone substitute materials in sinus augmentation procedures. A prospective, randomized-controlled, clinical multicenter study. **Clin Oral Investig,** v. 21, n. 3, p. 787-794, Apr 2017. ISSN 1436-3771 (Electronic) 1432-6981 (Linking). Disponível em: < http://www.ncbi.nlm.nih.gov/pubmed/27129584 >.

GINEBRA, M. P. et al. Bioceramics and bone healing. **EFORT Open Rev,** v. 3, n. 5, p. 173-183, May 2018. ISSN 2058-5241 (Print) 2058-5241 (Linking). Disponível em: < http://www.ncbi.nlm.nih.gov/pubmed/29951254 >.

GREENWALD, A. S. et al. Bone-graft substitutes: facts, fictions, and applications. **J Bone Joint Surg Am,** v. 83-A Suppl 2 Pt 2, p. 98-103, 2001. ISSN 0021-9355 (Print) 0021-9355 (Linking). Disponível em: < http://www.ncbi.nlm.nih.gov/pubmed/11712842 >.

HARRIS, G. M. et al. Strategies to direct angiogenesis within scaffolds for bone tissue engineering. **Curr Pharm Des,** v. 19, n. 19, p. 3456-65, 2013. ISSN 1873-4286 (Electronic) 1381-6128 (Linking). Disponível em: < http://www.ncbi.nlm.nih.gov/pubmed/23432671 >.

HOLTZCLAW, D. et al. The safety of bone allografts used in dentistry - A review. **Journal of the American Dental Association,** v. 139, n. 9, p. 1192-1199, Sep 2008. ISSN 0002-8177. Disponível em: < <Go to ISI>://WOS:000259241900012 >.

IEZZI, G. et al. Comparative histological results of different biomaterials used in sinus augmentation procedures: a human study at 6 months. **Clin Oral Implants Res,** v. 23, n. 12,

p. 1369-76, Dec 2012. ISSN 1600-0501 (Electronic) 0905-7161 (Linking). Disponível em: < http://www.ncbi.nlm.nih.gov/pubmed/22092377 >.

ISSA, J. P. et al. Bone repair of critical size defects treated with autogenic, allogenic, or xenogenic bone grafts alone or in combination with rhBMP-2. **Clin Oral Implants Res,** v. 27, n. 5, p. 558-66, May 2016. ISSN 1600-0501 (Electronic) 0905-7161 (Linking). Disponível em: < http://www.ncbi.nlm.nih.gov/pubmed/26260954 >.

JANICKI, P.; SCHMIDMAIER, G. What should be the characteristics of the ideal bone graft substitute? Combining scaffolds with growth factors and/or stem cells. **Injury,** v. 42 Suppl 2, p. S77-81, Sep 2011. ISSN 1879-0267 (Electronic) 0020-1383 (Linking). Disponível em: < http://www.ncbi.nlm.nih.gov/pubmed/21724186 >.

JENSEN, S. S. et al. Comparative study of biphasic calcium phosphates with different HA/TCP ratios in mandibular bone defects. A long-term histomorphometric study in minipigs. **J Biomed Mater Res B Appl Biomater,** v. 90, n. 1, p. 171-81, Jul 2009. ISSN 1552-4981 (Electronic) 1552-4973 (Linking). Disponível em: < http://www.ncbi.nlm.nih.gov/pubmed/19085941 >.

JENSEN, S. S.; TERHEYDEN, H. Bone augmentation procedures in localized defects in the alveolar ridge: clinical results with different bone grafts and bone-substitute materials. **Int J Oral Maxillofac Implants,** v. 24 Suppl, p. 218-36, 2009. ISSN 0882-2786 (Print) 0882-2786 (Linking). Disponível em: < http://www.ncbi.nlm.nih.gov/pubmed/19885447 >.

JENSEN, T. et al. Maxillary sinus floor augmentation with Bio-Oss or Bio-Oss mixed with autogenous bone as graft in animals: a systematic review. **Int J Oral Maxillofac Surg,** v. 41, n. 1, p. 114-20, Jan 2012a. ISSN 1399-0020 (Electronic) 0901-5027 (Linking). Disponível em: < http://www.ncbi.nlm.nih.gov/pubmed/22000958 >.

_____. Maxillary sinus floor augmentation with Bio-Oss or Bio-Oss mixed with autogenous bone as graft: a systematic review. **Clin Oral Implants Res,** v. 23, n. 3, p. 263-73, Mar 2012b. ISSN 1600-0501 (Electronic) 0905-7161 (Linking). Disponível em: < http://www.ncbi.nlm.nih.gov/pubmed/21443592 >.

JEONG, J. et al. Bioactive calcium phosphate materials and applications in bone regeneration. **Biomater Res,** v. 23, p. 4, 2019. ISSN 1226-4601 (Print) 1226-4601 (Linking). Disponível em: < http://www.ncbi.nlm.nih.gov/pubmed/30675377 >.

JUN, S. H. et al. A prospective study on the effectiveness of newly developed autogenous tooth bone graft material for sinus bone graft procedure. **J Adv Prosthodont,** v. 6, n. 6, p. 528-38, Dec 2014. ISSN 2005-7806 (Print) 2005-7806 (Linking). Disponível em: < http://www.ncbi.nlm.nih.gov/pubmed/25551014 >.

KIM, S. K. et al. Comparative study of BMP-2 alone and combined with VEGF carried by hydrogel for maxillary alveolar bone regeneration. **Tissue Eng Regen Med,** v. 13, n. 2, p. 171-181, Apr 2016. ISSN 2212-5469 (Electronic) 1738-2696 (Linking). Disponível em: < http://www.ncbi.nlm.nih.gov/pubmed/30603397 >.

KLIJN, R. J. et al. A meta-analysis of histomorphometric results and graft healing time of various biomaterials compared to autologous bone used as sinus floor augmentation material in humans. **Tissue Eng Part B Rev,** v. 16, n. 5, p. 493-507, Oct 2010. ISSN 1937-3376 (Electronic) 1937-3368 (Linking). Disponível em: < http://www.ncbi.nlm.nih.gov/pubmed/20334505 >.

KOLERMAN, R. et al. Histomorphometric analysis of newly formed bone after bilateral maxillary sinus augmentation using two different osteoconductive materials and internal collagen membrane. **Int J Periodontics Restorative Dent,** v. 32, n. 1, p. e21-8, Feb 2012. ISSN 1945-3388 (Electronic) 0198-7569 (Linking). Disponível em: < http://www.ncbi.nlm.nih.gov/pubmed/22254231 >.

LAMBERT, F. et al. Influence of space-filling materials in subantral bone augmentation: blood clot vs. autogenous bone chips vs. bovine hydroxyapatite. **Clin Oral Implants Res,** v. 22, n. 5, p. 538-45, May 2011. ISSN 1600-0501 (Electronic) 0905-7161 (Linking). Disponível em: < http://www.ncbi.nlm.nih.gov/pubmed/21198906 >.

LAMBERT, F. et al. The effect of collagenated space filling materials in sinus bone augmentation: a study in rabbits. **Clin Oral Implants Res,** v. 24, n. 5, p. 505-11, May 2013. ISSN 1600-0501 (Electronic) 0905-7161 (Linking). Disponível em: < http://www.ncbi.nlm.nih.gov/pubmed/22313247 >.

LEE, D. Z.; CHEN, S. T.; DARBY, I. B. Maxillary sinus floor elevation and grafting with deproteinized bovine bone mineral: a clinical and histomorphometric study. **Clin Oral Implants Res,** v. 23, n. 8, p. 918-24, Aug 2012. ISSN 1600-0501 (Electronic) 0905-7161 (Linking). Disponível em: < http://www.ncbi.nlm.nih.gov/pubmed/21707754 >.

LEGEROS, R. Z. Calcium phosphate-based osteoinductive materials. **Chem Rev,** v. 108, n. 11, p. 4742-53, Nov 2008. ISSN 1520-6890 (Electronic) 0009-2665 (Linking). Disponível em: < http://www.ncbi.nlm.nih.gov/pubmed/19006399 >.

LI, Y. et al. Bone defect animal models for testing efficacy of bone substitute biomaterials. **J Orthop Translat,** v. 3, n. 3, p. 95-104, Jul 2015. ISSN 2214-031X (Print) 2214-031X (Linking). Disponível em: < http://www.ncbi.nlm.nih.gov/pubmed/30035046 >.

LIM, H. C. et al. In Vivo Comparative Investigation of Three Synthetic Graft Materials with Varying Compositions Processed Using Different Methods. **Int J Oral Maxillofac Implants,** v. 30, n. 6, p. 1280-6, Nov-Dec 2015. ISSN 1942-4434 (Electronic) 0882-2786 (Linking). Disponível em: < http://www.ncbi.nlm.nih.gov/pubmed/26574853 >.

LIM, H. C. et al. Effect of different hydroxyapatite:beta-tricalcium phosphate ratios on the osteoconductivity of biphasic calcium phosphate in the rabbit sinus model. **Int J Oral Maxillofac Implants,** v. 30, n. 1, p. 65-72, Jan-Feb 2015. ISSN 1942-4434 (Electronic) 0882-2786 (Linking). Disponível em: < http://www.ncbi.nlm.nih.gov/pubmed/25265122 >.

LUTZ, R. et al. Sinus floor augmentation with autogenous bone vs. a bovine-derived xenograft - a 5-year retrospective study. **Clin Oral Implants Res,** v. 26, n. 6, p. 644-8, Jun 2015. ISSN 1600-0501 (Electronic) 0905-7161 (Linking). Disponível em: < http://www.ncbi.nlm.nih.gov/pubmed/25906198 >.

MANFRO, R. et al. Comparative, Histological and Histomorphometric Analysis of Three Anorganic Bovine Xenogenous Bone Substitutes: Bio-Oss, Bone-Fill and Gen-Ox Anorganic. **J Maxillofac Oral Surg,** v. 13, n. 4, p. 464-70, Dec 2014. ISSN 0972-8279 (Print) 0972-8270 (Linking). Disponível em: < http://www.ncbi.nlm.nih.gov/pubmed/26225012 >.

MATASSI, F. et al. New biomaterials for bone regeneration. **Clin Cases Miner Bone Metab,** v. 8, n. 1, p. 21-4, Jan 2011. ISSN 1971-3266 (Electronic) 1724-8914 (Linking). Disponível em: < http://www.ncbi.nlm.nih.gov/pubmed/22461799 >.

MOON, J. W. et al. Comparison of two kinds of bovine bone in maxillary sinus augmentation: a histomorphometric study. **Implant Dent,** v. 24, n. 1, p. 19-24, Feb 2015. ISSN 1538-2982 (Electronic) 1056-6163 (Linking). Disponível em: < http://www.ncbi.nlm.nih.gov/pubmed/25621547 >.

MORDENFELD, A.; LINDGREN, C.; HALLMAN, M. Sinus Floor Augmentation Using Straumann(R) BoneCeramic and Bio-Oss(R) in a Split Mouth Design and Later Placement of Implants: A 5-Year Report from a Longitudinal Study. **Clin Implant Dent Relat Res**, Sep 10 2015. ISSN 1708-8208 (Electronic) 1523-0899 (Linking). Disponível em: < http://www.ncbi.nlm.nih.gov/pubmed/26358740 >.

MUSCHLER, G. F. et al. The design and use of animal models for translational research in bone tissue engineering and regenerative medicine. **Tissue Eng Part B Rev,** v. 16, n. 1, p. 123-45, Feb 2010. ISSN 1937-3376 (Electronic) 1937-3368 (Linking). Disponível em: < http://www.ncbi.nlm.nih.gov/pubmed/19891542 >.

NADERI, H.; MATIN, M. M.; BAHRAMI, A. R. Review paper: critical issues in tissue engineering: biomaterials, cell sources, angiogenesis, and drug delivery systems. **J Biomater Appl,** v. 26, n. 4, p. 383-417, Nov 2011. ISSN 1530-8022 (Electronic) 0885-3282 (Linking). Disponível em: < http://www.ncbi.nlm.nih.gov/pubmed/21926148 >.

NEYT, J.; BUCKWALTER, J. A.; CARROLL, N. Use of animal models in musculoskeletal research. **The Iowa orthopaedic journal,** v. 18, p. 118, 1998.

NGUYEN, H.; MORGAN, D. A.; FORWOOD, M. R. Sterilization of allograft bone: is 25 kGy the gold standard for gamma irradiation? **Cell Tissue Bank,** v. 8, n. 2, p. 81-91, 2007. ISSN 1389-9333 (Print) 1389-9333 (Linking). Disponível em: < http://www.ncbi.nlm.nih.gov/pubmed/16821106 >.

NKENKE, E.; NEUKAM, F. W. Autogenous bone harvesting and grafting in advanced jaw resorption: morbidity, resorption and implant survival. **Eur J Oral Implantol,** v. 7 Suppl 2, p. S203-17, Summer 2014. ISSN 1756-2406 (Print) 1756-2406 (Linking). Disponível em: < http://www.ncbi.nlm.nih.gov/pubmed/24977256 >.

NKENKE, E.; STELZLE, F. Clinical outcomes of sinus floor augmentation for implant placement using autogenous bone or bone substitutes: a systematic review. **Clin Oral Implants Res,** v. 20 Suppl 4, p. 124-33, Sep 2009. ISSN 1600-0501 (Electronic) 0905-7161 (Linking). Disponível em: < http://www.ncbi.nlm.nih.gov/pubmed/19663959 >.

OH, J. S. et al. A Comparative Study with Biphasic Calcium Phosphate to Deproteinized Bovine Bone in Maxillary Sinus Augmentation: A Prospective Randomized and Controlled Clinical Trial. **Int J Oral Maxillofac Implants,** v. 34, n. 1, p. 233-242, January/February 2019. ISSN 1942-4434 (Electronic) 0882-2786 (Linking). Disponível em: < http://www.ncbi.nlm.nih.gov/pubmed/30521656 >.

OZDEMIR, H. et al. Effects of platelet rich fibrin alone used with rigid titanium barrier. **Arch Oral Biol,** v. 58, n. 5, p. 537-44, May 2013. ISSN 1879-1506 (Electronic) 0003-9969 (Linking). Disponível em: < http://www.ncbi.nlm.nih.gov/pubmed/23141995 >.

PAINI, S. et al. Concentration-dependent effects of latex F1-protein fraction incorporated into deproteinized bovine bone and biphasic calcium phosphate on the repair of critical-size bone defects. **J Biomed Mater Res B Appl Biomater,** May 2020. DOI: 10.1002/jbm.b.34664. (In press)

PAPAGEORGIOU, S. N. et al. Comparative effectiveness of natural and synthetic bone grafts in oral and maxillofacial surgery prior to insertion of dental implants: Systematic review and network meta-analysis of parallel and cluster randomized controlled trials. **J Dent,** v. 48, p. 1-8, May 2016. ISSN 1879-176X (Electronic) 0300-5712 (Linking). Disponível em: < http://www.ncbi.nlm.nih.gov/pubmed/27012858 >.

PEARCE, A. I. et al. Animal models for implant biomaterial research in bone: a review. **Eur Cell Mater,** v. 13, p. 1-10, 2007. ISSN 1473-2262 (Electronic) 1473-2262 (Linking). Disponível em: < http://www.ncbi.nlm.nih.gov/pubmed/17334975 >.

PERIC, M. et al. The rational use of animal models in the evaluation of novel bone regenerative therapies. **Bone,** v. 70, p. 73-86, Jan 2015. ISSN 1873-2763 (Electronic) 1873-2763 (Linking). Disponível em: < http://www.ncbi.nlm.nih.gov/pubmed/25029375 >.

PETROVIC, V. et al. Craniofacial bone tissue engineering. **Oral Surg Oral Med Oral Pathol Oral Radiol,** v. 114, n. 3, p. e1-9, Sep 2012. ISSN 2212-4411 (Electronic). Disponível em: < http://www.ncbi.nlm.nih.gov/pubmed/22862985 >.

PEYRIN, F. et al. Micro- and nano-CT for the study of bone ultrastructure. **Curr Osteoporos Rep,** v. 12, n. 4, p. 465-74, Dec 2014. ISSN 1544-2241 (Electronic) 1544-1873 (Linking). Disponível em: < http://www.ncbi.nlm.nih.gov/pubmed/25292366 >.

PILIPCHUK, S. P. et al. Tissue engineering for bone regeneration and osseointegration in the oral cavity. **Dent Mater,** v. 31, n. 4, p. 317-38, Apr 2015. ISSN 1879-0097 (Electronic) 0109-5641 (Linking). Disponível em: < http://www.ncbi.nlm.nih.gov/pubmed/25701146 >.

PRIPATNANONT, P.; NUNTANARANONT, T.; VONGVATCHARANON, S. Proportion of deproteinized bovine bone and autogenous bone affects bone formation in the treatment of calvarial defects in rabbits. **Int J Oral Maxillofac Surg,** v. 38, n. 4, p. 356-62, Apr 2009. ISSN 1399-0020 (Electronic) 0901-5027 (Linking). Disponível em: < http://www.ncbi.nlm.nih.gov/pubmed/19278833 >.

RH OWEN, G.; DARD, M.; LARJAVA, H. Hydoxyapatite/beta-tricalcium phosphate biphasic ceramics as regenerative material for the repair of complex bone defects. **J Biomed**

Mater Res B Appl Biomater, v. 106, n. 6, p. 2493-2512, Aug 2018. ISSN 1552-4981 (Electronic) 1552-4973 (Linking). Disponível em: < http://www.ncbi.nlm.nih.gov/pubmed/29266701 >.

ROBERTS, W. E. et al. Osseous adaptation to continuous loading of rigid endosseous implants. **Am J Orthod,** v. 86, n. 2, p. 95-111, Aug 1984. ISSN 0002-9416 (Print) 0002-9416 (Linking). Disponível em: < http://www.ncbi.nlm.nih.gov/pubmed/6589962 >.

ROCHA, C. A. **Avaliação comparativa da neoformação óssea após enxertia de HA/TCPp, Bio-Oss e osso autógeno associados ou não ao PRP em cirurgias de levantamento de seio maxilar de coelhos** 2015. 158 Universidade de São Paulo. Faculdade de Odontologia de Bauru

ROCHA, F. S. et al. Bovine anorganic bone graft associated with platelet-rich plasma: histologic analysis in rabbit calvaria. **J Oral Implantol,** v. 37, n. 5, p. 511-8, Oct 2011. ISSN 0160-6972 (Print) 0160-6972 (Linking). Disponível em: < http://www.ncbi.nlm.nih.gov/pubmed/20553125 >.

SALAI, M. et al. The effects of prolonged cryopreservation on the biomechanical properties of bone allografts: a microbiological, histological and mechanical study. **Cell Tissue Bank,** v. 1, n. 1, p. 69-73, 2000. ISSN 1573-6814 (Electronic) 1389-9333 (Linking). Disponível em: < http://www.ncbi.nlm.nih.gov/pubmed/15256969 >.

SAMAVEDI, S.; WHITTINGTON, A. R.; GOLDSTEIN, A. S. Calcium phosphate ceramics in bone tissue engineering: a review of properties and their influence on cell behavior. **Acta Biomater,** v. 9, n. 9, p. 8037-45, Sep 2013. ISSN 1878-7568 (Electronic) 1742-7061 (Linking). Disponível em: < http://www.ncbi.nlm.nih.gov/pubmed/23791671 >.

SANTOS, P. S. et al. Osteoinductive porous biphasic calcium phosphate ceramic as an alternative to autogenous bone grafting in the treatment of mandibular bone critical-size defects. **J Biomed Mater Res B Appl Biomater,** v. 106, n. 4, p. 1546-1557, May 2018. ISSN 1552-4981 (Electronic) 1552-4973 (Linking). Disponível em: < http://www.ncbi.nlm.nih.gov/pubmed/28755493 >.

SAUERBIER, S. et al. Bone marrow concentrate and bovine bone mineral for sinus floor augmentation: a controlled, randomized, single-blinded clinical and histological trial--per-protocol analysis. **Tissue Eng Part A,** v. 17, n. 17-18, p. 2187-97, Sep 2011. ISSN 1937-335X (Electronic) 1937-3341 (Linking). Disponível em: < http://www.ncbi.nlm.nih.gov/pubmed/21529247 >.

SBORDONE, L. et al. Apical and marginal bone alterations around implants in maxillary sinus augmentation grafted with autogenous bone or bovine bone material and simultaneous or delayed dental implant positioning. **Clin Oral Implants Res,** v. 22, n. 5, p. 485-91, May 2011. ISSN 1600-0501 (Electronic) 0905-7161 (Linking). Disponível em: < http://www.ncbi.nlm.nih.gov/pubmed/21087315 >.

SHARMA, S. et al. Biomaterials in tooth tissue engineering: a review. **J Clin Diagn Res,** v. 8, n. 1, p. 309-15, Jan 2014. ISSN 2249-782X (Print) 0973-709X (Linking). Disponível em: < http://www.ncbi.nlm.nih.gov/pubmed/24596804 >.

SOHN, J. Y. et al. Spontaneous healing capacity of rabbit cranial defects of various sizes. **J Periodontal Implant Sci,** v. 40, n. 4, p. 180-7, Aug 2010. ISSN 2093-2286 (Electronic) 2093-2278 (Linking). Disponível em: < http://www.ncbi.nlm.nih.gov/pubmed/20827327 >.

STACCHI, C. et al. Histologic and Histomorphometric Comparison between Sintered Nanohydroxyapatite and Anorganic Bovine Xenograft in Maxillary Sinus Grafting: A Split-Mouth Randomized Controlled Clinical Trial. **Biomed Res Int,** v. 2017, p. 9489825, 2017. ISSN 2314-6141 (Electronic). Disponível em: < http://www.ncbi.nlm.nih.gov/pubmed/28845435 >.

WANG, X.; MABREY, J. D.; AGRAWAL, C. M. An interspecies comparison of bone fracture properties. **Biomed Mater Eng,** v. 8, n. 1, p. 1-9, 1998. ISSN 0959-2989 (Print) 0959-2989 (Linking). Disponível em: < http://www.ncbi.nlm.nih.gov/pubmed/9713681 >.

WARD, B. B.; BROWN, S. E.; KREBSBACH, P. H. Bioengineering strategies for regeneration of craniofacial bone: a review of emerging technologies. **Oral Dis,** v. 16, n. 8, p. 709-16, Nov 2010. ISSN 1601-0825 (Electronic) 1354-523X (Linking). Disponível em: < http://www.ncbi.nlm.nih.gov/pubmed/20534013 >.

WERNIKE, E. et al. Vegf Incorporated into Calcium Phosphate Ceramics Promotes Vascularisation and Bone Formation in Vivo. **European Cells & Materials,** v. 19, p. 30-40, Jan-Jun 2010. ISSN 1473-2262. Disponível em: < <Go to ISI>://WOS:000278752500001 >.

XU, H. et al. Grafting of deproteinized bone particles inhibits bone resorption after maxillary sinus floor elevation. **Clin Oral Implants Res,** v. 15, n. 1, p. 126-33, Feb 2004. ISSN 0905-7161 (Print) 0905-7161 (Linking). Disponível em: < http://www.ncbi.nlm.nih.gov/pubmed/14731186 >.

YILDIRIM, M. et al. Maxillary sinus augmentation using xenogenic bone substitute material Bio-Oss in combination with venous blood. A histologic and histomorphometric study in humans. **Clin Oral Implants Res,** v. 11, n. 3, p. 217-29, Jun 2000. ISSN 0905-7161 (Print) 0905-7161 (Linking). Disponível em: < http://www.ncbi.nlm.nih.gov/pubmed/11168213 >.

YIP, I. et al. Defect healing with various bone substitutes. **Clin Oral Implants Res,** v. 26, n. 5, p. 606-14, May 2015. ISSN 1600-0501 (Electronic) 0905-7161 (Linking). Disponível em: < http://www.ncbi.nlm.nih.gov/pubmed/24702244 >.

ZHANG, L. et al. Three-dimensional (3D) printed scaffold and material selection for bone repair. **Acta Biomater,** v. 84, p. 16-33, Jan 15 2019. ISSN 1878-7568 (Electronic) 1742-7061 (Linking). Disponível em: < http://www.ncbi.nlm.nih.gov/pubmed/30481607 >.

ZIMMERMANN, G.; MOGHADDAM, A. Allograft bone matrix versus synthetic bone graft substitutes. **Injury,** v. 42 Suppl 2, p. S16-21, Sep 2011. ISSN 1879-0267 (Electronic) 0020-1383 (Linking). Disponível em: < http://www.ncbi.nlm.nih.gov/pubmed/21889142 >.

ANNEXES

Annex 1: Confirmation of submission of Article 1

Successfully received: submission MAXILLARY SINUS AUGMENTATION USING DIFFERENT CALCIUM PHOSPHATE-BASED CERAMICS: A MICROTOMOGRAPHIC, HISTOMORPHOMETRIC AND IMMUNOHISTOCHEMICAL STUDY for Materials Science & Engineering C

De: Materials Science & Engineering C (evisesupport@elsevier.com)

Para: santos_ps@yahoo.com.br

Data: segunda-feira, 16 de março de 2020 09:27 BRT

This message was sent automatically.

Ref: MSEC_2020_1036
Title: MAXILLARY SINUS AUGMENTATION USING DIFFERENT CALCIUM PHOSPHATE-BASED CERAMICS: A MICROTOMOGRAPHIC, HISTOMORPHOMETRIC AND IMMUNOHISTOCHEMICAL STUDY
Journal: Materials Science & Engineering C

Dear Ms. Santos,

Thank you for submitting your manuscript for consideration for publication in Materials Science & Engineering C. Your submission was received in good order.

To track the status of your manuscript, please log into EVISE® at: http://www.evise.com/evise/faces/pages/navigation/NavController.jspx?JRNL_ACR=MSEC and locate your submission under the header 'My Submissions with Journal' on your 'My Author Tasks' view.

Please note that we are currently handling a high volume of submissions and will assess your manuscript as soon as possible.

Thank you for submitting your work to this journal.

Kind regards,

Materials Science & Engineering C

Have questions or need assistance?
For further assistance, please visit our Customer Support site. Here you can search for solutions on a range of topics, find answers to frequently asked questions, and learn more about EVISE® via interactive tutorials. You can also talk 24/5 to our customer support team by phone and 24/7 by live chat and email.

Annex 2: Approval of Animal Ethical Committee (Article 1) – (CEEPA Process n. 028/2013)

Universidade de São Paulo
Faculdade de Odontologia de Bauru

Comissão de Ética no Ensino e Pesquisa em Animais

50 ANOS 1962 - 2012 FOB USP

CEEPA-Proc. Nº 028/2013

Bauru, 12 de agosto de 2013.

Senhor Professor,

O projeto de pesquisa encaminhado a esta Comissão de Ética no Ensino e Pesquisa em Animais, denominado ***Levantamento de seio maxilar bilateral em coelhos utilizando diferentes biomateriais cerâmicos a base de fosfato de cálcio. Avaliação microtomográfica e histomorfométrica***, de autoria de Paula Sanches dos Santos, sob sua orientação, foi enviado ao relator para avaliação e considerado APROVADO "ad referendum" desta Comissão, nesta data.

Solicitamos que qualquer alteração na pesquisa seja comunicada a esta Comissão, e que, ao final seja enviado um Relatório com os resultados obtidos, para análise ética e emissão de parecer final, o qual poderá ser utilizado para fins de publicação científica.

Atenciosamente,

Prof. Dr. Gustavo Pompermaier Garlet,
Presidente da Comissão de Ética no Ensino e Pesquisa em Animais, em exercício

Prof. Dr. Rumio Taga
Docente do Departamento de Ciências Biológicas

Al. Dr. Octávio Pinheiro Brisolla, 9-75 – Bauru-SP – CEP 17012-101 – C.P. 73
e-mail: mferrari@fob.usp.br – Fone/FAX (0xx14) 3235-8356
http://www.fob.usp.br

Annex 3: Approval of Animal Ethical Committee (Article 2) – (CEEPA Process n. 027/2013)

Universidade de São Paulo
Faculdade de Odontologia de Bauru

Comissão de Ética no Ensino e Pesquisa em Animais

50 ANOS 1962 - 2012 FOB USP

CEEPA-Proc. Nº 027/2013

Bauru, 12 de agosto de 2013.

Senhor Professor,

O projeto de pesquisa encaminhado a esta Comissão de Ética no Ensino e Pesquisa em Animais, denominado ***Reparo de defeitos ósseos no crânio de coelhos tratados com a proteína angiogênica F1 obtida do látex associada ao ácido hialurônico e ao GenOx Inorg®. Análise por microtomografia de raio-X e histomorfométrica***, de autoria de Tania Mary Cestari, sob sua orientação, foi enviado ao relator para avaliação e considerado APROVADO "ad referendum" desta Comissão, nesta data.

Solicitamos que qualquer alteração na pesquisa seja comunicada a esta Comissão, e que, ao final seja enviado um Relatório com os resultados obtidos, para análise ética e emissão de parecer final, o qual poderá ser utilizado para fins de publicação científica.

Atenciosamente,

Prof. Dr. Gustavo Pompermaier Garlet,
Presidente da Comissão de Ética no Ensino e Pesquisa em Animais, em exercício

Prof. Dr. Rumio Taga
Docente do Departamento de Ciências Biológicas

Al. Dr. Octávio Pinheiro Brisolla, 9-75 – Bauru-SP – CEP 17012-101 – C.P. 73
e-mail: mferrari@fob.usp.br – Fone/FAX (0xx14) 3235-8356
http://www.fob.usp.br

Annex 4: Approval of the report of Animal Ethical Committee (Article 2) – (CEEPA Process n. 027/2013)

Universidade de São Paulo
Faculdade de Odontologia de Bauru

CERTIFICADO

CERTIFICAMOS que a proposta intitulada "***Reparo de defeitos ósseos no crânio de coelhos tratados com a proteína angiogênica F1 obtida do látex associada ao ácido hialurônico e ao GenOx Inorg®. Análise por microtomografia de raio-X e histomorfométrica"***, *registrada sob nº* ***CEEPA Proc. nº 027/2013,*** sob a responsabilidade do Prof. Dr. Rumio Taga, que envolveu a utilização de animais pertencentes ao *filo Chordata, subfilo Vertebrata* (exceto humanos), para fins de pesquisa científica, encontra-se de acordo com os preceitos da Lei nº 11.794, de 8 de outubro de 2008, do Decreto nº 6.899, de 15 de julho de 2009, e com as normas editadas pelo Conselho Nacional de Controle de Experimentação Animal (CONCEA), e foi **aprovada** em reunião ordinária da Comissão de Ética no Ensino e Pesquisa em Animais (CEEPA), da Faculdade de Odontologia de Bauru-USP, realizada no dia 14 de março de 2017.

Finalidade	*( ) Ensino (X) Pesquisa Científica*
Vigência da autorização	*Agosto/2013 a Agosto/2014*
Espécie/Linhagem	*Coelho / Oryctolagus cuniculus*
N° de animais	*N=30*
Peso/Idade	*4 kg/5 meses*
Sexo	*Machos*
Origem	*Biotério de Criação ANILAB/Paulínia, SP*

21 de março de 2017.
Data

Profª Drª Ana Paula Campanelli
Presidente da Comissão de Ética no Ensino e Pesquisa em Animais

CEEPA
Comissão de Ética no Ensino e Pesquisa em Animais

Annex 5: Approval of Animal Ethical Committee (Article 2) – (CEEPA Process n. 003/2017)

Universidade de São Paulo
Faculdade de Odontologia de Bauru

Comissão de Ética no Ensino e Pesquisa em Animais

CEEPA-Proc. Nº 003/2017.

Bauru, 5 de maio de 2017.

Senhor Professor,

Informamos que Projeto de Pesquisa denominado ***"Avaliação microtomográfica, histomorfométrica e imunoistoquímica do efeito in vivo da fração F1 do látex (Hevea brasileiensis) carreada ao hidrogel de ácido hialurônico adsorvidos ao osso desproteinizado bovino no processo de reparo ósseo"*** tendo Vossa Senhoria como Pesquisador Responsável, que envolve a utilização de animais (logomorfos), para fins de pesquisa científica, encontra-se de acordo com os preceitos da Lei nº 11.794, de 8 de outubro de 2008, do Decreto nº 6.899, de 15 de julho de 2009, e com as normas editadas pelo Conselho Nacional de Controle da Experimentação Animal (CONCEA), foi analisado e considerado APROVADO em reunião ordinária da Comissão de Ética no Ensino e Pesquisa em Animais (CEEPA), realizada nesta data.

Vigência do projeto:	*Maio/2017 a Junho/2020*
Espécie/Linhagem:	*Amostras biológicas (crânio de coelhos incluídos em Histosec-Merck) provenientes do protocolo CEEPA 027/2013*
Nº de animais:	*Não se aplica*
Peso/Idade	*Não se aplica*
Sexo:	*Não se aplica*
Origem:	*Não se aplica*

Esta CEEPA solicita que ao final da pesquisa seja enviado um Relatório com os resultados obtidos para análise ética e emissão de parecer final, o qual poderá ser utilizado para fins de publicação científica.

Atenciosamente,

Profª Drª Ana Paula Campanelli
Presidente da Comissão de Ética no Ensino e Pesquisa em Animais

Prof. Dr. Gerson Francisco de Assis
Docente do Departamento de Ciências Biológicas

Al. Dr. Octávio Pinheiro Brisolla, 9-75 – Bauru-SP – CEP 17012-901 – C.P. 73
e-mail: ceepa@fob.usp.br – Fone/FAX (0xx14) 3235-8356
http://www.fob.usp.br